MycoKeys 55: 1–14 (2019)
doi: 10.3897/mycokeys.54.35015
http://mycokeys.pensoft.net

RESEARCH ARTICLE

A peer-reviewed open-access journal
MycoKeys
Launched to accelerate biodiversity research

Macrophomina vaccinii sp. nov. causing blueberry stem blight in China

Lin Zhao[1], Jing Cai[1], Wei He[1], Ying Zhang[2]

1 *Beijing Key Laboratory for Forest Pest Control, Beijing Forestry University, Beijing 100083, China* **2** *Institute of Microbiology, P.O. Box 61, Beijing Forestry University, Beijing 100083, China*

Corresponding author: *Wei He* (hewei@bjfu.edu.cn); *Ying Zhang* (yzhang@bjfu.edu.cn)

Academic editor: *Huzefa Raja* | Received 30 March 2019 | Accepted 22 May 2019 | Published 19 June 2019

Citation: Zhao L, Cai J, He W, Zhang Y (2019) *Macrophomina vaccinii* sp. nov. causing blueberry stem blight in China. MycoKeys 55: 1–14. https://doi.org/10.3897/mycokeys.55.35015

Abstract

Blueberries (*Vaccinium* spp.) have been widely cultivated in China because of their nutritional benefits and economic value. Blueberry stem blight has become one of the most severe diseases influencing blueberry productivity and quality in China. In this study, eight fungal isolates were obtained from twenty stem blight lesions of blueberry collected in Nanping, Fujian province, China. Asexual stage was observed after inducing sporulation, the morphology of which agrees with *Macrophomina* in the black, smooth, hard sclerotia and ellipsoid to obovoid, smooth hyaline conidia with apical sheath. Furthermore, DNA sequences of concatenated ITS, *tef1-a*, *TUB*, and *ACT* loci indicated that these isolates belong to a novel fungal species. The distinguishing morphological characteristics, such as the wider conidia and larger conidiomata pycnidial, also support its new status. Thus a novel fungus, *Macrophomina vaccinii*, was described in this study. Pathogenicity tests indicated that *M. vaccinii* could cause stem blight of blueberry.

Keywords

Vaccinium, stem blight, Botryosphaericeae, taxonomy, pathogenicity

Introduction

Blueberries (*Vaccinium* spp.) are popular fruits because of their health benefits health, such as enhancing brain memory and preventing heart disease (Shi and Liu 2009, Popović et al. 2018). Blueberries have been commercially cultivated worldwide, particularly in the USA, Canada and a few European countries (Evans and Ballen 2014). Blueberry cultivation in China started in 1981, and the planted area has reached 31,210 hectares with total production of 114, 905 t in 2017 (Li et al. 2018). Blueberries have

been widely cultivated mainly in Guizhou, Shandong and Liaoning province (Xu et al. 2015, Li et al. 2018). Stem blight disease was one of the most prevalent diseases in blueberry cultivation areas in China, which has seriously affected the growth of blueberry plants, fruit quality and productivity (Yu et al. 2012, 2013a, b, Xu et al. 2015, Xu 2016).

A number of fungal species have been reported causing stem blight, dieback or stem canker of blueberries. For instance, *Botryosphaeria dothidea*, *Lasiodiplodia theobromae*, *Neofusicoccum ribis*, and *N. parvum* caused stem blight of highbush or rabbiteyes blueberries in USA (Milholland 1972, Creswell and Milholland 1988, Smith 2004, Wright and Harmon 2009, 2010, Koike et al. 2014). *Macrophomina phaseolina* (Tassi) Goid caused stem blight of highbush blueberries in Serbia (Popović et al. 2018). *Neofusicoccum parvum* caused stem blight and dieback of highbush blueberries in Mexico (Boyzo-Marin et al. 2016). *Diaporthe ambigua*, *D. australafricana*, *D. neotheicola*, *D. passiflorae*, *Pestalotiopsis clavispora*, *P. neglecta*, and *Truncatella angustata* caused stem canker and dieback of highbush blueberries in Chile (Espinoza et al. 2008, Elfar et al. 2013), and *Godronia cassandrae* caused stem dieback of highbush blueberry in Norway (Stromeng and Stensvand 2011).

The genus *Macrophomina* was introduced based on *M. phaseolina*, and assigned in the Botryosphaeriaceae (Botryosphaeriales) (Crous et al. 2006, Phillips et al. 2013). Thus far, three species are accommodated within *Macrophomina*, *viz*. *M. phaseolina*, *M. pseudophaseolina* Crous, Sarr & Ndiaye, and *M. euphorbiicola* A.R. Machado, D.J. Soares & O.L. Pereira (Phillips et al. 2013, Sarr et al. 2014, Machado et al. 2019). *Macrophomina phaseolina* is a soil- or seed-borne polyphagous pathogen, causing charcoal rot disease on about 500 plant species of more than 100 families throughout the world (Su et al. 2001, Babu et al. 2007, Sarr et al. 2014). In Serbia, *M. phaseolina* was reported as a causal agent causing foliage death and brown discoloration of internal vascular stem tissues of highbush blueberry in 2015 (Popović et al. 2018). So far, *M. pseudophaseolina* has been reported causing charcoal rot disease on six plant species, *viz*. *Abelmoschus esculentus*, *Arachis hypogaea*, *Hibiscus sabdariffa*, *Vigna unguiculata*, *Gossypium hirsutum*, *Ricinus communis*, and associated with seed decay of *Jatropha curcas* (Sarr et al. 2014, Machado et al. 2019). *Macrophomia euphorbiicola* has only been reported as the causal agent of the charcoal rot on *Ricinus communis* and *Jatropha gossypiifolia* (Machado et al. 2019).

In the course of an ongoing survey of biodiversity of fungi causing stem blight of blueberries in China, a new taxon with general characteristics of *Macrophomina* was collected. The aim of this study was to identify the new isolates based on morphological characteristics and multigene phylogenetic analysis, and determine their pathogenicity on the blueberry.

Materials and methods

Sample collection, fungal isolation and morphological studies

This study was conducted at the Blueberry Production Garden in the suburb area of Nanping, Fujian province, China. Twenty diseased or dead stems (about 30 cm in length) were collected from blueberry branches in February, 2018. Wood segments (0.5 × 0.5

× 0.2 cm) cut from the diseased lesion boundary or dead tissue were surface sterilized (Pavlic et al. 2004) and incubated on malt extract agar (MEA, 2%) for fungal strains. Petri-dishes were incubated in the dark at 28 °C until fungal colonies were observed. Pure cultures were obtained by hyphal tips from the margin of the suspected *Macrophomina* colonies, which were subcultured on fresh MEA and maintained at 28 °C.

To induce sporulation of conidia, isolates were cultivated on synthetic nutrient-poor agar (SNA) with autoclaved pine needles placed onto the medium, and incubated at 25 °C under near-UV light (mainly 340 nm) (Dou et al. 2017b). Pycnidia produced on the pine needles were morphologically described and characterized following the protocol of Dou et al. (2017a, b). Measurements of conidia, conidiogenous cells and microconidia were made from water mounts. Measurements and digital photographs were made using a Nikon Coolpix 995 digital camera connected to a trinocular Leitz Orthoplan microscope and processed with Adobe Photoshop Elements 10 software. Fungal isolates and specimens were deposited at Beijing Forestry University (BJFU) with duplicates in the China General Microbiological Culture Collection Center (CGMCC) and the Mycological Herbarium of the Institute of Microbiology, Chinese Academy of Sciences (HMAS) (Table 1).

DNA extraction, PCR amplification and sequencing

DNA was extracted from mycelia grown on MEA plates with CTAB plant genome DNA fast extraction kit (Aidlab Biotechnologies Co., Ltd, Beijing, China). The internal transcribed spacer of rDNA (ITS) was amplified and sequenced with primers ITS-1 and ITS-4 (White et al. 1990). The translation elongation factor-1α (*tef1-a*) was amplified and sequenced with primers EF1-688F and EF1-1251R (Alves et al. 2008). The β-tubulin gene (*TUB*) was amplified and sequenced with primers Bt2a and Bt2b (Glass and Donaldson 1995). The actin gene (*ACT*) was amplified and sequenced with primers ACT-512F and ACT-2RD (Carbone and Kohn 1999, Sarr et al. 2014). PCR amplification and sequencing followed the protocols of Zhang et al. (2009).

Sequence alignment and phylogenetic analysis

DNA sequences of concatenated ITS, *tef1-a*, *TUB*, and *ACT* loci were analyzed to investigate the phylogenetic relationships among *Macrophomina* species with DNA sequences available from GenBank (http://www.ncbi.nlm.nih.gov/genbank/), as well as the sequences generated herein (Table 1). A multiple alignment was conducted with MEGA v. 6 (Tamura et al. 2013) and analyses were performed in PAUP V. 4.0b10 (Swofford 2002). Prior to phylogenetic analysis, ambiguous sequences at the start and the end were deleted and gaps manually adjusted to optimize the alignment. Maximum parsimony (MP) was conducted with heuristic searches as implemented in PAUP with the default options method (Zhang et al. 2008). Analyses with gaps treated as missing data were conducted under different parameters of maximum parsimonious criteria as outlined

Table 1. GenBank accession numbers of isolates included in this study (newly generated sequences are in bold).

Species	Sample number	GenBank accession number			
		ITS	*tef1-a*	*TUB*	*ACT*
Botryosphaeria dothidea	CBS 115476	AY236949	AY236898	AY236927	–
	CBS 110302	AY259092	AY573218	EU673106	–
Macrophomina euphorbiicola	CMM 4045	KU058928	KU058898	MF457657	MF457654
	CMM 4134	KU058936	KU058906	MF457658	MF457655
	CMM 4145	KU058937	KU058907	MF457659	MF457656
M. phaseolina	CBS 162.25	KF531826	KF951996	KF531805	KF951803
	CBS 227.33	KF531825	KF952000	KF531806	KF951807
	CPC 21388	KF951703	KF952074	KF952165	KF951843
	CPC 21392	KF951705	KF952076	KF952167	KF951844
	CPC 21395	KF951706	KF952077	KF952168	KF951846
	CPC 21399	KF951707	KF952078	KF952169	KF951847
	CPC 21443	KF951734	KF952104	KF952194	KF951872
	CPC 21444	KF951735	KF952105	KF952195	KF951873
	CPC 21445	KF951736	KF952106	KF952196	KF951874
M. pseudophaseolina	CPC 21394	KF951786	KF952148	KF952228	KF951913
	CPC 21402	KF951789	KF952151	KF952231	KF951916
	CPC 21403	KF951790	KF952152	KF952232	KF951917
	CPC 21417	KF951791	KF952153	KF952233	KF951918
	CPC 21459	KF951794	KF952156	KF952236	KF951921
	CPC 21501	KF951796	KF952158	KF952238	KF951923
	CPC 21524	KF951799	KF952161	KF952240	KF951925
	CPC 21527	KF951801	KF952163	KF952242	KF951927
	CPC 21528	KF951802	KF952164	KF952243	KF951928
M. vaccinii	CGMCC 3.19503	**MK687450**	**MK687426**	**MK687434**	**MK687442**
	CGMCC 3.19504	**MK687451**	**MK687427**	**MK687435**	**MK687443**
	CGMCC 3.19505	**MK687452**	**MK687428**	**MK687436**	**MK687444**
	CGMCC 3.19506	**MK687453**	**MK687429**	**MK687437**	**MK687445**
	CGMCC 3.19507	**MK687454**	**MK687430**	**MK687438**	**MK687446**
	CGMCC 3.19508	**MK687455**	**MK687431**	**MK687439**	**MK687447**
	CGMCC 3.19509	**MK687456**	**MK687432**	**MK687440**	**MK687448**
	CGMCC 3.19510	**MK687457**	**MK687433**	**MK687441**	**MK687449**

in Zhang et al. (2008). Clade stability was evaluated in a bootstrap analysis with 1,000 replicates, random sequence additions with the maxtrees set to 1,000 and other default parameters as implemented in PAUP. Maximum likelihood (ML) was also conducted using heuristic searches with the default options method as implemented in PAUP. For the ML analysis, best-fit model of nucleotide evolution (HKY+G) was selected by hierarchical likelihood ratio test (hLRT) in MrModeltest 2.3 (Posada and Crandall 2001). A bootstrap analysis with 1,000 replicates was used to test the statistical support of the branches. Trees were viewed in TreeView 1.6.6 (Page 1996). The nucleotide sequences reported in this paper were deposited in GenBank. Trees and alignments were deposited in TreeBase (https://treebase.org/treebase-web/home.html, submission ID: 24410).

Pathogenicity test

Three isolates of *Macrophomina vaccinii* (CGMCC 3.19503, CGMCC 3.19505, and CGMCC 3.19510) obtained in this study were used to conduct a pathogenicity test. The pathogenicity test was performed on 2-year blueberry stems (*cv*. O'Neal) in a humid chamber at 28 °C with semi-shaded conditions. Stems for inoculation were surface sterilized with 75% ethanol for 1 min before making a tangential cut (5 mm in length) on the bark (Espinoza et al. 2009). A 5-mm-diameter MEA medium with mycelial was taken from the 3-day colony, which was placed on to the wounded site, and subsequently covered with parafilm. Three replicates were conducted for each isolate. Noncolonized MEA agar plugs were used as negative controls. Pathogenicity was determined by the length of the necrotic lesion caused by the tested isolates three weeks after inoculation. Fungal isolates were re-isolated from the infected tissue, and morphological characterization and DNA sequence comparisons were conducted to fulfill Koch's postulates. Mean comparisons were conducted using Tukey's Honest Significant Difference test (HSD, $\alpha = 0.05$) in R (Version 3.2.2, R Inc. Auckland, NZL).

Results

Phylogeny

Phylogenetic analysis of the concatenated ITS, *tef1-a*, *TUB* and *ACT* sequence dataset comprising 1,426 bp revealed 129 parsimony-informative characters. The outgroup taxon was *Botryosphaeria dothidea*. The heuristic search with random addition of taxa (1,000 replicates) generated 5,000 most parsimonious trees of 141 steps (CI = 0.972, RI = 0.990, RC = 0.962, HI = 0.028). In both analyses (MP and ML), *M. phaseolina* and *M. vaccinii* formed a well-supported clade (MP BS = 99%, ML BS = 91%). *Macrophomina pseudophaseolina* and *M. euphorbiicola* formed another clade which lacks of bootstrap support (MP BS = 68%, ML BS = 67%, Fig. 1).

Taxonomy

Macrophomina vaccinii **Y. Zhang ter & L. Zhao, sp. nov.**
Mycobank: MB830282
Figure 2

Holotype. CHINA, Fujian province, Nanping city, Jianyang district, Huilong village, from blighted stem of southern high bush (*Vaccinium corymbosum* × *V. darrowii*), 26 Feb. 2018, L. Zhao (HMAS 255479): ex-type living culture, CGMCC 3.19503.

Etymology. from "*Vaccinium*", in reference to the host genus.

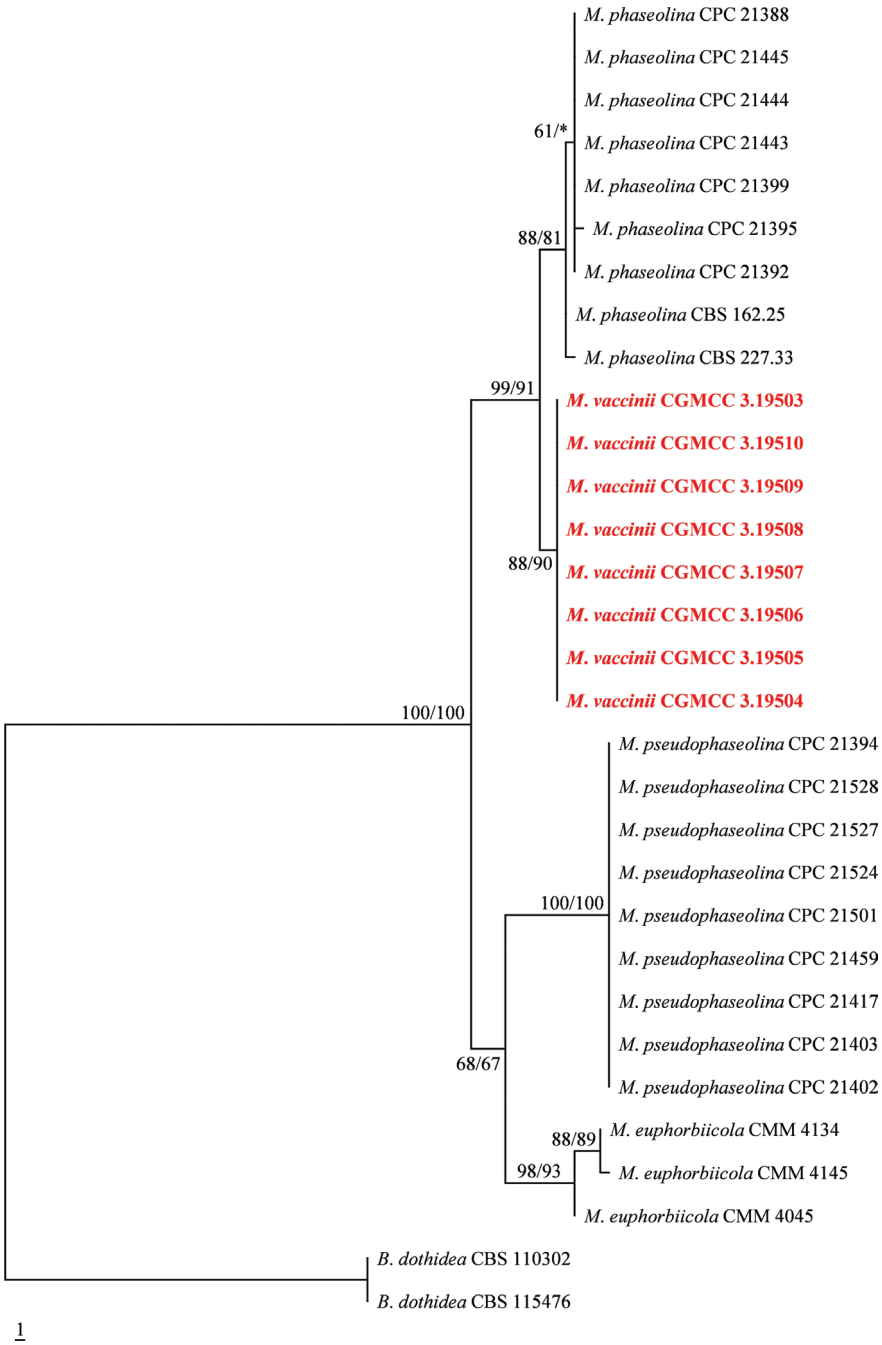

Figure 1. Maximum parsimony tree generated from sequence analysis of the concatenated ITS, *tef1-a*, *TUB* and *ACT* dataset. Designated out group taxa is *B. dothidea*. Maximum parsimony (MP) and maximum likelihood (ML) bootstrap support greater than or equal to 60% are shown above the nodes (* = value less than 60%). The positions of the *Macrophomina vaccinii* isolates are indicated in bold and red text.

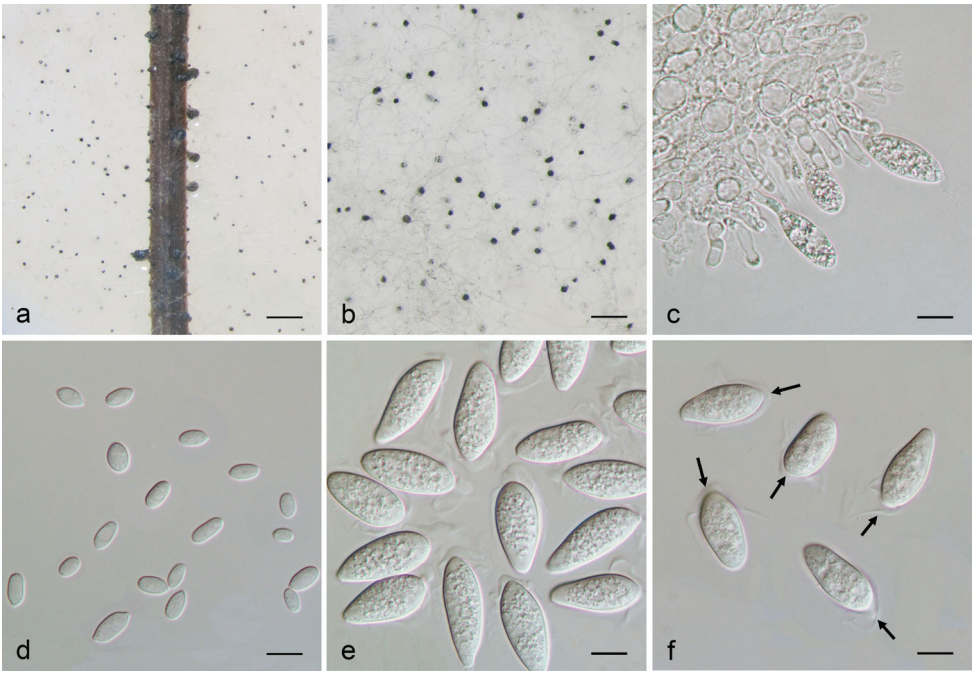

Figure 2. *Macrophomina vaccinii* (from ex-type: CGMCC 3.19503). **a** Pycnidia forming on pine needle **b** Sclerotia on the synthetic nutrient-poor agar **c** Conidiogenous cells **d** Microconidia **e–f** Conidia with apical appendages (arrows). Scale bars: 1 mm (**a**); 10 µm (**b–f**).

Description. Sexual stage not observed. Asexual stage: *Sclerotia* developing on SNA, black, smooth, hard, 40–100 µm diam. *Conidiomata* pycnidial, dark brown to black, solitary or gregarious, up to 400 µm diam., each opening by a central ostiole. *Conidiogenous cells* lining the inner surface of the conidioma, hyaline, subcylindrical, each proliferating several times percurrently near the apex, 9–16 × 3–4 µm, young conidiogenous cells each covered by a mucous layer that extends over the apex of the developing conidium. *Conidia* ellipsoid to obovoid, smooth, (18–)20–29(–33) × (8–)9–11(–12) µm (av. 24.8 × 10.1 µm, n = 60, L/W ratio = 2.5, range from 2.3 to 2.8), immature conidia hyaline, enclosed in a mucous sheath, that upon dehiscence encloses the top half of the conidium, transformed into two lateral tentaculiform, apical mucoid appendages (type C; Nag Raj 1993), no pigmented conidia observed after 30 days incubation. *Microconidia* aseptate, hyaline, smooth, guttulate to granular, straight to curved, ellipsoid to subcylindrical to irregular, 5–9(–10) × 3–5 µm.

Culture characteristics. *Colonies* on MEA at 25 °C in darkness, with even margins, sparse aerial mycelia. On MEA buff, turning pale olivaceous to olivaceous-black with dense, black sclerotial masses. Colonies reaching 58.6 mm on MEA after 2 d in the dark at 25 °C.

Figure 3. *Macrophomina vaccinii* causes stem blight of blueberry. **a** Death of the blueberry (*Vaccinium* spp.) plants in the field **b** Symptoms of stem blight of blueberry in the field **c** Symptoms of *Macrophomina vaccinii* after three days inoculation **d** Symptoms of *Macrophomina vaccinii* after one-week inoculation **e** Symptoms of *Macrophomina vaccinii* after three weeks inoculation **f** Symptoms of blueberry twig of *Macrophomina vaccinii* after three weeks inoculation.

Additional specimens examined. CHINA, Fujian province, Nanping city, Jianyang district, Huilong village, from blighted stem of southern high bush (*Vaccinium corymbosum* × *V. darrowii*), 26 February 2018, L. Zhao (Paratype, HMAS 255480): living culture, CGMCC 3.19505; (HMAS 255481): living culture, CGMCC 3.19510.

Note. Based on phylogenetic analysis, *M. vaccinii* and *M. phaseolina* formed a well-supported clade. Morphologically, the wider conidia of *Macrophomina vaccinii* can be distinguishable from *M. phaseolina* ((8–)9–11(–12) µm (av. 10.1 µm) *vs.* (6–)8(–9) µm (av. 8 µm)) (Sarr et al. 2014). In addition, the larger-sized pycnidia of *M. vaccinii* are also distinguishable from *M. phaseolina* (up to 400 µm diam. *vs.* up to 300 µm diam.) (Sarr et al. 2014). A comparison of the 264 nucleotides across the *tef1-a* gene region of *M. vaccinii* and *M. phaseolina* (CBS 227.33) reveals 5 base pair differences (1.9%) (Table 3).

Table 2. Pathogenicity on 2-year blueberry stems (*cv*. O'Neal) using mycelia of *Macrophomina vaccinii* after 3 weeks.

Species	Isolate	Blueberry stems inoculated with Mycelia ± SD (cm)
Macrophomina vaccinii	CGMCC 3.19503	12.63 ± 7.32 a
Macrophomina vaccinii	CGMCC 3.19505	12.38 ± 0.48 a
Macrophomina vaccinii	CGMCC 3.19510	10.75 ± 2.87 a
Noninoculated control	–	0.00 ± 0.00 b

Note: Data followed by different letters in each column are significantly different based on HSD tests at the P< 0.05 level.

Table 3. Major *tef1-a* and *TUB* and *ACT* base pair differences of *Macrophomina vaccinii*, *M. phaseolina*, *M. pseudophaseolina* and *M. euphorbiicola*.

Species	Base pair difference	Position of nucleotides difference		
		tef1-a	***TUB***	***ACT***
M. vaccinii and *M. phaseolina*	G instead of A	11	–	–
	C instead of T	41	–	–
	C instead of G	48	–	–
	A instead of C	75	–	–
	A instead of G	160	–	–
	T instead of C	–	–	76
M. vaccinii and *M. pseudophaseolina*	A instead of G	10, 24	–	–
	C instead of T	27, 31, 48, 103, 186	280, 313	–
	G instead of A	101, 144, 208	119, 192	–
	A instead of T	142	–	–
	T instead of C	145, 197, 217, 227, 247	56	76, 192
	T instead of A	219	–	–
	C instead of A	–	202	–
M. vaccinii and *M. euphorbiicola*	C instead of T	14, 23, 33, 193, 221	280, 313	–
	A instead of G	24	–	–
	T instead of C	43, 250	56	76, 192
	C instead of G	48	–	–
	C instead of A	106	202	–
	G instead of A	144, 211	119, 192	83
	A instead of C	185	–	–
	G instead of C	–	200	–

Pathogenicity test

All the three isolates of *Macrophomina vaccinii* (CGMCC 3.19503, CGMCC 3.19505, and CGMCC 3.19510) were pathogenic on the blueberry stems. Brown lesions appeared on the inoculated spots after 3 days of inoculation for mycelia (Fig. 3). The diseased spots turned brown and lesion area enlarged after 7 days inoculation (Fig. 3). After inoculation for 3 weeks, the length of necrotic lesion reached up to 20 cm, and the infected xylem tissue turned light-brown (Fig. 3). The wounded area of the inoculated stems was the one that was most significantly higher than those of the control groups, while no significant difference was detected among these three inoculated treatments (Fig. 3, Table 2).

Koch's postulates were performed by successful pathogen re-isolation from all the necrotic stems. The morphology and DNA sequences of these new isolates were consistent with the initial inoculate.

Discussion

Macrophomina is a cosmopolitan genus, with a broad host range and colonizing more than 500 crops and non-crop species, such as soybean, common bean, corn, sorghum, cowpea, peanut and cotton (Su et al. 2001, Ndiaye et al. 2010, Sarr et al. 2014, Sun et al. 2015). In this study, *Macrophomina vaccinii* was collected from the lesion of stem blight in Fujian province in China, a subtropical area in China. *Macrophomina phaseolina*, the most common species of *Macrophomina*, is considered as economically more important in subtropical and tropical countries with semi-arid climates, which tends to occur in hot and dry conditions (Wrather et al. 1997, 2001, Smith and Wyllie 1999, Radwan et al. 2014). Charcoal rot of beans is caused by *M. phaseolina*, however, this has frequently been reported in the northern part of China, with a disease incidence of 80% in Beijing and Tianjin (Zhang et al. 2009, 2011, Sun et al. 2015).

So far, seven species have been assigned within *Macrophomina*, *viz*. *M. euphorbiicola*, *M. limbalis*, *M. phaseoli*, *M. phaseolina*, *M. philippinensis*, *M. pseudeverniae* and *M. pseudophaseolina*. However, *M. limbalis* was transferred to *Dothiorella* (as *D. limbalis*), *M. pseudeverniae* to *Didymocyrtis* (as *D. pseudeverniae*), while *M. phaseoli* and *M. philippinensis* were treated as the synonym of *M. phaseolina*. Thus, only three species, *viz*. *M. euphorbiicola*, *M. phaseolina* and *M. pseudophaseolina* are currently accommodated within *Macrophomina*. Morphologically, wider conidia of *M. vaccinii* ((8–)9–11(–12) µm) are distinguishable from *M. phaseolina* ((6–)8(–9) µm) and *M. pseudophaseolina* ((7.5–)8(–9) µm) (Sarr et al. 2014). The larger-sized pycnidia of *M. vaccinii* (up to 400 µm diam.) can also be distinguishable from *M. phaseolina* (up to 300 µm diam.) and *M. pseudophaseolina* (up to 300 µm diam.) (Sarr et al. 2014). In addition, the smaller-sized sclerotia of *M. vaccinii* (40–100 µm diam.) also differs from *M. phaseolina* (100–400 µm diam.) and *M. pseudophaseolina* (100–400 µm diam.) (Sarr et al. 2014). *Macrophomina euphorbiicola* lacks morphological descriptions, and only DNA sequences are available for species comparison (Machado et al. 2019).

Phylogeny based on concatenated ITS, *tef1-a*, *TUB* and *ACT* DNA sequences indicated that the subclade comprising eight isolates of *Macrophomina vaccinii* are closely related to *M. phaseolina* (Fig. 1). A comparison of the *tef1-a* regions DNA sequence data of *M. vaccinii* and *M. phaseolina* revealed a 1.9% base pair difference. A comparison of the 266 nucleotides across the *tef1-a* gene region of *M. vaccinii* and *M. pseudophaseolina* (CPC 21417) reveals 17 base pair differences (6.39%). Although the morphological characteristics of *M. euphorbiicola* cannot be obtained, a comparison of the 269 nucleotides across the *tef1-a* gene region between *M. vaccinii* and *M. euphorbiicola* (CMM 4134) shows 13 base pair differences (4.83%) (Table 3). Following the

recommendations of Jeewon and Hyde (2016) and Tennakoon et al. (2018), there is sufficient evidence to justify our taxon as a new species.

Pathogenicity tests conducted on 2-year blueberry stems (*cv*. O'Neal) indicated that inoculation of *Macrophomina vaccinii* were pathogenic on blueberry stems which causes the stem turn brown with necrotic lesions. Similar symptoms caused by *M. phaseolina* have been reported on blueberry in Serbia, resulting in foliage death, and brown discoloration of internal vascular tissues at the basal part of the bush (Popović et al. 2018). The brown lesion caused by *M. vaccinii* and *M. phaseolina* on blueberries differs from the widely reported charcoal rot diseases caused by *Macrophomina phaseolina* and *M. pseudophaseolina* (Su et al. 2001, Salik 2007, Yang et al. 2005, Zhang et al. 2011, Sarr et al. 2014, Sun et al. 2015).

Acknowledgements

This work was supported by the National Natural Science Foundation of China (General Program, 31770015, 31370063), NSFC Projects of International Cooperation and Exchanges (3155461143028) and National Science and Technology Foundation Project (2014FY210400).

Reference

Alves A, Crous PW, Correia A, Phillips AJL (2008) Morphological and molecular data reveal cryptic speciation in *Lasiodiplodia theobromae*. Fungal Diversity 28: 1–13.

Babu BK, Saxena AK, Srivastava AK, Arora DK (2007) Identification and detection of *Macrophomina phaseolina* by using species-specific oligonucleotide primers and probe. Mycologia 99(6): 797–803. https://doi.org/10.1080/15572536.2007.11832511

Boyzo-Marin J, Rebollar-Alviter A, Silva-Rojas HV, Ramirez-Maldonado G (2016) First Report of *Neofusicoccum parvum* causing stem blight and dieback of blueberry in Mexico. Plant Disease 100(12): 2524. https://doi.org/10.1094/PDIS-03-16-0381-PDN

Carbone I, Kohn LM (1999) A method for designing primer sets for speciation studies in filamentous ascomycetes. Mycologia 91: 553–556. https://doi.org/10.2307/3761358

Creswell TC, Milholland RD (1988) Spore release and infection periods of *Botryosphaeria dothidea* on blueberry in North Carolina. Plant Disease 72: 342. https://doi.org/10.1094/pd-72-0342

Crous PW, Slippers B, Wingfield MJ, Rheeder J, Marasas WFO, Philips AJL, Alves A, Burgess T, Barber P, Groenewald JZ (2006) Phylogenetic lineages in the Botryosphaeriaceae. Studies in Mycology 55: 235–253. https://doi.org/10.3114/sim.55.1.235

Dou ZP, He, W, Zhang Y (2017a) *Lasiodiplodia chinensis* sp. nov., a new holomorphic species from China. Mycosphere 8: 521–532. https://doi.org/10.5943/mycosphere/8/2/3

Dou ZP, He W, Zhang Y (2017b) Does morphology matter in taxonomy of *Lasiodiplodia*? An answer from *Lasiodiplodia* hyalina sp. nov. Mycosphere 8: 1014–1027. https://doi.org/10.5943/mycosphere/8/2/5

Elfar K, Torres R, Díaz GA, Latorre BA (2013) Characterization of *Diaporthe australafricana* and *Diaporthe* spp. associated with stem canker of blueberry in Chile. Plant Disease 97: 1042–1050. https://doi.org/10.1094/PDIS-11-12-1030-RE

Espinoza JG, Briceño EX, Keith LM, Latorre BA (2008) Canker and twig dieback of blueberry (*Vaccinium* spp.) caused by *Pestalotiopsis* spp. and *Truncatella* sp. in Chile. Plant Disease 92: 1407–1414. https://doi.org/10.1094/PDIS-92-10-1407

Espinoza JG, Briceño EX, Chávez ER, Úrbez-Torres JR, Latorre BA (2009) *Neofusicoccum* spp. associated with stem canker and dieback of blueberry in Chile. Plant Disease 93: 1187–1194. https://doi.org/10.1094/PDIS-93-11-1187

Evans EA, Ballen FH (2014) An overview of US blueberry production, trade, and consumption, with special reference to Florida. University of Florida, IFAS, Extension, FE952. http://edis.ifas.ufl.edu

Glass NL, Donaldson GC (1995) Development of primer sets designed for use with the PCR to amplify conserved genes from filamentous ascomycetes. Applied and Environmental Microbiology 61(4): 1323–1330.

Jeewon R, Hyde KD (2016) Establishing species boundaries and new taxa among fungi: recommendations to resolve taxonomic ambiguities. Mycosphere 7(11): 1669–1677. https://doi.org/10.5943/mycosphere/7/11/4

Koike ST, Rooneylatham S, Wright AF (2014) First report of stem blight of blueberry in California caused by *Neofusicoccum parvum*. Plant Disease 98: 1280. https://doi.org/10.1094/PDIS-03-14-0325-PDN

Li YD, Pei JB, Sun HY (2018) Status and prospect of global blueberry industry. Journal of Jilin Agricultural University 40(04): 47–58.

Milholland RD (1972) Histopathology and pathogenicity of *Botryosphaeria dothidea* on blueberry stems. Phytopathology 62: 654–660. https://doi.org/10.1094/PHYTO-62-654

Machado AR, Pinho DB, Soares DJ, Gomes AAM, Pereira OL (2019) Bayesian analyses of five gene regions reveal a new phylogenetic species of *Macrophomina* associated with charcoal rot on oilseed crops in Brazil. European Journal of Plant Pathology. 153:89–100. https://doi.org/10.1007/s10658-018-1545-1

Nag Raj TR (1993) Coelomycetous anamorphs with appendage-bearing conidia. Mycologue Publications, Waterloo, Ontario.

Ndiaye M, Termorshuizen AJ, van Bruggen AHC (2010) Effects of compost amendment and the biocontrol agent *Clonostachys rosea* on the development of charcoal rot (*Macrophomina phaseolina*) on cowpea. Journal of Plant Pathology 92: 173–180.

Page RMD (1996) Treeview: an application to display phylogenetic trees on personal computers. Computer Applications in the Biosciences Cabios 12: 357–358. https://doi.org/10.1093/bioinformatics/12.4.357

Pavlic D, Slippers B, Coutinho TA, Gryenhout M, Wingfield MJ (2004) *Lasiodiplodia gonubiensis* sp. nov., a new *Botryosphaeria* anamorph from native *Syzygium cordatum* in South Africa. Studies in Mycology 50: 313–322.

Phillips AJL, Alves A, Abdollahzadeh J, Slippers B, Wingfield MJ, Groenewald JZ, Crous PW (2013) The Botryosphaeriaceae: genera and species known from culture. Studies in Mycology 76: 51–167. https://doi.org/10.3114/sim0021

Popović T, Blagojević J, Aleksić G, Jelušić A, Krnjajić S, Milovanović P (2018) A blight disease on highbush blueberry associated with *Macrophomina phaseolina* in Serbia. Canadian Journal of Plant Pathology 40: 121–127. https://doi.org/10.1080/07060661.2017.1415977

Posada D, Crandall KA (2001) Selecting the best-fit model of nucleotide substitution. Systematic Biology 50: 580–601. https://doi.org/10.1080/10635150118469

Radwan O, Rouhana LV, Hartman GL, Korban SS (2014) Genetic Mechanisms of Host-Pathogen Interactions for Charcoal Rot in Soybean. Plant Molecular Biology Reporter 32(3): 617–629. https://doi.org/10.1007/s11105-013-0686-9

Salik NK (2007) *Macrophomina phaseolina* as causal agent for charcoal rot of sunflower. Mycopath 5(2): 111–118.

Sarr MP, Ndiaye M, Groenewald JZ, Crous PW (2014) Genetic diversity in, *Macrophomina phaseolina*, the causal agent of charcoal rot. Phytopathologia Mediterranea 53(2): 250–268. https://doi.org/10.14601/PhytopatholMediterr-13736

Shi HZ, Liu HM (2009) The current research situation of Blueberry. Journal of Jiangsu Forestry Science & Technology 36: 48–51.

Smith BJ (2004) Susceptibility of southern highbush blueberry cultivars to *Botryosphaeria* stem blight. Small Fruits Review 3: 193–201. https://doi.org/10.1300/J301v03n01_19

Smith GS, Wyllie TD (1999) Charcoal rot. Compendium of soybean disease 4: 29–31.

Stromeng GM, Stensvand A (2011) Seasonal pattern in production of conidia of *Godronia cassandrae* f. sp. *vaccinii* in high bush blueberry in Norway. European Journal of Horticultural Science 76: 6–11.

Su G, Suh SO, Schneider RW, Russin JS (2001) Host Specialization in the Charcoal Rot Fungus, *Macrophomina phaseolina*. Phytopathology 91(2): 120–6. https://doi.org/10.1094/PHYTO.2001.91.2.120

Sun SL, Wang XM, Zhu ZD, Wang B, Wang M (2015) Occurrence of Charcoal Rot Caused by *Macrophomina phaseolina*, an Emerging Disease of Adzuki Bean in China. Journal of Phytopathology 164(3): 212–216. https://doi.org/10.1111/jph.12413

Swofford DL (2002) PAUP*: phylogenetic analysis using parsimony (*and other methods). Version 4.0b10. Sinauer Associates, Sunderland, Massachusetts.

Tamura K, Stecher G, Peterson D, Filipski A, Kumar S (2013) MEGA6: molecular evolutionary genetics analysis version 6.0. Molecular Biology and Evolution 30: 2725–2729. https://doi.org/10.1093/molbev/mst197

Tennakoon SD, Jeewon R, Kuo CH, Hyde KD (2018) Phylogenetic and morphological characterization of *Byssosphaeria macarangae* sp. nov., and *B. taiwanense* sp. nov. from *Macaranga tanarius*. Phytotaxa 364(3): 211–226 https://doi.org/10.11646/phytotaxa.364.3.1

White TJ, Bruns T, Lee S, Taylor JL (1990) Amplification and direct sequencing of fungal ribosomal RNA genes for phylogenetics. PCR Protocols: a guide to methods and applications 18: 315–322. https://doi.org/10.1016/B978-0-12-372180-8.50042-1

Wrather JA, Anderson TR, Arsyad DM, Gai J, Ploper LD, Porta-Puglia A, Ram HH, Yorinori JT (1997) Soybean disease loss estimates for the top 10 soybean producing countries in 1994. Plant Disease 81: 107–110. https://doi.org/10.1094/PDIS.1997.81.1.107

Wrather JA, Anderson TR, Arsyad DM, Tan Y, Ploper LD, Porta-Puglia A, Ram HH, Yorinori JT (2001) Soybean disease loss estimates for the top 10 soybean produc-

ing countries in 1998. Canadian Journal of Plant Pathology 23: 115–221. https://doi.org/10.1080/07060660109506918

Wright AF, Harmon PF (2009) First report of *Lasiodiplodia theobromae* associated with stem blight of southern highbush blueberries in Florida. Plant Disease 93: 962. https://doi.org/10.1094/PDIS-93-9-0962C

Wright AF, Harmon PF (2010) Identification of species in the Botryosphaeriaceae family causing stem blight on southern highbush blueberry in Florida. Plant Disease 94: 966–971. https://doi.org/10.1094/pdis-94-8-0966

Xu CN (2016) Etiology, Molecular Detection and Control of Blueberry Stem Blight in China. PhD Thesis, Hebei Agricultural University.

Xu CN, Zhang HJ, Zhou ZS, Hu T, Wang ST, Wang YN, Cao KQ (2015) Identification and distribution of Botryosphaeriaceae species associated with blueberry stem blight in China. European Journal of Plant Pathology 143: 737–752. https://doi.org/10.1007/s10658-015-0724-6

Yang XB, Navi SS (2005) First report of charcoal rot epidemics caused by *Macrophomina phaseolina* in soybean in Iowa. Plant Disease 89(5): 526. https://doi.org/10.1094/PD-89-0526B

Yu L, Rasisara I, Xu SG, Wu X, Zhao JR (2012) First report of stem blight of blueberry caused by *Botryosphaeria dothidea* in China. Plant Disease 96: 1697. https://doi.org/10.1094/PDIS-05-12-0500-PDN

Yu L, Impaprasert R, Zhao JR, Xu SG, Wu X (2013a) Stem dieback of highbush blueberries caused by *Neofusicoccum parvum* in China. New Disease Reports 27: 3. https://doi.org/10.5197/j.2044-0588.2013.027.003

Yu L, Zhao JR, Impaprasert R, Xu SG, Wu X (2013b) Identification of the pathogen causing twigs and stem dieback in blueberry. Acta Phytopathologica Sinica 43: 421–425. https://doi.org/10.13926/j.cnki.apps.2013.04.013

Zhang JQ, Cui YL, Duan CX, Wu XF, Wang XM, Zhu ZD (2009) Identification of pathogen causing soybean charcoal rot. Acta Agriculturae Boreali-Sinica 24: 192–196.

Zhang JQ, Zhu ZD, Duan CX, Wang XM, Li HJ (2011) First report of charcoal rot caused by *Macrophomina phaseolina* on mungbean in China. Plant Disease 95: 872. https://doi.org/10.1094/PDIS-01-11-0010

Zhang Y, Jeewon R, Fournier J, Hyde KD (2008) Multi-gene phylogeny and morphotaxonomy of *Amniculicola lignicola*: a novel freshwater fungus from France and its relationships to the Pleosporales. Mycological Research 112: 1186–1194. https://doi.org/10.1016/j.mycres.2008.04.004

Zhang Y, Wang HK, Fournier J, Crous PW, Jeewon R, Pointing SB, Hyde KD (2009) Towards a phylogenetic clarification of *Lophiostoma* / *Massarina* and morphologically similar genera in the Pleosporales. Fungal Diversity 38: 225–251.

MycoKeys 55: 15–28 (2019)
doi: 10.3897/mycokeys.55.35522
http://mycokeys.pensoft.net

RESEARCH ARTICLE

A peer-reviewed open-access journal
MycoKeys
Launched to accelerate biodiversity research

Elbamycella rosea gen. et sp. nov. (Juncigenaceae, Torpedosporales) isolated from the Mediterranean Sea

Anna Poli[1], Elena Bovio[1], Gerard Verkley[2], Valeria Prigione[1], Giovanna Cristina Varese[1]

1 *Department of Life Sciences and Systems Biology, Mycotheca Universitatis Taurinensis (MUT), University of Torino, Viale Mattioli 25, 10125 Torino, Italy* **2** *Westerdijk Fungal Biodiversity Institute, Uppsalalaan 8, 3584CT Utrecht, The Netherlands*

Corresponding author: *Valeria Prigione* (valeria.prigione@unito.it)

Academic editor: *Marc Stadler* | Received 18 April 2019 | Accepted 16 May 2019 | Published 19 June 2019

Citation: Poli A, Bovio E, Verkley G, Prigione V, Varese GC (2019) *Elbamycella rosea* gen. et sp. nov. (Juncigenaceae, Torpedosporales) isolated from the Mediterranean Sea. MycoKeys 55: 15–28. https://doi.org/10.3897/mycokeys.55.35522

Abstract

Elbamycella rosea **sp. nov.**, introduced in the new genus *Elbamycella*, was collected in the Mediterranean Sea in association with the seagrass *Posidonia oceanica* and with the brown alga *Padina pavonica*. The affiliation of the new taxon to the family Juncigenaceae is supported by both morphology and phylogenetic inference based on a combined nrSSU and nrLSU sequence dataset. Maximum-likelihood and Bayesian phylogeny proved *Elbamycella* **gen. nov.** as a distinct genus within Juncigenaceae. The new genus has been compared with closely related genera and is characterised by a unique suite of characters, such as ascospores with polar appendages and peculiar shape and dimension of ascomata and asci.

Keywords

Marine fungi, new taxon, TBM clade

Introduction

Marine fungi are a considerable part of the huge diversity of microorganisms that inhabit the Oceans (Richards et al. 2012). These organisms, which are distributed worldwide, live on a broad range of biotic and abiotic substrates (e.g. algae, sponges, corals, sediments) (Jones and Pang 2012) and are divided in two major ecological categories, namely obligate and facultative marine fungi. The former grow and reproduce exclusively in the sea, the latter are terrestrial species that can actively grow and reproduce in marine environments. Those fungi whose obligate or facultative marine nature is undefined are called marine-derived (Raghukumar 2017).

The number of marine fungi has been estimated to exceed 10,000 taxa, but the most recent update in marine mycology listed only 1,206 species belonging to Ascomycota, Basidiomycota, Chytridiomycota, and Mucoromycota. Thus fungal diversity is largely undescribed (Pang and Jones 2017).

In an attempt to clarify the phylogeny of the genera *Swampomyces* Kohlm. & Volkm.-Kohlm. and *Torpedospora* Meyers, Sakayaroj et al. (2005) recognised a distinct lineage of marine Ascomycota within the class Sordariomycetes that was then named TBM (*Torpedospora*/*Bertia*/*Melanospora*) clade (Schoch et al. 2007). Following a re-evaluation of the marine fungi affiliated to the TBM clade, together with the terrestrial genus *Falcocladium*, new families were introduced to accommodate its four subclades: Juncigenaceae, Etheirophoraceae, Falcocladiaceae, and Torpedosporaceae, all belonging to the order Torpedosporales (Jones et al. 2014; Abdel-Wahab et al. 2018). Based on phylogeny and morphological data, Maharachchikumbura et al. (2015) introduced the order Falcocladiales (Falcocladiaceae) under the class Sordariomycetes.

Recently, during a survey focused on the fungal diversity in the Mediterranean Sea, two unidentified Sordariomycetes were isolated from the seagrass *Posidonia oceanica* (L.) Delile (Panno et al. 2013) and from the brown alga *Padina pavonica* (L.) Thivy (Garzoli et al. 2018). The present paper provides a phylogenetic and morphological study of the two strains that turn out to represent a new genus within the family Juncigenaceae.

Material and methods

Fungal isolates

The fungal isolates investigated in this paper were previously retrieved from *P. oceanica* (MUT 4937 = CBS 130520) and *P. pavonica* (MUT 5443) from the coastal waters of Elba island, in the Mediterranean Sea (Panno et al. 2013; Garzoli et al. 2018) (Table 1). The two strains were originally isolated on corn meal agar medium supplemented with sea salts (CMASS; 3.4% w/v sea salt mix, Sigma-Aldrich, Saint Louis, USA, in ddH_2O) and are preserved at the *Mycotheca Universitatis Taurinensis*

(MUT), Italy, and CBS Collection of the Westerdijk Fungal Biodiversity Institute, the Netherlands.

Morphological analysis

MUT 4937 and MUT 5443 were pre-grown on CMA-sea water (CMASW; 17 g corn meal agar in 1 L of sea water) for one month at 21 °C prior to inoculation in triplicate onto Petri dishes (9 cm Ø) containing CMASS, CMASW, Potato Dextrose Agar (PDA) SS or PDASW. Petri dishes were incubated at 10 °C and 21 °C. The colony growth, together with macroscopic and microscopic traits, were monitored for 28 days.

Reproductive structures were observed and captured using an optical microscope (Leica DM4500B, Leica microsystems GmbH, Germany) equipped with a camera (Leica DFC320, Leica microsystems GmbH, Germany). Macro- and microscopic features were compared with the available description of Juncigenaceae (Kohlmeyer et al. 1997; Abdel-Wahab et al. 2001; Jones et al. 2014; Abdel-Wahab et al. 2018).

DNA extraction, PCR amplification, and data assembling

Genomic DNA was extracted from about 100 mg of mycelium carefully scraped from CMASS plates. Mycelium was transferred to a 2 mL Eppendorf tubes and disrupted in a MM400 tissue lyzer (Retsch GmbH, Haan, Germany). Extraction was accomplished using a NucleoSpin kit (Macherey Nagel GmbH, Duren, DE, USA) following the manufacturer's instructions. The quality and quantity of DNA samples were measured spectrophotometrically with Infinite 200 PRO NanoQuant (TECAN, Switzerland) and stored at –20 °C.

The primer pairs ITS1/ITS4 (White et al. 1990), LROR/LR7 (Vilgalys and Hester 1990), and NS1/NS4 (White et al. 1990) were used to amplify the partial sequences of the internal transcribed spacers including the 5.8S rDNA gene (ITS), partial large ribosomal subunit (nrLSU), and partial small ribosomal subunit (nrSSU), respectively. Ribosomal genes were amplified in a T100 Thermal Cycler (Bio-Rad, Hercules, CA, USA), as previously described (Bovio et al. 2018). Reaction mixtures consisted of 60–80 ng DNA template, 10× PCR Buffer (15 mM $MgCl_2$,500 mM KCl, 100 mM Tris-HCl, pH 8.3), 200 µM each dNTP, 1 µM each primer, 2.5 U Taq DNA Polymerase (Qiagen, Chatsworth, CA, USA), in 50 µL final volume. Following visualization of the amplicons on a 1.5% agarose gel stained with 5 mL 100 mL^{-1} ethidium bromide, PCR products were purified and sequenced at Macrogen Europe Laboratory (Madrid, Spain). The resulting ABI chromatograms were processed and assembled to obtain consensus sequences using Sequencer v. 5.0 (GeneCodes Corporation, Ann Arbor, Michigan, USA http://www.genecodes.com). Newly generated sequences were deposited in GenBank (Table 1).

Table 1. Dataset used for phylogenetic analysis. Genbank sequences including newly generated ITS, LSU and SSU amplicons relative to *Elbamycella rosea* sp. nov. and *Torpedospora ambispinosa* MUT 3537.

Species	Strain Code	Source	ITS	SSU	LSU
HYPOCREALES					
Bionectria pityrodes (Mont.) Schroers	GJS95-26	Bark	–	AY489696	AY489728
Clonostachys rosea (Link.) Schroers	GJS90-227	Bark	–	AY489684	AY489716
Cordyceps militaris (L.) Fr.	NRRL 28021	–	–	AF049146	AF327374
Fusarium solani (Mart.) Sacc.	GJS89-70	Bark	–	AY489697	AY489729
Trichoderma deliquescens (Sopp.) Jaklitsch	ATCC 208838	Pine wood	–	AF543768	AF543791
MICROASCALES					
Cephalotrichum stemonitis (Pers.) Nees	AFTOL 1380	Seed	–	DQ836901	DQ836907
Halosphaeria appendiculata Linder	NTOU4004	Driftwood	–	KX686781	KX686782
Lignincola laevis Hohnk	JK5180A	Wooden stake	–	U46873	U46890
Microascus trigonosporus Emmons & Dodge	AFTOL 914	–	–	DQ471006	DQ470958
Nimbospora effusa Kock	NTOU4018	Intertidal wood	–	KX686793	KX686794
Nohea umiumi Kohlm. & Volkm. Kohlm.	NTOU4006	Driftwood	–	KX686795	KX686796
Petriella setifera (Schmidt) Curzi	AFTOL 956	Wood panel in coastal water	–	DQ471020	DQ470969
TORPEDOSPORALES					
Etheirophoraceae					
Etheirophora blepharospora (Kohlm. & E. Kohlm.) Kohlm. & Volkm. Kohlm.	JK5397A	Bark on submerged proproots	–	EF027717	EF027723
E. unijubata Kohlm. & Volkm. Kohlm.	JK5443B	Submerged wood	–	EF027718	EF027725
Swampomyces armeniacus Kohlm. & Volkm. Kohlm.	JK5059C	Mangroves	–	EF027721	EF027728
S. triseptatus Hyde & Nakagiri	CY2802	Submerged wood	–	AY858942	AY858953
Juncigenaceae					
Juncigena adarca Kohlm., Volkm. Kohlm. & Erikss	JK5548A	*Juncus roemerianus*	–	EF027720	EF027727
J. fruticosae (Abdel-Wahab, Abdel-Aziz & Nagah.) Mill. & Shearer	EF14	Driftwood	–	GU252146	GU252145
	IMI391650	Driftwood	–	NG_061097	NG_060791
Khaleijomyces marinus Abdel-Wahab	MD1348	Driftwood	–	MG717679	MG717678
Marinokulati chaetosa (Kohlm.) Jones & Panf	BCRC FU30271	Driftwood	–	KJ866929	KJ866931
	BCRC FU30272	Driftwood	–	KJ866930	KJ866932
Fulvocentrum aegyptiacum (Abdel-Wahab, El-Shar. & Jones) Jones & Abdel-Wahab	CY2973	Mangroves	–	AY858943	AY858950
F. clavatisporum (Abdel-Wahab, El-Shar. & Jones) Jones & Abdel-Wahab	LP83	Mangroves	–	AY858945	AY858952
***Elbamycella rosea* sp. nov.**	MUT 4937	*P. oceanica*	MK775496*	MK775501*	MK775499*
***Elbamycella rosea* sp. nov.**	MUT 5443	*P. pavonica*	MK775497*	MK775502*	MK775500*
Torpedosporaceae					
Torpedospora ambispinosa Kohlm.	CY3386	Driftwood	–	AY858941	AY858946
	BCC16003	Driftwood	–	AY858940	AY858949
	MUT 3537	Driftwood	MK775503*	MK775498*	MK775495*
T. mangrovei (Abdel-Wahab & Nagah.) Jones & Abdel-Wahab	NBRC 105264	Mangroves	NR_138418	GU252150	GU252149
T. radiata Meyers	BCC11269	Driftwood	–	AY858938	AY858948
	PP7763	Driftwood	–	AY858939	AY858947
FALCOCLADIALES					
Falcocladiaceae					
Falcocladium multivesiculatum Silveira, Alfenas, Crous & Wingf	CBS 120386	Leaves	–	JF831928	JF831932
F. sphaeropedunculatum Crous & Alfenas	CBS 111292	Leaves	–	JF831929	JF831933
F. thailandicum Crous & Himaman	CBS 121717	Leaves	–	JF831930	JF831934
F. turbinatum Somrith., Sudhom, Tippawan & Jones	BCC22055	Dead leaves	–	JF831931	JF831935
XYLARIALES					
Daldinia concentrica (Bolton) Ces. & De Not.	ATCC 36659	*Fraxinus* sp.	–	U32402	U47828
Hypoxylon fragiforme (Pers.) Kickx	HKUCC 1022	Bark	–	AY083810	AY083829
Xylaria hypoxylon (L.) Grev.	AFTOL 51	Rotting wood	–	AY544692	AY544648

* = newly generated sequences

Sequence alignment and phylogenetic analysis

A dataset consisting of nrLSU and nrSSU was assembled on the basis of BLASTn results and of a recent phylogenetic study focused on Torpedosporales (Abdel-Wahab et al. 2018). Reference sequences were retrieved from GenBank. Although nrITS regions were amplified for MUT 4937 and MUT 5443, they were not used for phylogenetic analyses, due to the lack of available ITS sequences for the strains present in the tree. Alignments were generated using MUSCLE (default conditions for gap openings and gap extension penalties), implemented in MEGA v. 7.0 (Molecular Evolutionary Genetics Analysis), visually inspected and trimmed by TrimAl v. 1.2 (http://trimal.cgenomics.org) to delimit and discard ambiguously aligned regions. nrITS alignment was not performed, due to the lack of reference sequences. Preliminary analyses suggested no incongruence among single-loci phylogenetic trees, as assessed through the Incongruence Length Difference (ILD) test (de Vienne et al. 2007). As a consequence, alignments were concatenated into a single data matrix with SequenceMatrix (Vaidya et al. 2011). The appropriate evolutionary model under the Akaike Information Criterion (AIC) was determined with jModelTest 2 (Darriba et al. 2012).

Phylogenetic inference was estimated using both Maximum Likehood (ML) and Bayesian Inference (BI). The ML analysis was performed using RAxML v. 8.1.2 (Stamatakis 2014) under GTR + I + G evolutionary model (best model) and 1,000 bootstrap replicates. Support values from bootstrapping runs (MLB) were mapped on the globally best tree using the "-f a" option of RAxML and "-x 12345" as a random seed to invoke the novel rapid bootstrapping algorithm. BI was performed with MrBayes 3.2.2 (Ronquist et al. 2012) with the same substitution model (GTR + I + G). The alignment was run for 10 million generations with two independent runs each containing four Markov Chains Monte Carlo (MCMC) and sampling every 100 iterations. The first quarter of the trees were discarded as "burn-in". A consensus tree was generated using the "sumt" function of MrBayes and Bayesian posterior probabilities (BPP) were calculated. Consensus trees were visualized in FigTree v. 1.4.2 (http://tree.bio.ed.ac.uk/software/figtree). Members of Xylariales (i.e. *Xylaria hypoxylon*, *Hypoxylon fragiforme*, and *Daldinia concentrica*) were used as outgroup taxa. Due to topological similarity of the two resulting trees, only ML analysis with MLB and BPP values is reported (Fig. 1).

Sequence alignments and phylogenetic tree were deposited in TreeBASE (http://www.treebase.org, submission number 24426).

Results

Phylogenetic inference

Preliminary analyses were carried out individually with nrSSU and nrLSU. The topology of the single-locus trees was very similar and the ILD test confirmed the congruence between them ($p = 0.001$). The combined dataset consisted of an equal number

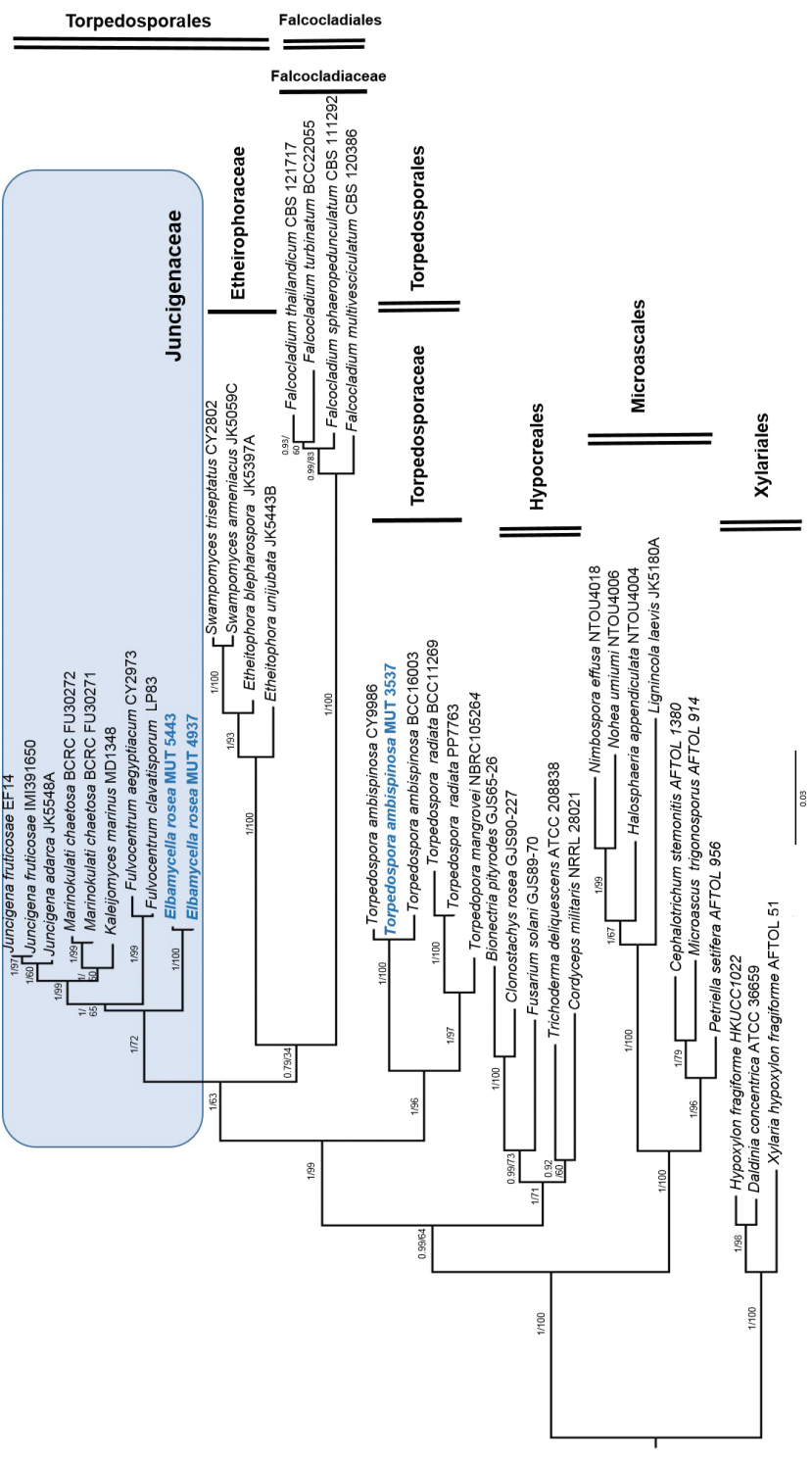

Figure 1. Phylogenetic inference of *Elbamycella rosea* sp. nov. based on a combined nrSSU and nrLSU dataset. The tree is rooted to *Xylaria hypoxylon*. Branch numbers indicate BPP/MLB values; Bar = expected changes per site (0.03).

of nrSSU and nrLSU sequences relative to 39 taxa (including MUT 4937 and MUT 5443) that represented 23 genera and 33 species (Table 1). Nine sequences (3 nrSSU, 3 nrLSU, and 3 nrITS) were newly generated while 72 were retrieved from GeneBank. SSU and LSU sequences relative to MUT 4937 and MUT 5443 displayed 100% and 99% similarity (3 bp substitutions). The combined dataset had an aligned length of 1676 characters, of which 1208 were constant, 92 were parsimony-uninformative and 376 parsimony informative (TL = 315, CI = 0.603715, RI = 0.802773, RC = 0.549296, HI = 0.396285).

The two isolates MUT 4937 and MUT 5443 clustered within the family Juncigenaceae together with *Marinokulati chaetosa*, *Khaleijomyces marinus*, *Juncigena adarca*, *J. fruticosae*, *Fulvocentrum aegyptiacum*, and *F. clavatisporum* (Fig. 1; BPP = 1; MLB = 72%) and formed a strongly supported monophyletic lineage (Fig. 1; BPP = 1; MLB = 100%) indicating that these strains are phylogenetically different from the other members of the family.

Taxonomy

***Elbamycella* gen. nov. A. Poli, E. Bovio, V. Prigione & G.C. Varese**
Mycobank: MB830648

Type species. *Elbamycella rosea* sp. nov.

Etymology. In reference to the geographic isolation site, Elba Island, Tuscany (Italy)

Phylogenetic placement. Juncigenaceae, Sordariomycetes, Ascomycota. The genus *Elbamycella* gen. nov. clusters together with genera *Marinokulati*, *Khaleijomyces*, *Juncigena*, and *Fulvocentrum* (Fig. 1).

Description. Ascomata superficial, erumpent or immersed, perithecial, scattered or gregarious, olivaceous-brown to black at maturity, globose, subglobose, ovoid or pyriform, glabrous; ostiolar neck long, pale-coloured; peridium of textura prismatica in the outer layers and textura globulosa in the inner layers. Asci evanescent, hyaline, cylindrical to clavate.

Ascopores cylindrical rounded at both ends, thin-walled, hyaline, straight or slightly curved, 3-septate, bearing subpolar, appendages.

Asexual morph unknown.

***Elbamycella rosea* sp. nov. A. Poli, E. Bovio, V. Prigione & G.C. Varese**
Mycobank: MB830649
Figures 2, 3

Type. Italy, Tuscany, Mediterranean Sea, Elba Island (LI), Ghiaie ISL, 14–15m depth, 42°49'04"N, 10°19'20"E, on the brown alga *Padina pavonica*, 20 March 2010, R. Mussat-Sartor and N. Nurra, MUT 5443 holotype, living culture permanently preserved

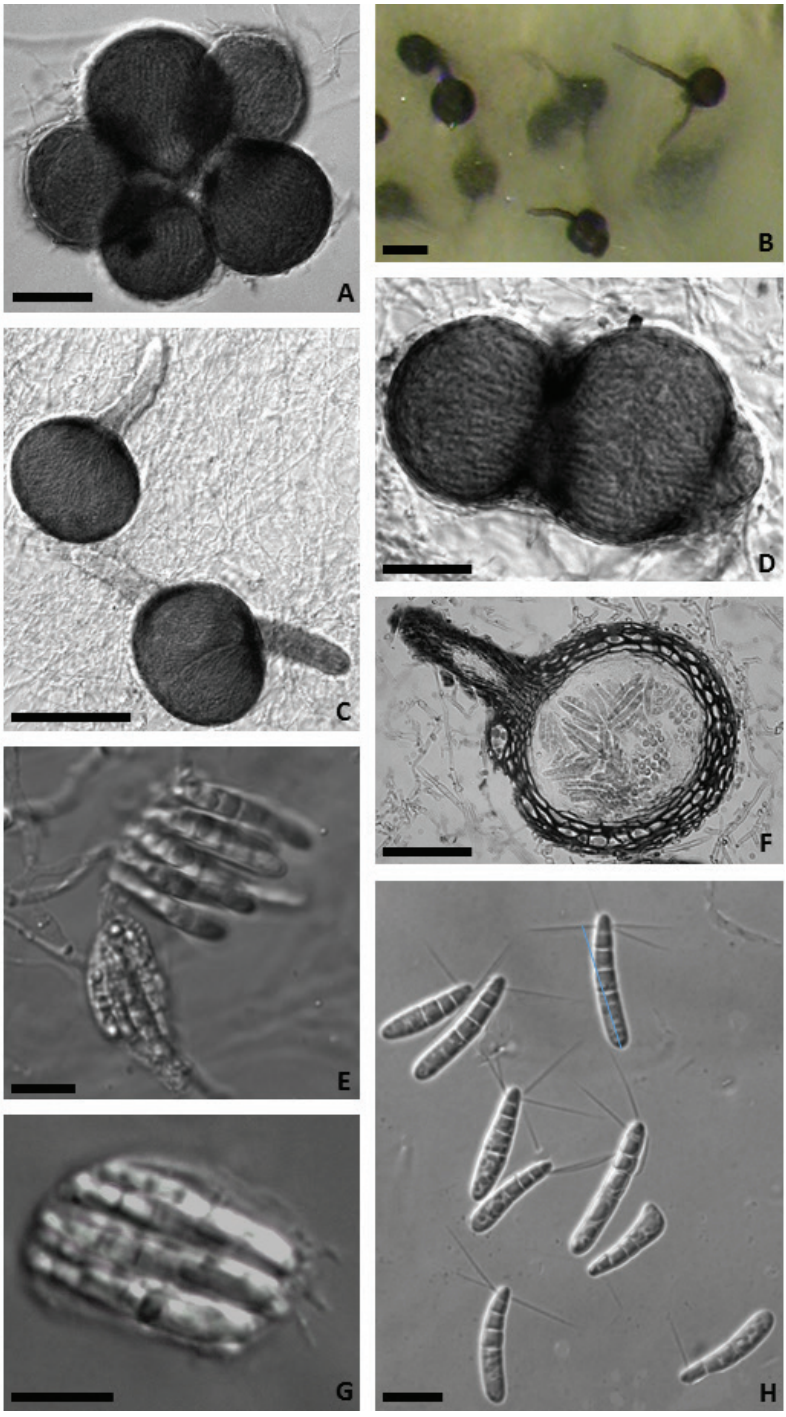

Figure 2. *Elbamycella rosea* sp. nov. **A, D** group of young subglobose ascomata **B, C** globose ascomata with one or two necks **E** immature (bottom) and dehiscent (top) asci **F** ascoma in cross section **G** mature ascus with 8 ascospores **H** ascospores. Scale bars: 50 µm (**A, D, F**); 100 µm (**B, C**); 10 µm (**E, G, H**).

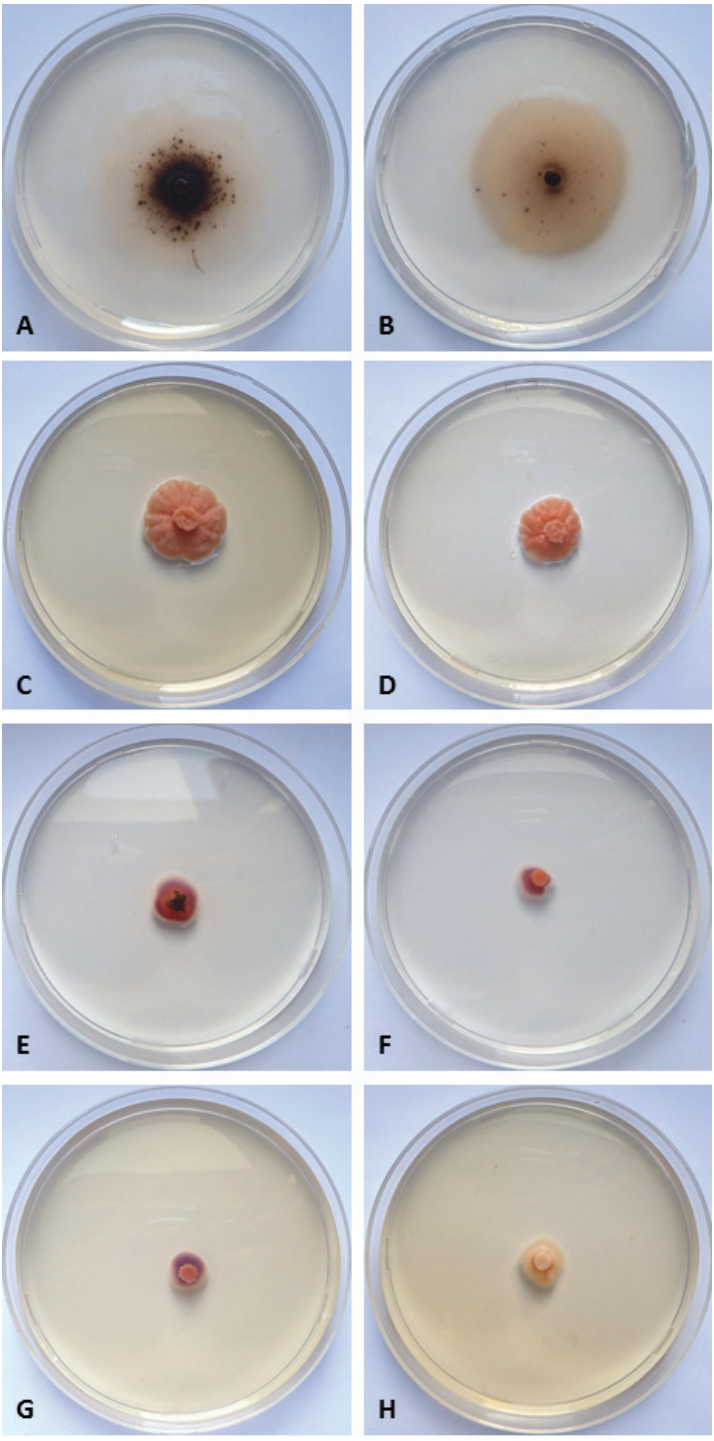

Figure 3. *Elbamycella rosea* sp. nov.: 28-days-old colonies at 21 °C on **A** CMASW **B** CMASS **C** PDASW **D** PDASS; 28-days-old colonies at 10 °C on **E** CMASW **F** CMASS **G** PDASW **H** PDASS.

Table 2. Comparison of the main sexual morpholgical features of genera belonging to Juncigenaceae.

Fungus	Ascomata	Periphyses/ Paraphyses	Asci	Ascospores	Reference
Marinokulati chaetosa	Immersed to superficial, dark brown, ostiolate, papillate; neck 20 × 70 µm	Both present, septate, wide	102–135 × 12–18 µm; cylindrical to clavate, attenuate at the base, thick-walled at the apex, containing 8 spores	25.5–36.5 × 7.5–11.5 µm; 3-septate, hyaline, fusiform to ellipsoidal with polar and equatorial appendages	Jones et al. 2014
Khaleijomyces marinus	Superficial to immersed, hyaline to yellow-orange to reddish brown, ostiolate; 110–175 × 100–115 µm; neck 120-175 × 40-50 µm	Periphyses present in the neck	60–98 × 12–16 µm; cymbiform to fusiform, thin-walled, with no apical apparatus, containing 8 spores	12–26 × 6-8 µm; 1-4-septate; ellipsoidal to fusiform; hyaline, smooth-walled	Abdel-Wahab et al. 2018
Juncigena adarca	Immersed, ostiolate, papillate, 225–400 × 135-200 µm; neck 85–170 × 50–85 µm	Both present; Paraphyses thin, branched, septate	115–140 × 10–13 µm; fusiform to cylindrical, short pedunculate, apical apparatus with a ring, containing 8 spores	26.5–34.5 × 6–7 µm; 3-septate, hyaline, fusiform to ellipsoidal, no appendages, smooth wall, constricted	Kohlmeyer et al. 1997
Fulvocentrum aegyptiacum	Immersed, dark brown, ostiolate; 240–280 × 170–190 µm; neck 70–80 µm diameter	Both present; Paraphyses numerous, in a gel, unbranched	145–155 × 9–10 µm; Short pedicellate, apically thickened, containing 8 spores	15–20 × 6–8 µm; 3-septate, ellipsoidal, hyaline	Abdel-Wahab et al. 2001
Fulvocentrum clavatisporum	Immersed, dark brown, ostiolate; 160–170 × 160–190 µm; neck 50 µm long	Both present; Paraphyses numerous, in a gel, unbranched	80–96 × 10–13µm; Pedicellate, apically thickened, containing 8 spores	25–28 × 5–6 µm; 3-septate, clavate, hyaline	Abdel-Wahab et al. 2001
Fulvocentrum rubrum	Erumpent to superficial, olive-brown to dark brown, ostiolate; 145–270 µm; neck 310–390 × 50–55 µm	Both present	Fusiform or obclavate, 95–130 × 13–19 µm; persistent, thin-walled, containing 8 spores	Ellipsoidal to clavate, no appendages, 25–33 × 6–9 µm; hyaline to faint apricot, smooth walled, 3–5-septate	Abdel-Wahab et al. 2019
Elbamycella rosea sp. nov.	Superficial, erumpent or immersed; 100–140 µm diam; olivaceous-brown to black; ostiolar neck 55–70 × 20–50 µm		Cylindrical to clavate 22–26 × 12–16 µm containing 8 spores	Cylindrical 23–28 × 4–5 µm; hyaline, generally 3-septate, bearing 3(4) subpolar appendages 10–20 × 0.5–1 µm	This study

in metabolically inactively state by deep-freezing at *Mycotheca Universitatis Taurinensis*. A dried specimen of this culture grown on CMASS and CMASW has been deposited in the herbarium of the Department of Life Sciences and Systems Biology (TO Cryptogamia 3446).

Additional material examined. Italy, Tuscany, Mediterranean Sea, Elba island (LI), Ghiaie ISL, 14–15m depth, 42°49'04"N, 10°19'20"E, on the seagrass *Posidonia oceanica*, 20 March 2010, R. Mussat-Sartor and N. Nurra, MUT 4937 = CBS 130520.

Etymology. In reference to the colour of the colony on the culture media.

Description. Ascomata were produced on both CMASS and CMASW at 21 °C only, after 28 days of incubation. Mycelium hyaline to pale brown consisting of smooth-walled hyphae 2.5–4 µm wide (Fig. 2A–D, F).

Ascomata perithecial, scattered or gregarious (from 2 to 6-8), superficial, erumpent or immersed, olivaceous-brown to black at maturity, globose, subglobose, ovoid or pyriform, glabrous, up to 100–140 µm diameter; ostiolar neck, pale-coloured, single (sometimes 2, rarely 3), 55–70 µm long and 20–50 µm wide at the base; peridium 5–10 µm thick of textura prismatica in the outer layers and textura globulosa in the

inner layers with cells with olivaceous-brown walls, in the neck consisting of hyaline, more elongated cells, from which numerous hyaline blunt hyphal projections 5–15 × 3–5 µm arise. Asci evanescent, hyaline, cylindrical to clavate 22–26 × 12–16 µm containing 8 spores; sterile elements not observed (Fig. 2E, G).

Ascopores cylindrical 23–28 × 4–5 µm, rounded at both ends, thin-walled, hyaline, straight or slightly curved, 3-septate, with a large basal cell 10–15 µm long and 3 shorter, upper cells, slightly constricted around the septa, the apical cell somewhat attenuated just below the blunt tip, bearing 3(4) subpolar, straight or slightly bent, acuminate, hyaline, smooth-walled cellular appendages 10–20 µm long (about 0.5–1 µm wide). In some spores the apical cell is divided by an additional septum; each cell of the spore contains a few oil-droplets 1.5–3.0 µm diameter (Fig. 2H).

Asexual morph not observed.

Colony description. Colonies reaching 21–23 mm diameter on CMASW and 19–29 mm diameter on CMASS in 28 days at 21 °C, plane, thin, mycelium mainly submerged. Colonies pale pink in the centre becoming brown with age, colourless at the margins. Black spots due to ascomata groups in fruiting colonies. Reverse of the same colour of the surface (Fig. 3A, B).

Colonies on PDASW and PDASS reaching 10–14 mm diameter in 28 days at 21 °C, convolute, developing in height with irregular margins, salmon. Reverse of the same colour of the surface (Fig. 3C, D).

At 10 °C colony growth on all media very poor, attaining 5–8 mm diameter in 28 days. Colonies plane to slightly convolute with regular margins, pale pink to cyclamen. Reverse of the same colour of the surface (Fig. 3E–H).

Discussion

The novel genus *Elbamycella* is introduced in this study and has been compared to the closest genera. Herein, the two strains MUT 4937 and MUT 5443 represented a new species that formed a well-supported cluster phylogenetically distant from the related genera of Juncigenaceae.

From a morphological point of view, the relatedness with the other species belonging to Juncigenaceae is confirmed by i) 3-septate spores (1–4 only in *K. marinus*), ii) 8-spored asci, and iii) ascomata with an elongated neck (Kohlmeyer et al. 1997; Abdel-Wahab et al. 2001; Abdel-Wahab et al. 2010; Jones et al. 2014; Abdel-Wahab et al. 2018). *Elbamycella rosea* sp. nov. is furthermore characterised by the presence of polar appendages on the ascospores. *Marinokulati chaetosa* displays this feature too, although it can be distinguished from *E. rosea* sp. nov. by additional, equatorially placed appendages. Additonally, in the new species, spores are cylindrical, not fusiform-ellipsoidal as in *M. chaetosa* (Jones et al. 2014). *Khaleijomyces marinus*, *Juncigena adarca*, *Fulvocentrum aegyptiacum*, *F. clavatisporum*, and the recently described *F. rubrum* differ in the shape and dimensions of the ascospores (Jones et al. 2014; Abdel-Wahab et al. 2018; Abdel-Wahab et al. 2019); generally asci and ascomata are larger than those observed in *E. rosea* sp. nov.

As no sexual form is known for *J. fruticosae*, the comparison with *E. rosea* sp. nov. is not possible. However, the similarity or identity to this species is excluded by the phylogenetical distance.

Ecologically, the described Juncigenaceae are species having a marine origin. So far, they have all been retrieved from driftwood in the intertidal of salt marshes (Kohlmeyer et al. 1997; Jones et al. 2014). The new species was found for the first time underwater, in association with the seagrass *P. oceanica* and the brown alga *P. pavonica*, two different organisms that were sampled in close proximity. This could be related to a successful spore dispersal; indeed polar appendages are known to facilitate floatation and attachment (Overy et al. 2019).

Acknowledgements

This work was funded by Fondazione CRT, Turin, Italy. The authors are grateful to Pelagosphera s.c.r.l. for harvesting algal and seagrasses samples.

References

Abdel-Wahab MA, El-Sharouney H, Jones EBG (2001) Two new intertidal lignicolous Swampomyces species from Red Sea mangroves in Egypt. Fungal Diversity 8: 35–40.

Abdel-Wahab MA, Pang KL, Nagahama T, Abdel-Aziz FA, Jones EBG (2010) Phylogenetic evaluation of anamorphic species of *Cirrenalia* and *Cumulospora* with the description of eight new genera and four new species. Mycological Progress 9: 537–558. https://doi.org/10.1007/s11557-010-0661-x

Abdel-Wahab MA, El-Samawaty AMA, El Gorban AM, Yassin MA, Alsaadi MH (2018) *Kaleijomyces marinus* gen. et sp nov. (Juncigenaceae, Torpedosporales) a new lignicolous marine fungus from Saudi Arabia. Phytotaxa 340: 277–285. https://doi.org/10.11646/phytotaxa.340.3.8

Abdel-Wahab MA, Jones EBG, Bahkali AHA, El-Gorban AM (2019) Marine fungi from Red Sea mangroves in Saudi Arabia with *Fulvocentrum rubrum* sp. nov. (Torpedosporales, Ascomycota). Nova Hedwigia 108: 365–377. https://doi.org/10.1127/nova_hedwigia/2018/0511

Bovio E, Garzoli L, Poli A, Prigione V, Firsova D, McCormack G, Varese G (2018) The culturable mycobiota associated with three Atlantic sponges, including two new species: *Thelebolus balaustiformis* and *T. spongiae*. Fungal Systematics and Evolution 1: 141–167. https://doi.org/10.3114/fuse.2018.01.07

Darriba D, Taboada GL, Doallo R, Posada D (2012) jModelTest 2: more models, new heuristics and parallel computing. Nature Methods 9: 772–772. hhttps://doi.org/10.1038/nmeth.2109

de Vienne DM, Giraud T, Martin OC (2007) A congruence index for testing topological similarity between trees. Bioinformatics 23: 3119–3124. https://doi.org/10.1093/bioinformatics/btm500

Garzoli L, Poli A, Prigione V, Gnavi G, Varese GC (2018) Peacock's tail with a fungal cocktail: first assessment of the mycobiota associated with the brown alga *Padina pavonica*. Fungal Ecology 35: 87–97. https://doi.org/10.1016/j.funeco.2018.05.005

Jones EG, Pang K-L (2012) Marine fungi and fungal-like organisms. Walter de Gruyter. https://doi.org/10.1515/9783110264067

Jones EBG, Suetrong S, Cheng WH, Rungjindamai N, Sakayaroj J, Boonyuen N, Somrothipol S, Abdel-Wahab MA, Pang KL (2014) An additional fungal lineage in the Hypocreomycetidae (Falcocladium species) and the taxonomic re-evaluation of *Chaetosphaeria chaetosa* and *Swampomyces* species, based on morphology, ecology and phylogeny. Cryptogamie Mycologie 35: 119–138. https://doi.org/10.7872/crym.v35.iss2.2014.119

Kohlmeyer J, Volkmann-Kohlmeyer B, Eriksson OE (1997) Fungi on *Juncus roemerianus* .9. New obligate and facultative marine ascomycotina. Botanica Marina 40: 291–300. https://doi.org/10.1515/botm.1997.40.1-6.291

Maharachchikumbura SSN, Hyde KD, Jones EBG, McKenzie EHC, Huang SK, Abdel-Wahab MA, Daranagama DA, Dayarathne M, D'Souza MJ, Goonasekara ID, Hongsanan S, Jayawardena RS, Kirk PM, Konta S, Liu JK, Liu ZY, Norphanphoun C, Pang KL, Perera RH, Senanayake IC, Shang QJ, Shenoy BD, Xiao YP, Bahkali AH, Kang JC, Somrothipol S, Suetrong S, Wen TC, Xu JC (2015) Towards a natural classification and backbone tree for Sordariomycetes. Fungal Diversity 72: 199–301. https://doi.org/10.1007/s13225-015-0331-z

Overy DP, Rama T, Oosterhuis R, Walker AK, Pang KL (2019) The neglected marine fungi, sensu stricto, and their isolation for natural products' discovery. Marine Drugs 17: 20. https://doi.org/10.3390/md17010042

Pang KL, Jones EBG (2017) Recent advances in marine mycology. Botanica Marina 60: 361–362. https://doi.org/10.1515/bot-2017-0048

Panno L, Bruno M, Voyron S, Anastasi A, Gnavi G, Miserere L, Varese GC (2013) Diversity, ecological role and potential biotechnological applications of marine fungi associated to the seagrass *Posidonia oceanica*. New Biotechnology 30: 685–694. https://doi.org/10.1016/j.nbt.2013.01.010

Raghukumar S (2017) Fungi in Coastal and Oceanic Marine Ecosystems: Marine Fungi. Springer, Cham, 1–36. https://doi.org/10.1007/978-3-319-54304-8_1

Richards TA, Jones MD, Leonard G, Bass D (2012) Marine fungi: their ecology and molecular diversity. Annual Review of Marine Science 4: 495–522. https://doi.org/10.1146/annurev-marine-120710-100802

Ronquist F, Teslenko M, van der Mark P, Ayres DL, Darling A, Hohna S, Larget B, Liu L, Suchard MA, Huelsenbeck JP (2012) MrBayes 3.2: efficient Bayesian phylogenetic inference and model choice across a large model space. Systematic Biology 61: 539–542. https://doi.org/10.1093/sysbio/sys029

Sakayaroj J, Pang KL, Jones EBG, Phongpaichit S, Vrijmoed LLP, Abdel-Wahab MA (2005) A systematic reassessment of the marine ascomycetes Torpedospora and Swampomyces. Botanica Marina 48: 395–406. https://doi.org/10.1515/bot.2005.053

Schoch CL, Sung GH, Volkmann-Kohlmeyer B, Kohlmeyer J, Spatafora JW (2007) Marine fungal lineages in the Hypocreomycetidae. Mycological Research 111: 154–162. https://doi.org/10.1016/j.mycres.2006.10.005

Stamatakis A (2014) RAxML version 8: a tool for phylogenetic analysis and post-analysis of large phylogenies. Bioinformatics 30: 1312–1313. https://doi.org/10.1093/bioinformatics/btu033

Vaidya G, Lohman DJ, Meier R (2011) SequenceMatrix: concatenation software for the fast assembly of multi-gene datasets with character set and codon information. Cladistics 27: 171–180. https://doi.org/10.1111/j.1096-0031.2010.00329.x

Vilgalys R, Hester M (1990) Rapid genetic identification and mapping of enzymatically amplified ribosomal DNA from several *Cryptococcus* species. Journal of Bacteriology 172: 4238–4246. https://doi.org/10.1128/jb.172.8.4238-4246.1990

White TJ, Bruns T, Lee S, Taylor J (1990) Amplification and direct sequencing of fungal ribosomal RNA genes for phylogenetics. PCR Protocols: a Guide to Methods and Applications 18: 315–322. https://doi.org/10.1016/B978-0-12-372180-8.50042-1

MycoKeys 55: 29–57 (2019)
doi: 10.3897/mycokeys.55.34570
http://mycokeys.pensoft.net

RESEARCH ARTICLE

A peer-reviewed open-access journal
MycoKeys
Launched to accelerate biodiversity research

Two new *Erythrophylloporus* species (Boletaceae) from Thailand, with two new combinations of American species

Santhiti Vadthanarat[1,2,8], Mario Amalfi[4], Roy E. Halling[5], Victor Bandala[6], Saisamorn Lumyong[1,8,9], Olivier Raspé[4,7]

1 *Department of Biology, Faculty of Science, Chiang Mai University, Chiang Mai, 50200, Thailand* **2** *PhD's Degree Program in Biodiversity and Ethnobiology, Department of Biology, Faculty of Science, Chiang Mai University, Chiang Mai, 50200, Thailand* **3** *Academy of Science, The Royal Society of Thailand, Bangkok 10300, Thailand* **4** *Botanic Garden Meise, Nieuwelaan 38, 1860 Meise, Belgium* **5** *New York Botanical Garden, 2900 Southern Blvd, Bronx, New York 10458, USA* **6** *Red Biodiversidad y Sistemática, Instituto de Ecología A.C., P.O. Box 63, Xalapa, Veracruz, 91000, México* **7** *Fédération Wallonie–Bruxelles, Service général de l'Enseignement universitaire et de la Recherche scientifique, Rue A. Lavallée 1, 1080 Bruxelles, Belgium* **8** *Center of Excellence in Microbial Diversity and Sustainable Utilization, Faculty of Science, Chiang Mai University, Chiang Mai, 50200, Thailand* **9** *Academy of Science, The Royal Society of Thailand, Bangkok, 10300, Thailand*

Corresponding author: *Olivier Raspé* (olivier.raspe@botanicgardenmeise.be)

Academic editor: *Alfredo Vizzini* | Received 15 March 2019 | Accepted 24 May 2019 | Published 21 June 2019

Citation: Vadthanarat S, Amalfi M, Halling RE, Bandala V, Lumyong S, Raspé O (2019) Two new *Erythrophylloporus* species (Boletaceae) from Thailand, with two new combinations of American species. MycoKeys 55: 29–57. https://doi.org/10.3897/mycokeys.55.34570

Abstract

Erythrophylloporus is a lamellate genus in the family Boletaceae that has been recently described from China based on *E. cinnabarinus*, the only known species. Typical characters of *Erythrophylloporus* are reddish-orange to yellowish-red basidiomata, including lamellae, bright yellow basal mycelium and smooth, broadly ellipsoid, ellipsoid to nearly ovoid basidiospores. During our survey on diversity of Boletaceae in Thailand, several yellowish-orange to reddish- or brownish-orange lamellate boletes were collected. Based on both morphological evidence and molecular analyses of a four-gene dataset (*atp*6, *tef*1, *rpb*2 and *cox*3), they were recognised as belonging in *Erythrophylloporus* and different from the already known species. Two new species, *E. paucicarpus* and *E. suthepensis* are therefore introduced from Thailand with detailed descriptions and illustrations. Moreover, two previously described *Phylloporus* species, *P. aurantiacus* and *P. fagicola*, were also revised and recombined in *Erythrophylloporus*. A key to all known *Erythrophylloporus* species is provided.

Keywords
atp6, *cox3*, Taxonomy, *Phylloporus*, *Pulveroboletus* group, multigene phylogeny, Boletales, Southeast Asia

Introduction

Most fungi in the family Boletaceae are pileate-stipitate with poroid hymenophore, but some have a lamellate hymenophore. Lamellate Boletaceae are currently classified in four genera, *Phylloporus* Quél, which contains about 84 species worldwide, *Phylloboletellus* Singer from South America and Mexico, the two recently described genera *Phylloporopsis* Angelini et al., from the New World and *Erythrophylloporus* Ming Zhang & T.H. Li from Asia, each of which circumscribes only one species (http://www.indexfungorum.org, Farid et al. 2018; Zhang and Li 2018).

The genus *Erythrophylloporus* was recently described from China, with *E. cinnabarinus* Ming Zhang & T.H. Li as the type species. According to Zhang & Li (2018), the typical characters of the genus are orange to reddish-orange basidiomes, reddish-orange to yellowish-red lamellae turning greyish-green when bruised, bright yellow to orange yellow context staining blackish-blue to dark blue when exposed, bright yellow basal mycelium, smooth and broadly ellipsoid to nearly ovoid basidiospores and yellowish-brown pigmented cystidia. During our survey on the diversity of Boletaceae in Thailand, several collections of lamellate boletes were discovered. Some collections were recognised to belong to *Erythrophylloporus* by possessing yellowish-orange to deep orange to reddish-orange basidiomata with bright yellow basal mycelium and smooth basidiospores. We also found that two described *Phylloporus* species, *P. aurantiacus* Halling & G.M. Mueller from Costa Rica and *P. fagicola* Montoya & Bandala from Mexico (Halling et al. 1999, Montoya and Bandala 2011), share similar morphological characters with the genus *Erythrophylloporus*, but until now, have not been included in a molecular phylogeny. In this study, a combination of phylogenetic and morphological evidence indicated that our Thai collections were new species, that, together with the two aforementioned American *Phylloporus* species, belong in *Erythrophylloporus*. Therefore, we introduce two new species with detailed descriptions and illustrations and propose two new combinations. As some of the species we studied have some characters that do not fit with the protologue of the genus, we emend its description.

Materials and methods

Specimen collecting

Specimens were obtained and photographed from community forests and Doi Suthep-Pui National Park, Chiang Mai Province, northern Thailand during the rainy season in 2015 to 2016. The specimens were wrapped in aluminium foil and taken to the laboratory. After description of macroscopic characters, all specimens were dried in an electric drier at 45–50 °C. Examined specimens were deposited in the herbaria CMUB, MFLU, BKF or BR (Index Herbariorum; Thiers, continuously updated).

Morphological studies

Macroscopic descriptions were made based on detailed field notes and photos of fresh basidiomata. Colour codes follow Kornerup and Wanscher (1978). Macrochemical reactions (colour reactions) of fresh basidiomata were determined using 10% potassium hydroxide (KOH) and 28–30% ammonium hydroxide (NH_4OH) in water. Microscopic structures were observed from dried specimens mounted in 5% KOH, NH_4OH, Melzer's reagent or 1% ammoniacal Congo red. A minimum of 50 basidiospores, 20 basidia and 20 cystidia were randomly measured at 1000× with a calibrated ocular micrometer using an Olympus CX51 microscope. The notation '[*m*/*n*/*p*]' represents the number of basidiospores *m* measured from *n* basidiomata of *p* collections. Dimensions of microscopic structures are presented in the following format: (*a*–)*b*–*c*–*d*(–*e*), in which *c* represents the average, *b* the 5th percentile, *d* the 95th percentile and *a* and *e* the minimum and maximum values, respectively. *Q*, the length/width ratio, is presented in the same format. A section of the pileus surface was radially and perpendicularly cut at a point halfway between the centre and margin of the pileus. Sections of stipitipellis were taken from halfway up the stipe and longitudinally cut, perpendicularly to the surface. All microscopic features were drawn by free hand using an Olympus Camera Lucida model U–DA, fitted to the microscope cited above. For scanning electron microscopy (SEM), a spore print was mounted on to a SEM stub with double-sided tape. The sample was coated with gold, examined and photographed with a JEOL JSM–5910 LV SEM (JEOL, Japan).

DNA isolation, PCR amplification and DNA sequencing

Genomic DNA was extracted from fresh tissue preserved in CTAB or about 10–15 mg of dried specimens using a CTAB isolation procedure adapted from Doyle and Doyle (1990). Portions of the genes *atp*6, *tef*1, *rpb*2 and *cox*3 were amplified by the polymerase chain reaction (PCR) technique. The tailed primers ATP6-1M40F and ATP6-2M (Raspé et al. 2016) and the primer pairs EF1-983F/EF1-2218R (Rehner and Buckley 2005) and bRPB2-6F/bRPB2-7.1R (Matheny 2005) were used to amplify *atp*6, *tef*1 and *rpb*2, respectively. PCR conditions were the same as in Raspé et al. (2016). Part of the mitochondrial gene *cox*3 was amplified with the primers COX3M1-F and COX3M1-R (Vadthanarat et al. 2019), using KAPA2G™ Robust HotStart polymerase (Kapa Biosystems, Wilmington, MA, USA) and the following PCR programme: 2 min 30 s at 95 °C; 35 cycles of 25 s at 95 °C, 30 s at 48 °C, 30 s at 72 °C; 3 min at 72 °C. PCR products were purified by adding 1 U of Exonuclease I and 0.5 U FastAP Alkaline Phosphatase (Thermo Scientific, St. Leon-Rot, Germany) and incubated at 37 °C for 1 h, followed by inactivation at 80 °C for 15 min. Sequencing was performed by Macrogen Inc. (Korea and The Netherlands) with PCR primers, except for *atp*6, for which universal primers M13F-pUC(-40) and M13F(-20) were used; for *tef*1, additional sequencing was performed with two internal primers, EF1-1577F and EF1-1567R (Rehner and Buckley 2005).

Alignment and phylogeny inference

The sequences were assembled in GENEIOUS Pro v. 6.0.6 (Biomatters) and introns were removed prior to alignment, based on the amino acid sequence of previously published sequences. All sequences, including sequences from GenBank, were aligned using MAFFT version 7 (Katoh and Standley 2013) on the server accessed at http://mafft.cbrE.jp/alignment/server/.

Maximum Likelihood (ML) phylogenetic tree inference was performed using RAxML-HPC2 version 8.2.10 (Stamatakis 2006) on the CIPRES web portal (Miller et al. 2009). The phylogenetic tree was inferred from a four-partitions combined dataset, using the GTRCAT model with 25 categories. Two *Buchwaldoboletus* and nine *Chalciporus* species from subfamily Chalciporoideae were used as the outgroup. Statistical support of clades was obtained with 1,000 rapid bootstrap replicates.

For Bayesian Inference (BI), the best-fit model of substitution amongst those implementable in MrBayes was estimated separately for each gene using jModeltest (Darriba et al. 2012) on the CIPRES portal, based on the Bayesian Information Criterion (BIC). The selected models were GTR+I+G for *atp*6 and *cox*3, SYM+I+G for *tef*1 and K80+I+G for *rpb*2. Partitioned Bayesian analysis was performed with MrBayes 3.2 (Ronquist et al. 2012) on the CIPRES portal. Two runs of five chains were run for 15,000,000 generations and sampled every 1,000 generations. The chain temperature was decreased to 0.02 to improve convergence. At the end of the run, the average deviation of split frequencies was 0.007058 and the Potential Scale Reduction Factor (PSRF) values of all parameters were close to 1. The burn-in phase (25%) was estimated by checking the stationarity in the plot generated by the sump command.

Results

Phylogenetic analysis

Twenty-five sequences were newly generated and deposited in GenBank (Table 1). The sequences from three specimens, OR0689, OR1135 (*E. paucicarpus*) and OR0615B (*E. suthepensis*), were not included in our phylogenic analyses because they were identical to the sequences of the type specimens of *E. paucicarpus* and *E. suthepensis*. The alignment contained 906 sequences (179 for *atp*6, 313 for *tef*1, 279 for *rpb*2, 135 for *cox*3) from 315 voucher specimens and was 2946 characters long (TreeBase number 24078). ML and BI trees showed similar topologies without any supported conflict (Bootstrap Support values, BS ≥ 70% and posterior probabilities, PP ≥ 0.90; Fig. 1). The four-gene phylogram indicated that the included taxa formed seven major clades, representing the Austroboletoideae, Boletoideae, Chalciporoideae, Leccinoideae, Xerocomoideae, Zangioideae and the *Pulveroboletus* group. *Erythrophylloporus cinnabarinus* (typus generis) grouped with the two new *Erythrophylloporus* species, *E. paucicarpus* and *E. suthepensis*, in a highly supported clade (BS = 100% and PP = 1). The two New World *Phylloporus* species (*P. aurantiacus* voucher REH7271 and *P. fagicola* voucher Garay215)

Table 1. List of collections used in this study, with origin and GenBank accession numbers. Newly generated sequences are presented in bold.

Species	Voucher	Origin	*atp6*	*tef1*	*rpb2*	*cox3*	References
Afroboletus aff. *multijugus*	JD671	Burundi	MH614651	MH614700	MH614747	MH614794	Vadthanarat et al. 2019
Afroboletus costatisporus	ADK4644	Togo	KT823958	KT824024	KT823991	MH614795*	Raspé et al. 2016; *Vadthanarat et al. 2019
Afroboletus luteolus	ADK4844	Togo	MH614652	MH614701	MH614748	MH614796	Vadthanarat et al. 2019
Aureoboletus catenarius	HKAS54467	China	–	KT990711	KT990349	–	Wu et al. 2016
Aureoboletus duplicatoporus	HKAS50498	China	–	KF112230	KF112754	–	Wu et al. 2014
Aureoboletus gentilis	ADK4865	Belgium	KT823961	KT824027	KT823994	MH614797*	Raspé et al. 2016; *Vadthanarat et al. 2019
Aureoboletus mirabilis	HKAS57776	China	–	KF112229	KF112743	–	Wu et al. 2014
Aureoboletus moravicus	VDKO1120	Belgium	MG212528	MG212573	MG212615	MH614798*	Vadthanarat et al. 2018; *Vadthanarat et al. 2019
Aureoboletus nephrosporus	HKAS67931	China	–	KT990720	KT990357	–	Wu et al. 2016
Aureoboletus projectellus	AFTOL-ID-713	USA	DQ534604*	AY879116	AY787218	–	*Binder & Hibbett 2006; Binder, Matheny & Hibbett, Unpublished
Aureoboletus shichianus	HKAS76852	China	–	KF112237	KF112756	–	Wu et al. 2014
Aureoboletus sp.	HKAS56317	China	–	KF112239	KF112753	–	Wu et al. 2014
Aureoboletus sp.	OR0245	China	MH614653	MH614702	MH614749	MH614799	Vadthanarat et al. 2019
Aureoboletus sp.	OR0369	Thailand	MH614654	MH614703	MH614750	MH614800	Vadthanarat et al. 2019
Aureoboletus thibetanus	HKAS76655	China	–	KF112236	KF112752	–	Wu et al. 2014
Aureoboletus thibetanus	AFTOL-ID-450	China	DQ534600*	DQ029199	DQ366279	–	*Binder and Hibbett 2006; Unpublished
Aureoboletus tomentosus	HKAS80485	China	–	KT990715	KT990353	–	Wu et al. 2016
Aureoboletus viscosus	OR0361	Thailand	MH614655	MH614704	MH614751	MH614801	Vadthanarat et al. 2019
Aureoboletus zangii	HKAS74766	China	–	KT990726	KT990363	–	Wu et al. 2016
Austroboletus cf. *dictyotus*	OR0045	Thailand	KT823966	KT824032	KT823999	MH614802*	Raspé et al. 2016; *Vadthanarat et al. 2019
Austroboletus cf. *subvirens*	OR0573	Thailand	MH614656	MH614705	MH614752	MH614803	*Vadthanarat et al. 2019
Austroboletus eburneus	REH9487	Australia	–	JX889708	–	–	Halling et al. 2012b
Austroboletus olivaceoglutinosus	HKAS57756	China	–	KF112212	KF112764	–	Wu et al. 2014
Austroboletus sp.	HKAS59624	China	–	KF112217	KF112765	–	Wu et al. 2014
Austroboletus sp.	OR0891	Thailand	MH614657	MH614706	MH614753	MH614804	Vadthanarat et al. 2019
Baorangia pseudocalopus	HKAS63607	China	–	KF112167	KF112677	–	Wu et al. 2014
Baorangia pseudocalopus	HKAS75739	China	–	KJ184570	KM605179	–	Wu et al. 2015
Baorangia pseudocalopus	HKAS75081	China	–	KF112168	KF112678	–	Wu et al. 2014
Baorangia rufomaculata	BOTH4144	USA	MG897415	MG897425	MG897435	MH614805*	Phookamsak et al. 2019; *Vadthanarat et al. 2019
Baorangia major	OR0209	Thailand	MG897421	MG897431	MG897441	MK372295*	Phookamsak et al. 2019; *Vadthanarat et al. 2019
Boletellus aff. *ananas*	NY815459	Costa Rica	–	KF112308	KF112760	–	Wu et al. 2014
Boletellus aff. *emodensis*	OR0061	Thailand	KT823970	KT824036	KT824003	MH614806*	Raspé et al. 2016; *Vadthanarat et al. 2019
Boletellus ananas	K(M)123769	Belize	MH614658	MH614707	MH614754	MH614807	Vadthanarat et al. 2019

Species	Voucher	Origin	*atp6*	*tef1*	*rpb2*	*cox3*	References
Boletellus sp.	OR0621	Thailand	MG212529	MG212574	MG212616	MH614808*	Vadthanarat et al. 2018; *Vadthanarat et al. 2019
Boletellus sp.	HKAS58713	China	–	KF112307	KF112759	–	Wu et al. 2014
Boletellus sp.	HKAS59536	China	–	KF112306	KF112758	–	Wu et al. 2014
Boletus aereus	VDKO1055	Belgium	MG212530	MG212575	MG212617	MH614809*	Vadthanarat et al. 2018; *Vadthanarat et al. 2019
Boletus albobrunnescens	OR0131	Thailand	KT823973	KT824039	KT824006	MH614810*	Raspé et al. 2016; *Vadthanarat et al. 2019
Boletus botryoides	HKAS53403	China	–	KT990738	KT990375	–	Wu et al. 2016
Boletus edulis	HMJAU4637	Russia	–	KF112202	KF112704	–	Wu et al. 2014
Boletus edulis	VDKO0869	Belgium	MG212531	MG212576	MG212618	MH614811*	Vadthanarat et al. 2018; *Vadthanarat et al. 2019
Boletus p.p. sp	JD0693	Burundi	MH645583	MH645591	MH645599	–	Vadthanarat et al. 2019
Boletus p.p. sp.	OR0832	Thailand	MH645584	MH645592	MH645600	MH645605	Vadthanarat et al. 2019
Boletus p.p. sp.	OR1002	Thailand	MH645585	MH645593	MH645601	MH645606	Vadthanarat et al. 2019
Boletus pallidus	BOTH4356	USA	MH614659	MH614708	–	MH614812	Vadthanarat et al. 2019
Boletus pallidus	TDB-1231-Bruns	–	AF002142	–	–	AF002154	Kretzer and Bruns 1999
Boletus reticuloceps	HKAS57671	China	–	KF112201	KF112703	–	Wu et al. 2014
Boletus s.s. sp.	OR0446	China	MG212532	MG212577	MG212619	MH614813*	Vadthanarat et al. 2018; *Vadthanarat et al. 2019
Boletus sp.	HKAS59660	China	–	KF112153	KF112664	–	Wu et al. 2014
Boletus sp.	HKAS63598	China	–	KF112152	KF112663	–	Wu et al. 2014
Boletus violaceofuscus	HKAS62900	China	–	KF112219	KF112762	–	Wu et al. 2014
Borofutus dhakanus	HKAS73789	Bangladesh	–	JQ928576	JQ928597	–	Hosen et al. 2013
Borofutus dhakanus	OR0345	Thailand	MH614660	MH614709	MH614755	MH614814	Vadthanarat et al. 2019
Buchwaldoboletus lignicola	HKAS76674	China	–	KF112277	KF112819	–	Wu et al. 2014
Buchwaldoboletus lignicola	VDKO1140	Belgium	MH614661	MH614710	MH614756	MH614815	Vadthanarat et al. 2019
Butyriboletus appendiculatus	VDKO0193b	Belgium	MG212537	MG212582	MG212624	MH614816*	Vadthanarat et al. 2018; *Vadthanarat et al. 2019
Butyriboletus cf. *roseoflavus*	OR0230	China	KT823974	KT824040	KT824007	MH614819*	Raspé et al. 2016; *Vadthanarat et al. 2019
Butyriboletus frostii	NY815462	USA	–	KF112164	KF112675	–	Wu et al. 2014
Butyriboletus pseudoregius	VDKO0925	Belgium	MG212538	MG212583	MG212625	MH614817*	Vadthanarat et al. 2018; *Vadthanarat et al. 2019
Butyriboletus pseudospeciosus	HKAS63513	China	–	KT990743	KT990380	–	Wu et al. 2016
Butyriboletus roseoflavus	HKAS54099	China	–	KF739779	KF739703	–	Wu et al. 2014
Butyriboletus roseopurpureus	BOTH4497	USA	MG897418	MG897428	MG897438	MH614818*	Phookamsak et al. 2019; *Vadthanarat et al. 2019
Butyriboletus sp.	HKAS52525	China	–	KF112163	KF112671	–	Wu et al. 2014
Butyriboletus sp.	HKAS59814	China	–	KF112199	KF112699	–	Wu et al. 2014
Butyriboletus sp.	HKAS57774	China	–	KF112155	KF112670	–	Wu et al. 2014
Butyriboletus subsplendidus	HKAS50444	China	–	KT990742	KT990379	–	Wu et al. 2016
Butyriboletus yicibus	HKAS55413	China	–	KF112157	KF112674	–	Wu et al. 2014
Caloboletus calopus	ADK4087	Belgium	MG212539	KJ184566	KP055030	MH614820	Vadthanarat et al. 2018; Zhao et al. 2014a; Zhao et al. 2014b; Vadthanarat et al. 2019
Caloboletus inedulis	BOTH3963	USA	MG897414	MG897424	MG897434	MH614821*	Phookamsak et al. 2019; *Vadthanarat et al. 2019
Caloboletus panniformis	HKAS55444	China	–	KF112165	KF112666	–	Wu et al. 2014
Caloboletus radicans	VDKO1187	Belgium	MG212540	MG212584	MG212626	MH614822*	Vadthanarat et al. 2018; *Vadthanarat et al. 2019
Caloboletus sp.	HKAS53353	China	–	KF112188	KF112668	–	Wu et al. 2014

Species	Voucher	Origin	*atp6*	*tef1*	*rpb2*	*cox3*	References
Caloboletus sp.	OR0068	Thailand	MH614662	MH614711	MH614757	MH614823	Vadthanarat et al. 2019
Caloboletus yunnanensis	HKAS69214	China	–	KJ184568	KT990396	–	Zhao et al. 2014a; Wu et al. 2016
Chalciporus aff. *piperatus*	OR0586	Thailand	KT823976	KT824042	KT824009	MH614824*	Raspé et al. 2016; *Vadthanarat et al. 2019
Chalciporus aff. *rubinus*	OR0139	China	MH614663	MH614712	MH614758	–	Vadthanarat et al. 2019
Chalciporus africanus	JD517	Cameroon	KT823963	KT824029	KT823996	MH614825*	Raspé et al. 2016; *Vadthanarat et al. 2019
Chalciporus piperatus	VDKO1063	Belgium	MH614664	MH614713	MH614759	MH614826	Vadthanarat et al. 2019
Chalciporus rubinus	AF2835	Belgium	KT823962	KT824028	KT823995	–	Raspé et al. 2016
Chalciporus sp.	HKAS53400	China	–	KF112279	KF112821	–	Wu et al. 2014
Chalciporus sp.	HKAS74779	China	–	KF112278	KF112820	–	Wu et al. 2014
Chalciporus sp.	OR0363	Thailand	MH645586	MH645594	MH645602	MH645607	Vadthanarat et al. 2019
Chalciporus sp.	OR0373	Thailand	MH645587	MH645595	MH645603	MH645608	Vadthanarat et al. 2019
Chiua sp.	OR0141	China	MH614665	MH614714	MH614760	MH614827	Vadthanarat et al. 2019
Chiua virens	HKAS76678	China	–	KF112272	KF112793	–	Wu et al. 2014
Chiua virens	OR0266	China	MG212541	MG212585	MG212627	MH614828*	Vadthanarat et al. 2018; *Vadthanarat et al. 2019
Chiua viridula	HKAS74928	China	–	KF112273	KF112794	–	Wu et al. 2014
Crocinoboletus cf. *laetissimus*	OR0576	Thailand	KT823975	KT824041	KT824008	MH614833*	Raspé et al. 2016; *Vadthanarat et al. 2019
Crocinoboletus rufoaureus	HKAS53424	China	–	KF112206	KF112710	–	Wu et al. 2014
Cyanoboletus brunneoruber	OR0233	China	MG212542	MG212586	MG212628	MH614834*	Vadthanarat et al. 2018; *Vadthanarat et al. 2019
Cyanoboletus instabilis	HKAS59554	China	–	KF112186	KF112698	–	Wu et al. 2014
Cyanoboletus pulverulentus	RW109	Belgium	KT823980	KT824046	KT824013	MH614835*	Raspé et al. 2016; *Vadthanarat et al. 2019
Cyanoboletus sinopulverulentus	HKAS59609	China	–	KF112193	KF112700	–	Wu et al. 2014
Cyanoboletus sp.	OR0257	China	MG212543	MG212587	MG212629	MH614836*	Vadthanarat et al. 2018; *Vadthanarat et al. 2019
Cyanoboletus sp.	HKAS76850	China	–	KF112187	KF112697	–	Wu et al. 2014
Cyanoboletus sp.	OR0322	Thailand	MH614673	MH614722	MH614768	MH614837	Vadthanarat et al. 2019
Cyanoboletus sp.	OR0491	China	MH614674	MH614723	MH614769	MH614838	Vadthanarat et al. 2019
Cyanoboletus sp.	OR0961	Thailand	MH614675	MH614724	MH614770	MH614839	Vadthanarat et al. 2019
Erythrophylloporus aurantiacus	REH7271	Costa Rica	**MH614666**	**MH614715**	**MH614761**	**MH614829**	This study
Erythrophylloporus cinnabarinus	GDGM70536	China	–	MH378802	MH374035	–	Zhang and Li 2018
Erythrophylloporus fagicola	Garay215	Mexico	**MH614667**	**MH614716**	**MH614762**	**MH614830**	This study
Erythrophylloporus paucicarpus	OR1151	Thailand	**MH614670**	**MH614719**	**MH614765**	**MH614831**	This study
Erythrophylloporus paucicarpus	OR0689	Thailand	**MH614668**	**MH614717**	**MH614763**	–	This study
Erythrophylloporus paucicarpus	OR1135	Thailand	**MH614669**	**MH614718**	**MH614764**	–	This study
Erythrophylloporus suthepensis	SV0236	Thailand	**MH614672**	**MH614721**	**MH614767**	**MH614832**	This study
Erythrophylloporus suthepensis	OR0615B	Thailand	**MH614671**	**MH614720**	**MH614766**	–	This study
Fistulinella prunicolor	REH9880	Australia	MH614676	MH614725	MH614771	MH614840	Vadthanarat et al. 2019
Fistulinella prunicolor	REH9502	Australia	MG212544	MG212588	MG212630	–	Vadthanarat et al. 2018
Gymnogaster boletoides	NY01194009	Australia	–	KT990768	KT990406	–	Wu et al. 2016
Harrya atriceps	REH7403	Costa Rica	–	JX889702	–	–	Halling et al. 2012b

Species	Voucher	Origin	*atp6*	*tef1*	*rpb2*	*cox3*	References
Harrya chromapes	HKAS50527	China	–	KF112270	KF112792	–	Wu et al. 2014
Harrya chromapes	HKAS49416	China	HQ326840	HQ326863	–	–	Li et al. 2011
Harrya moniliformis	HKAS49627	China	–	KT990881	KT990500	–	Wu et al. 2016
Heimioporus cf. *mandarinus*	OR0661	Thailand	MG212545	MG212589	MG212631	MH614841*	Vadthanarat et al. 2018; *Vadthanarat et al. 2019
Heimioporus japonicus	OR0114	Thailand	KT823971	KT824037	KT824004	MH614842*	Raspé et al. 2016; *Vadthanarat et al. 2019
Heimioporus retisporus	HKAS52237	China	–	KF112228	KF112806	–	Wu et al. 2014
Heimioporus sp.	OR0218	Thailand	MG212546	MG212590	MG212632	–	Vadthanarat et al. 2018
Hemileccinum depilatum	AF2845	Belgium	MG212547	MG212591	MG212633	MH614843*	Vadthanarat et al. 2018; *Vadthanarat et al. 2019
Hemileccinum impolitum	ADK4078	Belgium	MG212548	MG212592	MG212634	MH614844*	Vadthanarat et al. 2018; *Vadthanarat et al. 2019
Hemileccinum indecorum	OR0863	Thailand	MH614677	MH614726	MH614772	MH614845	Vadthanarat et al. 2019
Hemileccinum rugosum	HKAS84970	China	–	KT990773	KT990412	–	Wu et al. 2016
Hortiboletus amygdalinus	HKAS54166	China	–	KT990777	KT990416	–	Wu et al. 2016
Hortiboletus rubellus	VDKO0403	Belgium	MH614679	–	MH614774	MH614847	*Vadthanarat et al. 2019
Hortiboletus sp.	HKAS51239	China	–	KF112184	KF112695	–	Wu et al. 2014
Hortiboletus sp.	HKAS50466	China	–	KF112183	KF112694	–	Wu et al. 2014
Hortiboletus sp.	HKAS51292	China	–	KF112181	KF112692	–	Wu et al. 2014
Hortiboletus sp.	HKAS76673	China	–	KF112182	KF112693	–	Wu et al. 2014
Hortiboletus subpaludosus	HKAS59608	China	–	KF112185	KF112696	–	Wu et al. 2014
Hourangia cf. *pumila*	OR0762	Thailand	MH614680	MH614728	MH614775	MH614848	Vadthanarat et al. 2019
Hourangia cheoi	HKAS74744	China	–	KF112285	KF112772	–	Wu et al. 2014
Hourangia cheoi	Zhu108	China	–	KP136979	KP136928	–	Zhu et al. 2015
Hourangia nigropunctata	HKAS 57427	China	–	KP136927	KP136978	–	Zhu et al. 2015
Hymenoboletus luteopurpureus	HKAS46334	China	–	KF112271	KF112795	–	Wu et al. 2014
Imleria badia	VDKO0709	Belgium	KT823983	KT824049	KT824016	MH614849*	Raspé et al. 2016; *Vadthanarat et al. 2019
Imleria obscurebrunnea	OR0263	China	MH614681	MH614729	MH614776	MH614850	Vadthanarat et al. 2019
Imleria subalpina	HKAS74712	China	–	KF112189	KF112706	–	Wu et al. 2014
Lanmaoa angustispora	HKAS74759	China	–	KM605155	KM605178	–	Wu et al. 2015
Lanmaoa angustispora	HKAS74765	China	–	KF112159	KF112680	–	Wu et al. 2014
Lanmaoa asiatica	HKAS54094	China	–	KF112161	KF112682	–	Wu et al. 2014
Lanmaoa asiatica	HKAS63603	China	–	KM605153	KM605176	–	Wu et al. 2015
Lanmaoa asiatica	OR0228	China	MH614682	MH614730	MH614777	MH614851	Vadthanarat et al. 2019
Lanmaoa carminipes	BOTH4591	USA	MG897419	MG897429	MG897439	MH614852*	Phookamsak et al. 2019, *Vadthanarat et al. 2019
Lanmaoa flavorubra	NY775777	Costa Rica	–	KF112160	KF112681	–	Wu et al. 2014
Lanmaoa pallidorosea	BOTH4432	USA	MG897417	MG897427	MG897437	MH614853*	Phookamsak et al. 2019, *Vadthanarat et al. 2019
Lanmaoa sp.	HKAS52518	China	–	KF112162	KF112683	–	Wu et al. 2014
Lanmaoa sp.	OR0130	Thailand	MH614683	MH614731	MH614778	MH614854	Vadthanarat et al. 2019
Lanmaoa sp.	OR0370	Thailand	MH614684	MH614732	MH614779	MH614855	Vadthanarat et al. 2019
Leccinellum aff. *crocipodium*	HKAS76658	China	–	KF112252	KF112728	–	Wu et al. 2014
Leccinellum aff. *griseum*	KPM-NC-0017832	Japan	KC552164	JN378450*	–	–	unpublished, *Orihara et al. 2012
Leccinellum corsicum	Buf4507	USA	–	KF030435	–	–	Nuhn et al. 2013

Species	Voucher	Origin	*atp6*	*tef1*	*rpb2*	*cox3*	References
Leccinellum cremeum	HKAS90639	China	–	KT990781	KT990420	–	Wu et al. 2016
Leccinellum crocipodium	VDKO1006	Belgium	KT823988	KT824054	KT824021	MH614856*	Raspé et al. 2016; *Vadthanarat et al. 2019
Leccinellum sp.	KPM-NC-0018041	Japan	KC552165	KC552094	–	–	Orihara et al. 2016
Leccinellum sp.	OR0711	Thailand	MH614685	MH614733	MH614780	–	Vadthanarat et al. 2019
Leccinum monticola	HKAS76669	China	–	KF112249	KF112723	–	Wu et al. 2014
Leccinum quercinum	HKAS63502	China	–	KF112250	KF112724	–	Wu et al. 2014
Leccinum scabrum	RW105a	Belgium	KT823979	KT824045	KT824012	MH614857*	Raspé et al. 2016; *Vadthanarat et al. 2019
Leccinum scabrum	VDKO0938	Belgium	MG212549	MG212593	MG212635	MH614858*	Vadthanarat et al. 2018; *Vadthanarat et al. 2019
Leccinum scabrum	KPM-NC-0017840	Scotland	KC552170	JN378455	–	–	Orihara et al. 2016; Orihara et al. 2012
Leccinum schistophilum	VDKO1128	Belgium	KT823989	KT824055	KT824022	MH614859*	Raspé et al. 2016; *Vadthanarat et al. 2019
Leccinum variicolor	VDKO0844	Belgium	MG212550	MG212594	MG212636	MH614860*	Vadthanarat et al. 2018; *Vadthanarat et al. 2019
Mucilopilus castaneiceps	HKAS75045	China	–	KF112211	KF112735	–	Wu et al. 2014
Neoboletus brunneissimus	HKAS52660	China	–	KF112143	KF112650	–	Wu et al. 2014
Neoboletus brunneissimus	HKAS57451	China	–	KM605149	KM605172	–	Wu et al. 2015
Neoboletus brunneissimus	OR0249	China	MG212551	MG212595	MG212637	MH614861*	Vadthanarat et al. 2018; *Vadthanarat et al. 2019
Neoboletus hainanensis	HKAS59469	China	–	KF112175	KF112669	–	Wu et al. 2014
Neoboletus junquilleus	AF2922	France	MG212552	MG212596	MG212638	MH614862*	Vadthanarat et al. 2018; *Vadthanarat et al. 2019
Neoboletus magnificus	HKAS54096	China	–	KF112149	KF112654	–	Wu et al. 2014
Neoboletus magnificus	HKAS74939	China	–	KF112148	KF112653	–	Wu et al. 2014
Neoboletus sanguineoides	HKAS55440	China	–	KF112145	KF112652	–	Wu et al. 2014
Neoboletus sp.	HKAS76851	China	–	KF112144	KF112651	–	Wu et al. 2014
Neoboletus sp.	OR0128	Thailand	MH614686	MH614734	MH614781	MH614863	Vadthanarat et al. 2019
Neoboletus tomentulosus	HKAS53369	China	–	KF112154	KF112659	–	Wu et al. 2014
Neoboletus erythropus	VDKO0690	Belgium	KT823982	KT824048	KT824015	MH614864*	Raspé et al. 2016; *Vadthanarat et al. 2019
Octaviania asahimontana	KPM-NC-17824	Japan	KC552154	JN378430	–	–	Orihara et al. 2016; Orihara et al. 2012
Octaviania asterosperma	AQUI3899	Italy	KC552159	KC552093	–	–	Orihara et al. 2016
Octaviania celatifilia	KPM-NC-17776	Japan	KC552147	JN378416	–	–	Orihara et al. 2016; Orihara et al. 2012
Octaviania cyanescens	PNW-FUNGI-5603	USA	KC552160	JN378438	–	–	Orihara et al. 2016; Orihara et al. 2012
Octaviania decimae	KPM-NC17763	Japan	KC552145	JN378409	–	–	Orihara et al. 2016; Orihara et al. 2012
Octaviania tasmanica	MEL2128484	Australia	KC552157	JN378437	–	–	Orihara et al. 2016; Orihara et al. 2012
Octaviania tasmanica	MEL2341996	Australia	KC552156	JN378436	–	–	Orihara et al. 2016; Orihara et al. 2012
Octaviania zelleri	MES270	USA	KC552161	JN378440	–	–	Orihara et al. 2016; Orihara et al. 2012
Parvixerocomus pseudoaokii	OR0155	China	MG212553	MG212597	MG212639	MH614865	Vadthanarat et al. 2019
Phylloporus bellus	OR0473	China	MH580778	MH580798	MH580818	MH614866*	Chuankid et al. 2019; *Vadthanarat et al. 2019

Species	Voucher	Origin	*atp6*	*tef1*	*rpb2*	*cox3*	References
Phylloporus brunneiceps	OR0050	Thailand	KT823968	KT824034	KT824001	MH614867*	Raspé et al. 2016; *Vadthanarat et al. 2019
Phylloporus castanopsidis	OR0052	Thailand	KT823969	KT824035	KT824002	MH614868*	Raspé et al. 2016; *Vadthanarat et al. 2019
Phylloporus imbricatus	HKAS68642	China	–	KF112299	KF112786	–	Wu et al. 2014
Phylloporus luxiensis	HKAS75077	China	–	KF112298	KF112785	–	Wu et al. 2014
Phylloporus maculatus	OR0285	China	MH580780	MH580800	MH580820	–	Chuankid et al. 2019
Phylloporus pelletieri	WU18746	Austria	MH580781	MH580801	MH580821	MH614869*	Chuankid et al. 2019; *Vadthanarat et al. 2019
Phylloporus pusillus	OR1158	Thailand	MH580783	MH580803	MH580823	MH614870*	Chuankid et al. 2019; *Vadthanarat et al. 2019
Phylloporus rhodoxanthus	WU17978	USA	MH580785	MH580805	MH580824	MH614871*	Chuankid et al. 2019; *Vadthanarat et al. 2019
Phylloporus rubeolus	OR0251	China	MH580786	MH580806	MH580825	MH614872*	Chuankid et al. 2019; *Vadthanarat et al. 2019
Phylloporus rubiginosus	OR0169	China	MH580788	MH580808	MH580827	MH614873*	Chuankid et al. 2019; *Vadthanarat et al. 2019
Phylloporus sp.	OR0896	Thailand	MH580790	MH580810	MH580829	MH614874*	Chuankid et al. 2019; *Vadthanarat et al. 2019
Phylloporus subbacillisporus	OR0436	China	MH580792	MH580812	MH580831	MH614875*	Chuankid et al. 2019; *Vadthanarat et al. 2019
Phylloporus subrubeolus	BC022	Thailand	MH580793	MH580813	MH580832	MH614876*	Chuankid et al. 2019; *Vadthanarat et al. 2019
Phylloporus yunnanensis	OR0448	China	MG212554	MG212598	MG212640	MH614877*	Vadthanarat et al. 2018; *Vadthanarat et al. 2019
Porphyrellus castaneus	OR0241	China	MG212555	MG212599	MG212641	MH614878*	Vadthanarat et al. 2018; *Vadthanarat et al. 2019
Porphyrellus cf. *nigropurpureus*	ADK3733	Benin	MH614687	MH614735	MH614782	MH614879	Vadthanarat et al. 2019
Porphyrellus nigropurpureus	HKAS74938	China	–	KF112246	KF112763	–	Wu et al. 2014
Porphyrellus porphyrosporus	MB97-023	Germany	DQ534609	GU187734	GU187800	–	Binder & Hibbett 2006; Binder et al. 2010
Porphyrellus sp.	HKAS53366	China	–	KF112241	KF112716	–	Wu et al. 2014
Porphyrellus sp.	JD659	Burundi	MH614688	MH614736	MH614783	MH614880	Vadthanarat et al. 2019
Porphyrellus sp.	OR0222	Thailand	MH614689	MH614737	MH614784	MH614881	Vadthanarat et al. 2019
Pulveroboletus aff. *ravenelii*	ADK4360	Togo	KT823957	KT824023	KT823990	MH614882*	Raspé et al. 2016; *Vadthanarat et al. 2019
Pulveroboletus aff. *ravenelii*	ADK4650	Togo	KT823959	KT824025	KT823992	MH614883*	Raspé et al. 2016; *Vadthanarat et al. 2019
Pulveroboletus aff. *ravenelii*	HKAS53351	China	–	KF112261	KF112712	–	Wu et al. 2014
Pulveroboletus fragrans	OR0673	Thailand	KT823977	KT824043	KT824010	MH614884*	Raspé et al. 2016; *Vadthanarat et al. 2019
Pulveroboletus ravenelii	REH2565	USA	KU665635	KU665636	KU665637	MH614885*	Raspé et al. 2016; *Vadthanarat et al. 2019
Pulveroboletus sp.	HKAS74933	China	–	KF112262	KF112713	–	Wu et al. 2014
Retiboletus aff. *nigerrimus*	OR0049	Thailand	KT823967	KT824033	KT824000	MH614886*	Raspé et al. 2016; *Vadthanarat et al. 2019
Retiboletus brunneolus	HKAS52680	China	–	KF112179	KF112690	–	Wu et al. 2014
Retiboletus fuscus	HKAS59460	China	–	JQ928580	JQ928601	–	Hosen et al. 2013
Retiboletus fuscus	OR0231	China	MG212556	MG212600	MG212642	MH614887*	Vadthanarat et al. 2018; *Vadthanarat et al. 2019
Retiboletus griseus	MB03-079	USA	KT823964	KT824030	KT823997	MH614888*	Raspé et al. 2016; *Vadthanarat et al. 2019
Retiboletus kauffmanii	OR0278	China	MG212557	MG212601	MG212643	MH614889*	Vadthanarat et al. 2018; *Vadthanarat et al. 2019
Retiboletus nigerrimus	HKAS53418	China	–	KT990824	KT990462	–	Wu et al. 2016

Species	Voucher	Origin	*atp6*	*tef1*	*rpb2*	*cox3*	References
Retiboletus sinensis	HKAS59832	China	–	KT990827	KT990464	–	Wu et al. 2016
Retiboletus zhangfeii	HKAS59699	China	–	JQ928582	JQ928603	–	Hosen et al. 2013
Rhodactina himalayensis	CMU25117	Thailand	MG212558	MG212602, MG212603	–	–	Vadthanarat et al. 2018
Rhodactina rostratispora	SV170	Thailand	MG212560	MG212605	MG212645	–	Vadthanarat et al. 2018
Rossbeevera cryptocyanea	KPM-NC17843	Japan	KT581441	KC552072	–	–	Orihara et al. 2016
Rossbeevera eucyanea	TNS-F-36986	Japan	KC552115	KC552068	–	–	Orihara et al. 2016
Rossbeevera griseovelutina	TNS-F-36989	Japan	KC552124	KC552076	–	–	Orihara et al. 2016
Rossbeevera pachydermis	KPM-NC23336	New Zealand	KJ001064	KP222912	–	–	Orihara et al. 2016
Rossbeevera vittatispora	OSC61484	Australia	KC552109	JN378446	–	–	Orihara et al. 2016; Orihara et al. 2012
Royoungia reticulata	HKAS52253	China	–	KT990786	KT990427	–	Wu et al. 2016
Royoungia rubina	HKAS53379	China	–	KF112274	KF112796	–	Wu et al. 2014
Rubroboletus latisporus	HKAS80358	China	–	KP055020	KP055029	–	Zhao et al. 2014b
Rubroboletus legaliae	VDKO0936	Belgium	KT823985	KT824051	KT824018	MH614890*	Raspé et al. 2016; *Vadthanarat et al. 2019
Rubroboletus rhodosanguineus	BOTH4263	USA	MG897416	MG897426	MG897436	MH614891*	Phookamsak et al. 2019, *Vadthanarat et al. 2019
Rubroboletus rhodoxanthus	HKAS84879	Germany	–	KT990831	KT990468	–	Wu et al. 2016
Rubroboletus satanas	VDKO0968	Belgium	KT823986	KT824052	KT824019	MH614892*	Raspé et al. 2016; *Vadthanarat et al. 2019
Rubroboletus sinicus	HKAS68620	China	–	KF112146	KF112661	–	Wu et al. 2014
Rubroboletus sp.	HKAS68679	China	–	KF112147	KF112662	–	Wu et al. 2014
Rugiboletus brunneiporus	HKAS68586	China	–	KF112197	KF112719	–	Wu et al. 2014
Rugiboletus brunneiporus	HKAS83209	China	–	KM605144	KM605168	–	Wu et al. 2015
Rugiboletus extremiorientalis	HKAS63635	China	–	KF112198	KF112720	–	Wu et al. 2014
Rugiboletus extremiorientalis	HKAS76663	China	–	KM605147	KM605170	–	Wu et al. 2015
Rugiboletus extremiorientalis	OR0406	Thailand	MG212562	MG212607	MG212647	MH614893*	Vadthanarat et al. 2018; *Vadthanarat et al. 2019
Rugiboletus sp.	HKAS55373	China	–	KF112303	KF112804	–	Wu et al. 2014
Singerocomus inundabilis	TWH9199	Guyana	MH645588	MH645596	LC043089*	MH645609	*Henkel et al. 2016; Vadthanarat et al. 2019
Singerocomus rubriflavus	TWH9585	Guyana	MH645589	MH645597	–	MH645610	Vadthanarat et al. 2019
Spongiforma thailandica	DED7873	Thailand	MG212563	KF030436*	MG212648	MH614894**	*Nuhn et al. 2013; Vadthanarat et al. 2018; **Vadthanarat et al. 2019
Strobilomyces atrosquamosus	HKAS55368	China	–	KT990839	KT990476	–	Wu et al. 2016
Strobilomyces echinocephalus	OR0243	China	MG212564	MG212608	MG212649	–	Vadthanarat et al. 2018
Strobilomyces strobilaceus	RW103	Belgium	KT823978	KT824044	KT824011	MH614895*	Raspé et al. 2016; *Vadthanarat et al. 2019
Strobilomyces strobilaceus	MB-03-102	USA	DQ534607*	AY883428	AY786065	–	Binder and Hibbett 2006*, Unpublished
Strobilomyces mirandus	OR0115	Thailand	KT823972	KT824038	KT824005	MH614896*	Raspé et al. 2016; *Vadthanarat et al. 2019
Strobilomyces sp.	OR0259	China	MG212565	MG212609	MG212650	MH614897*	Vadthanarat et al. 2018; *Vadthanarat et al. 2019
Strobilomyces sp.	OR0778	Thailand	MG212566	MG212610	MG212651	MH614899*	Vadthanarat et al. 2018; *Vadthanarat et al. 2019

Species	Voucher	Origin	*atp6*	*tef1*	*rpb2*	*cox3*	References
Strobilomyces sp.	OR0319	Thailand	MH614690	MH614738	MH614785	MH614898	Vadthanarat et al. 2019
Strobilomyces sp.	OR1092	Thailand	MH614691	MH614739	MH614786	MH614900	Vadthanarat et al. 2019
Strobilomyces verruculosus	HKAS55389	China	–	KF112259	KF112813	–	Wu et al. 2014
Suillellus amygdalinus	112605ba	USA	–	JQ327024	–	–	Halling et al. 2012a
Suillellus luridus	VDKO0241b	Belgium	KT823981	KT824047	KT824014	MH614901*	Raspé et al. 2016; *Vadthanarat et al. 2019
Suillellus queletii	VDKO1185	Belgium	MH645590	MH645598	MH645604	MH645611	Vadthanarat et al. 2019
Suillellus subamygdalinus	HKAS57262	China	–	KF112174	KF112660	–	Wu et al. 2014
Sutorius australiensis	REH9441	Australia	MG212567	JQ327032*	MG212652	–	*Halling et al. 2012a; Vadthanarat et al. 2018
Sutorius eximius	REH9400	USA	MG212568	JQ327029*	MG212653	MH614902**	*Halling et al. 2012a; Vadthanarat et al. 2018; **Vadthanarat et al. 2019
Sutorius ferrugineus	HKAS77718	China	–	KT990789	KT990431	–	Wu et al. 2016
Sutorius flavidus	HKAS59443	China	–	KU974136	KU974144	–	Wu et al. 2016
Sutorius rubriporus	HKAS83026	China	–	KT990795	KT990437	–	Wu et al. 2016
Sutorius sanguineus	HKAS80823	China	–	KT990802	KT990442	–	Wu et al. 2016
Sutorius sp.	OR0378B	Thailand	MH614692	MH614740	MH614787	MH614903	Vadthanarat et al. 2019
Sutorius sp.	OR0379	Thailand	MH614693	MH614741	MH614788	MH614904	Vadthanarat et al. 2019
Tengioboletus glutinosus	HKAS53425	China	–	KF112204	KF112800	–	Wu et al. 2014
Tengioboletus reticulatus	HKAS53426	China	–	KF112313	KF112828	–	Wu et al. 2014
Tengioboletus sp.	HKAS76661	China	–	KF112205	KF112801	–	Wu et al. 2014
Turmalinea persicina	KPM-NC18001	Japan	KC552130	KC552082	–	–	Orihara et al. 2016
Turmalinea yuwanensis	KPM-NC18011	Japan	KC552138	KC552089	–	–	Orihara et al. 2016
Tylocinum griseolum	HKAS50281	China	–	KF112284	KF112730	–	Wu et al. 2014
Tylopilus alpinus	HKAS55438	China	–	KF112191	KF112687	–	Wu et al. 2014
Tylopilus atripurpureus	HKAS50208	China	–	KF112283	KF112799	–	Wu et al. 2014
Tylopilus balloui s.l.	OR0039	Thailand	KT823965	KT824031	KT823998	MH614905*	Raspé et al. 2016; *Vadthanarat et al. 2019
Tylopilus brunneirubens	HKAS53388	China	–	KF112192	KF112688	–	Wu et al. 2014
Tylopilus felleus	VDKO0992	Belgium	KT823987	KT824053	KT824020	MH614906*	Raspé et al. 2016; *Vadthanarat et al. 2019
Tylopilus ferrugineus	BOTH3639	USA	MH614694	MH614742	MH614789	MH614907	Vadthanarat et al. 2019
Tylopilus otsuensis	HKAS53401	China	–	KF112224	KF112797	–	Wu et al. 2014
Tylopilus sp.	HKAS74925	China	–	KF112222	KF112739	–	Wu et al. 2014
Tylopilus sp.	HKAS50229	China	–	KF112216	KF112769	–	Wu et al. 2014
Tylopilus sp.	JD598	Gabon	MH614695	MH614743	MH614790	MH614908	Vadthanarat et al. 2019
Tylopilus sp.	OR0252	China	MG212569	MG212611	MG212654	MH614909*	Vadthanarat et al. 2018; *Vadthanarat et al. 2019
Tylopilus sp.	OR0542	Thailand	MG212570	MG212612	MG212655	MH614910*	Vadthanarat et al. 2018; *Vadthanarat et al. 2019
Tylopilus sp.	OR0583	Thailand	MH614696	MH614744	–	–	Vadthanarat et al. 2019
Tylopilus sp.	OR1009	Thailand	MH614697	–	MH614791	MH614911	Vadthanarat et al. 2019
Tylopilus vinaceipallidus	HKAS50210	China	–	KF112221	KF112738	–	Wu et al. 2014
Tylopilus vinaceipallidus	OR0137	China	MG212571	MG212613	MG212656	MH614912*	Vadthanarat et al. 2018; *Vadthanarat et al. 2019
Tylopilus violaceobrunneus	HKAS89443	China	–	KT990886	KT990504	–	Wu et al. 2016
Tylopilus virens	KPM-NC-0018054	Japan	KC552174	KC552103	–	–	Unpublished

Species	Voucher	Origin	*atp6*	*tef1*	*rpb2*	*cox3*	References
Veloporphyrellus alpinus	HKAS68301	China	JX984515	JX984550	–	–	Li et al. 2014
Veloporphyrellus conicus	REH8510	Belize	MH614698	MH614745	MH614792	MH614913	Vadthanarat et al. 2019
Veloporphyrellus gracilioides	HKAS53590	China	–	KF112210	KF112734	–	Wu et al. 2014
Veloporphyrellus pseudovelatus	HKAS59444	China	JX984519	JX984553	–	–	Li et al. 2014
Veloporphyrellus velatus	HKAS63668	China	JX984523	JX984554	–	–	Li et al. 2014
Xanthoconium affine	NY00815399	USA	–	KT990850	KT990486	–	Wu et al. 2016
Xanthoconium porophyllum	HKAS90217	China	–	KT990851	KT990487	–	Wu et al. 2016
Xanthoconium sinense	HKAS77651	China	–	KT990853	KT990488	–	Wu et al. 2016
Xerocomellus chrysenteron	VDKO0821	Belgium	KT823984	KT824050	KT824017	MH614914*	Raspé et al. 2016; *Vadthanarat et al. 2019
Xerocomellus cisalpinus	ADK4864	Belgium	KT823960	KT824026	KT823993	MH614915*	Raspé et al. 2016; *Vadthanarat et al. 2019
Xerocomellus communis	HKAS50467	China	–	KT990858	KT990494	–	Wu et al. 2016
Xerocomellus corneri	HKAS90206	Philippines	–	KT990857	KT990493	–	Wu et al. 2016
Xerocomellus porosporus	VDKO0311	Belgium	MH614678	MH614727	MH614773	MH614846	Vadthanarat et al. 2019
Xerocomellus ripariellus	VDKO0404	Belgium	MH614699	MH614746	MH614793	MH614916	Vadthanarat et al. 2019
Xerocomellus sp.	HKAS56311	China	–	KF112170	KF112684	–	Wu et al. 2014
Xerocomus aff. *macrobbii*	HKAS56280	China	–	KF112265	KF112708	–	Wu et al. 2014
Xerocomus fulvipes	HKAS76666	China	–	KF112292	KF112789	–	Wu et al. 2014
Xerocomus magniporus	HKAS58000	China	–	KF112293	KF112781	–	Wu et al. 2014
Xerocomus s.s. sp.	OR0237	China	MH580796	MH580816	MH580835	–	Chuankid et al. 2019
Xerocomus s.s. sp.	OR0443	China	MH580797	MH580817	MH580836	MH614917*	Chuankid et al. 2019; *Vadthanarat et al. 2019
Xerocomus sp.	OR0053	Thailand	MH580795	MH580815	MH580834	MH614918*	Chuankid et al. 2019; *Vadthanarat et al. 2019
Xerocomus subtomentosus	VDKO0987	Belgium	MG212572	MG212614	MG212657	MH614919*	Vadthanarat et al. 2018; *Vadthanarat et al. 2019
Zangia citrina	HKAS52684	China	HQ326850	HQ326872	–	–	Li et al. 2011
Zangia olivacea	HKAS45445	China	HQ326854	HQ326873	–	–	Li et al. 2011
Zangia olivaceobrunnea	HKAS52272	China	HQ326857	HQ326876	–	–	Li et al. 2011
Zangia roseola	HKAS75046	China	–	KF112269	KF112791	–	Wu et al. 2014
Zangia roseola	HKAS51137	China	HQ326858	HQ326877	–	–	Li et al. 2011

also clustered in the *Erythrophylloporus* clade indicating that they are close relatives. *Erythrophylloporus* formed a clade sister to the genus *Singerocomus* T.W. Henkel & M.E. Sm. with high Bootstrap support (96%) but low posterior probability support (0.86) within the *Pulveroboletus* group. Some undescribed species formed two different generic clades in the *Pulveroboletus* group. *Boletus* p.p. spp. clade 1 contains two specimens, HKAS63598 and HKAS9660, named "*Boletus* sp." in Wu et al. (2016), as well as two of our specimens, OR0832 and OR1002. *Boletus* p.p. sp. clade 2 contains a single African specimen, JD0693, sister to and morphologically different from *Cyanoboletus*.

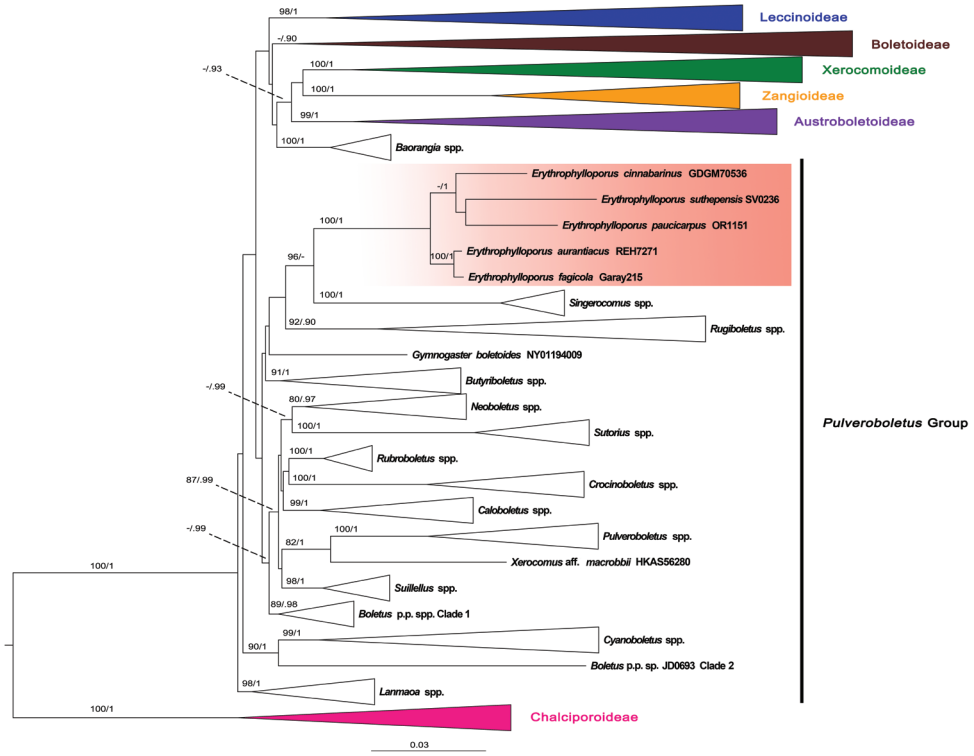

Figure 1. Phylogenetic tree inferred from the four-gene dataset (*atp6*, *rpb2*, *tef1* and *cox3*), including *Erythrophylloporus* species and selected Boletaceae using Maximum Likelihood and Bayesian Inference methods (ML tree is presented). The two *Buchwaldoboletus* and nine *Chalciporus* species in subfamily Chalciporoideae were used as outgroup. Most of the taxa not belonging to the *Pulveroboletus* group were collapsed into subfamilies. All generic clades, including one undescribed generic clade in *Pulveroboletus* group that were highly supported, were also collapsed. Bootstrap support values (BS ≥ 70%) and posterior probabilities (PP ≥ 0.90) are shown above the supported branches.

Taxonomy

Erythrophylloporus Ming Zhang & T.H. Li, Mycosystema 37(9): 1111–1126 (2018)

Description. *Basidiomata* stipitate-pileate with lamellate hymenophore, small to medium-sized; *Pileus* subhemispheric to convex when young becoming convex to plano-convex to plano-subdepressed when old, dry, pruinose or velutinous, subtomentose to tomentose, yellowish-orange to red; *pileus context* vivid yellow to yellowish-orange. *Hymenophore* lamellae, slightly thick, decurrent, deeply yellowish-orange to deep orange or reddish-orange to orange red or brownish-orange to red. *Stipe* central to slightly excentric, cylindrical or clavate, yellowish- to reddish-orange to yellowish red, with scattered yellowish- to reddish-orange to red scales on surface, with bright yellow basal mycelium; *stipe context* solid, yellow to reddish-yellow or yellow with olivaceous

brown. *Staining* none or slightly reddening or greening or gradually bluing or dark violet, greyish to blackish-blue when bruised on the basidiomata or context or lamellae. *Spore print* olivaceous brown. *Basidiospores* ovoid or ellipsoid to broadly ellipsoid to subovoid, thin-walled, with non-bacillate surface. *Basidia* clavate to narrowly clavate. *Cheilocystidia and pleurocystidia* present, subcylindrical or narrowly conical to narrowly fusiform to ventricose with slightly or obtuse apex, thin-walled, sometimes thick-walled, originating more or less deeply in the sub hymenium or from hymenophoral trama, hyaline or sometimes containing yellowish-brown pigments. *Pileipellis* a subcutis to cutis to trichoderm to palisadoderm, composed of thin to slightly thick-walled hyphae. *Clamp connection* absent in all tissues.

Typus species. *Erythrophylloporus cinnabarinus* Ming Zhang & T.H. Li.

Known Distribution. Asia (China and Thailand), North America (Mexico) and Central America (Costa Rica).

Remarks. *Erythrophylloporus* is easily distinguished from other lamellate Boletaceae genera by a combination of the following characters: the intense orange to red colour of the pileus and lamellae; bright yellow basal mycelium; ovoid or ellipsoid to broadly ellipsoid to subovoid basidiospores with non-bacillate surface; pleurocystidia originating more or less deeply in the subhymenium or from hymenophoral trama.

***Erythrophylloporus paucicarpus* Raspé, Vadthanarat & Lumyong, sp. nov.**
MycoBank: MB823605
Figs. 2A, 3A, 4A and 5

Holotype. THAILAND, Chiang Mai Province, Mae On District, Huay Kaew, 18°52'0"N, 99°17'30"E, elev. 700 m, 16 August 2016, *O. Raspé & S. Vadthanarat*, OR1151, (holotype: CMUB, isotype: BR).

Etymology. from Latin "pauci-" meaning few and "carpus" meaning fruits or what is harvested, refers to the low number of basidiomata produced.

Description. *Basidiomata* stipitate-pileate with lamellate hymenophore, small to medium-sized. *Pileus* 2.3–5.5 cm in diameter, plano-convex with involute margin at first becoming almost plane to slightly depressed with inflexed to straight margin, irregularly and coarsely crenate in age, sometimes with low and broad umbo and a few to several verrucae, especially when young; *surface* more or less even, tomentose, dull, slightly moist, colour distribution patchy with red to brownish-orange (9B8 to 9C8), brownish-red (10E8 to 10D8) becoming orange-red to orange (8B/C8 to 6B7) at the margin when old, abruptly paler at the margin. *Pileus context* 3–4 mm thick half-way to the margin, tough, colour distribution even, yellow (3A6) to yellowish-orange (4A5), slowly reddening when exposed, especially at the centre and above lamellae. *Stipe* 2.4–4.5 × 0.7–1.3 cm, central or sometimes slightly eccentric, clavate with strigose base, straight to curved, terete, even, dull, dry, tomentose, yellowish-orange (4–5A7–8) to orange (6–7A7–8) with orange to yellowish-orange (7B/C7–8 to 4A7–8) coarse scales, with bright yellow (2A6–7) basal mycelium. *Stipe context* solid, fleshy fibrous, yellow

marbled with olivaceous brown (4D5, 5D5). *Hymenophore* lamellate; lamellae decurrent, close, thick, 40–42 lamellae, with 4–6 different lengths of lamellullae, 2–4.5 mm wide half-way to margin, somewhat anastomosing, especially near the stipe, yellowish-orange (4-5A6-7) with orange to red tinge, slightly reddening when bruised. *Odour* rubbery; *Taste* not recorded. *Spore print* olive-brown (4E7).

Macrochemical reactions. KOH on pileus and stipe surface deep red at first, then red-brown to brown, with pale orange aura on the pileus; brown on pileus context, dark red-brown on stipe context; brownish-orange on hymenophore. NH_4OH on pileus first red, then orange; on pileus context bluing at first then with a greenish tinge; on stipe surface and context briefly bluing; no reaction on hymenophore.

Basidiospores [208/4/4] (5.9–)6.1–6.8–7.5(–8) × (4.1–)4.6–5.1–5.5(–6) µm, *Q* = (1.2–)1.23–1.33–1.48(–1.56); from the type (OR1151) (6–)6.3–6.8–7.5(–7.8) × (4.6–)4.8–5.2–5.5(–6) µm, *Q* = (1.2–)1.22–1.31–1.48(–1.56), *N* = 88, broadly ellipsoid to ellipsoid, smooth under light microscope and SEM, yellowish to pale brown in water, hyaline in 5% KOH, thin-walled, inamyloid. *Basidia* 4–spored, (37.8–)38–45.6–54.7(–54.8) × (6.2–)–6.3–8–9.5(–9.6) µm, narrowly clavate to subcylindrical, attenuated towards the base, clampless, hyaline to yellowish hyaline in water, Melzer's reagent and 5% KOH; *sterigmata* up to 5.5 µm long. *Cheilocystidia* (35.4–)35.5–49.9–61.8(–61.9) × (3.9–)3.9–6–7.7(–7.7) µm, narrowly fusiform with obtuse apex, projecting up to 30 µm, thin-walled, smooth, yellowish hyaline in water, in 5% KOH and NH_4OH, inamyloid. *Pleurocystidia* (66.9–)67.4–80.3–93.5(–94.7) × (8.8–)8.9–11.7–16.1(–16.2) µm, abundant, narrowly conical with obtuse, somewhat prolonged apex, projecting up to 32 µm, thin-walled, smooth, yellowish hyaline in water, in 5% KOH and NH_4OH, arising more or less deeply in the subhymenium or from hymenophoral trama, inamyloid. *Hymenophoral trama* subregular near the pileus context becoming slightly divergent near the edge, 87–238 µm wide, widest near the pileus context then getting narrower when close to the edge, composed of clampless hyphae 4.5–8 µm wide, yellowish hyaline in water, hyaline in 5% KOH and NH_4OH. *Pileipellis* a palisadoderm to trichoderm 83–165 µm thick, composed of slightly thick-walled, cylindrical hyphae, terminal cells 16–46 × 4–6.5 µm with rounded apex, hyaline or yellowish hyaline to yellowish-orange hyaline hyphae ornamented with scattered fine epiparietal encrustation when observed in water, hyaline to yellowish hyaline in 5% KOH and NH_4OH, inamyloid. *Pileus trama* composed of slightly thick-walled, strongly interwoven hyphae, 4.5–8.5 µm wide, inamyloid. *Stipitipellis* a disrupted palisadoderm perpendicular to the stipe axis, 63–145 µm thick, composed of slightly thick-walled, slightly rough, cylindrical, yellow to yellowish-orange in water, yellowish hyaline hyphae in 5% KOH and NH_4OH, terminal cells 13–57 × 3–8 µm, cylindrical to irregular hyphae with rounded to notched apex; wall covered by dispersed fine encrustations when observed in water. *Caulocystidia* not seen. *Stipe trama* composed of parallel hyphae, densely packed, 4–8.5 µm wide; hyphae wall covered by dispersed encrustations when observed in water. *Clamp connections* not seen in any tissue.

Habit and habitat. On soil, mostly solitary in dipterocarp forest dominated by *Dipterocarpus tuberculatus*, *D. obtusifolius*, *Shorea obtusa*, *S. siamensis*, *Quercus* spp. and *Lithocarpus* spp.

Figure 2. Habits of Thai *Erythrophylloporus* species **A** *E. paucicarpus* **B** *E. suthepensis*. Scale bars: 1 cm.

Known distribution. Currently known only from Chiang Mai Province, northern Thailand.

Additional specimens examined. – THAILAND, Chiang Mai Province, Muang District, Doi Suthep-Pui National Park, 18°48'05"N–98°55'40"E, elev. 800 m, 17 May 2015, *O. Raspé*, OR0615A (CMUB, BKF, BR); Mae Taeng District, Baan Tapa,

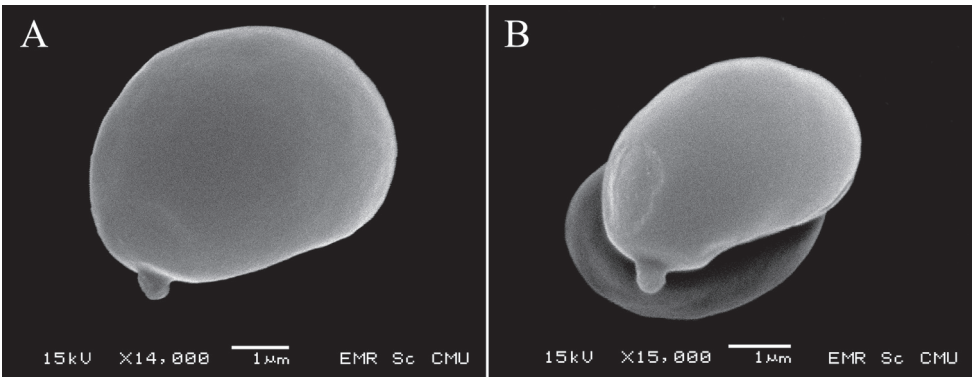

Figure 3. Scanning electron micrographs of basidiospores from Thai *Erythrophylloporus* show smooth surfaces **A** *E. paucicarpus* **B** *E. suthepensis*. Scale bars: 1 µm.

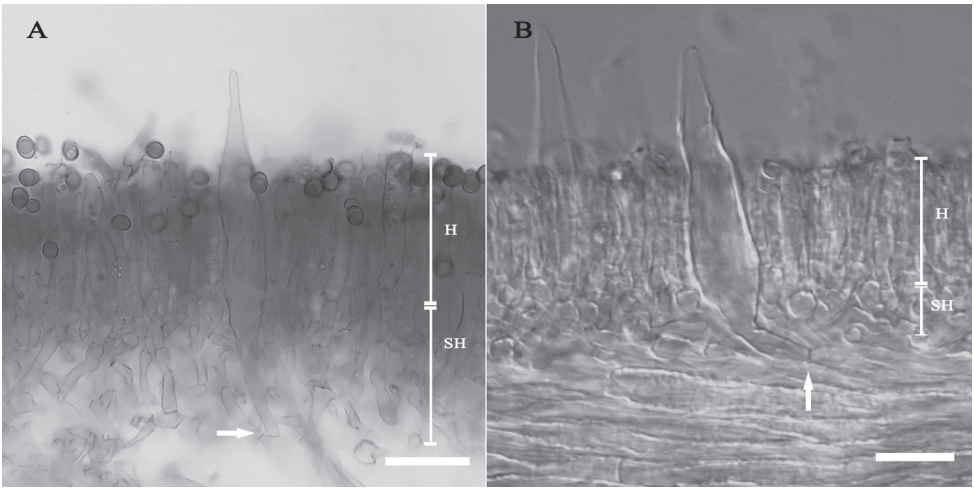

Figure 4. Origin of pleurocystidia (white arrow), more or less deep in the subhymenium or from hymenophoral trama **A** *E. paucicarpus* **B** *E. suthepensis* – hymenium (H), subhymenium (SH), Scale bars: 25 µm (**A–B**).

19°08'29"N, 98°45'47"E, elev. 1035 m, 4 August 2015, *O. Raspé & A. Thawthong*, OR0689 (MFLU, BR); Mae On District, Huay Kaew, 18°52'12"N, 99°18'12"E, elev. 780 m, 15 August 2016, *O. Raspé & S. Vadthanarat*, OR1135 (CMUB, BR).

Remarks. *E. paucicarpus* is characterised by the following combination of features: orange to brownish- to orange-red basidiomata, yellowish-orange lamellae that turn slightly red when bruised; pileus context yellow to yellowish-orange that slowly reddens when exposed and mostly occurring as solitary basidiomata.

In the inferred molecular phylogeny, *E. paucicarpus* clustered close to *E. suthepensis* and *E. cinnabarinus* (65% BS and 1 PP), but the two species are different from

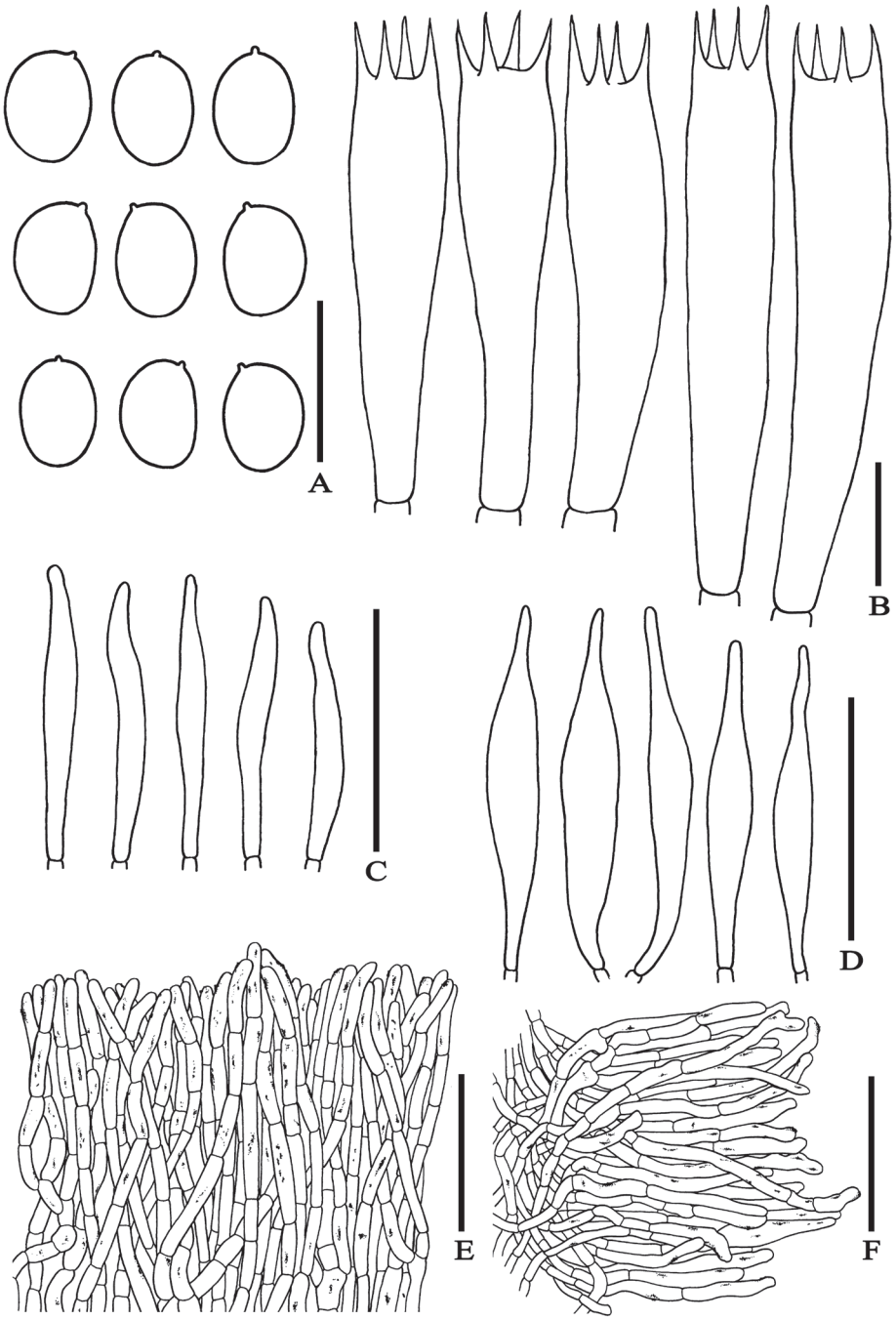

Figure 5. Microscopic features of *Erythrophylloporus paucicarpus* **A** basidiospores **B** basidia **C** cheilocystidia **D** pleurocystidia **E** pileipellis **F** stipitipellis. – Scale bars: 10 µm (**A–B**); 50 µm (**C–F**). All drawings were made from the type (OR1151).

E. paucicarpus in that they have darker lamellae which are orange to orange red or brownish-orange. Moreover, spores of *E. paucicarpus* are wider and longer (5.9–8 × 4.1–6 µm) than those of *E. suthepensis* (4.6–5.9 × 3.5–4.5 µm) and, on average, longer than those of *E. cinnabarinus* (5.5–7 × 4.5–5.5 µm) (Zhang and Li 2018). *Erythrophylloporus paucicarpus* also differs from both species by the slight reddening of the context and lamellae when exposed or bruised, whereas *E. suthepensis* context seems unchanging when exposed and lamellae turn blue when bruised. In *E. cinnabarinus*, the context slowly turns dark violet, blackish-blue to dark blue when exposed and lamellae turn greyish-blue, or greyish-green when bruised (Zhang and Li 2018).

Erythrophylloporus paucicarpus is different from the two New World species by the reddening of the context, whereas in *E. fagicola*, it turns blue and, in *E. aurantiacus*, the colour remains unchanged when exposed. Moreover, *E. fagicola* has somewhat thick-walled (0.8–3.5 µm) pleurocystidia (Montoya and Bandala 2011), which are not found in *E. paucicarpus*. Although the basidiospores of *E. paucicarpus* and *E. aurantiacus* are similar in size (*E. aurantiacus* = 6.0–7.5 × 4–5.5 µm), they differ in shape, being more ovoid in *E. aurantiacus* than in *E. paucicarpus*. *Erythrophylloporus paucicarpus* also differs from *E. aurantiacus* by macro-chemical reactions. In the latter, the pileus surface and pileus context are unchanging with NH_4OH (Halling et al. 1999), while in *E. paucicarpus*, the pileus becomes orange to red and the pileus context initially turns blue then with a greenish tinge.

Erythrophylloporus suthepensis **Vadthanarat, Raspé & Lumyong, sp. nov.**
MycoBank: MB823606
Figs. 2B, 3B, 4B and 6

Holotype. THAILAND, Chiang Mai Province, Muang District, Doi Suthep-Pui National Park, 18°48'47"N, 98°55'56"E, elev. 645 m, 25 August 2015, *S. Vadthanarat*, SV0236, (holotype CMUB, isotype BKF, BR).

Etymology. Refers to the type locality Doi Suthep.

Description. *Basidiomata* stipitate-pileate with lamellate hymenophore, small-sized. *Pileus* (1.0–)2.5– 3.5 cm in diameter, subumbonate with involute margin at first, becoming convex to plano-convex with inflexed margin; surface even with some small pustules, tomentose, dull, slightly moist, yellow (3–4A4– 5) becoming light orange to orange-red (5–6A5–7 to 7–8A–B7–8) with patches of light yellow to light orange (4–5A5–6) becoming brownish-orange to dull red (7B–C8 to 8B–D8) with age, the colour of the margin when young clearly paler than the rest of the pileus, bluing when bruised. *Pileus context* 2–3 mm thick half-way to the margin, tough, yellowish-orange (4A5), unchanging when bruised. *Stipe* 2.5– 4.5 × 0.3– 0.8 cm, central, slightly curved, terete, dull, dry, yellowish-orange (2A6–7) with greyish-orange (5–6 B 7–8) coarse scales at first, then light yellow or reddish-yellow to brownish-orange (4A/B5–6 to 7C6) with brownish-red to reddish-dark brown (7F4–5, 8C7–8, 8F5–7) scales, sub-bulbous, with bright yellow to greyish-yellow (2A6–7 to 3A/B5–6) sparse basal mycelium that extends half-way up the stipe. *Stipe context* solid, tough, reddish-yellow (4A6) near the pileus

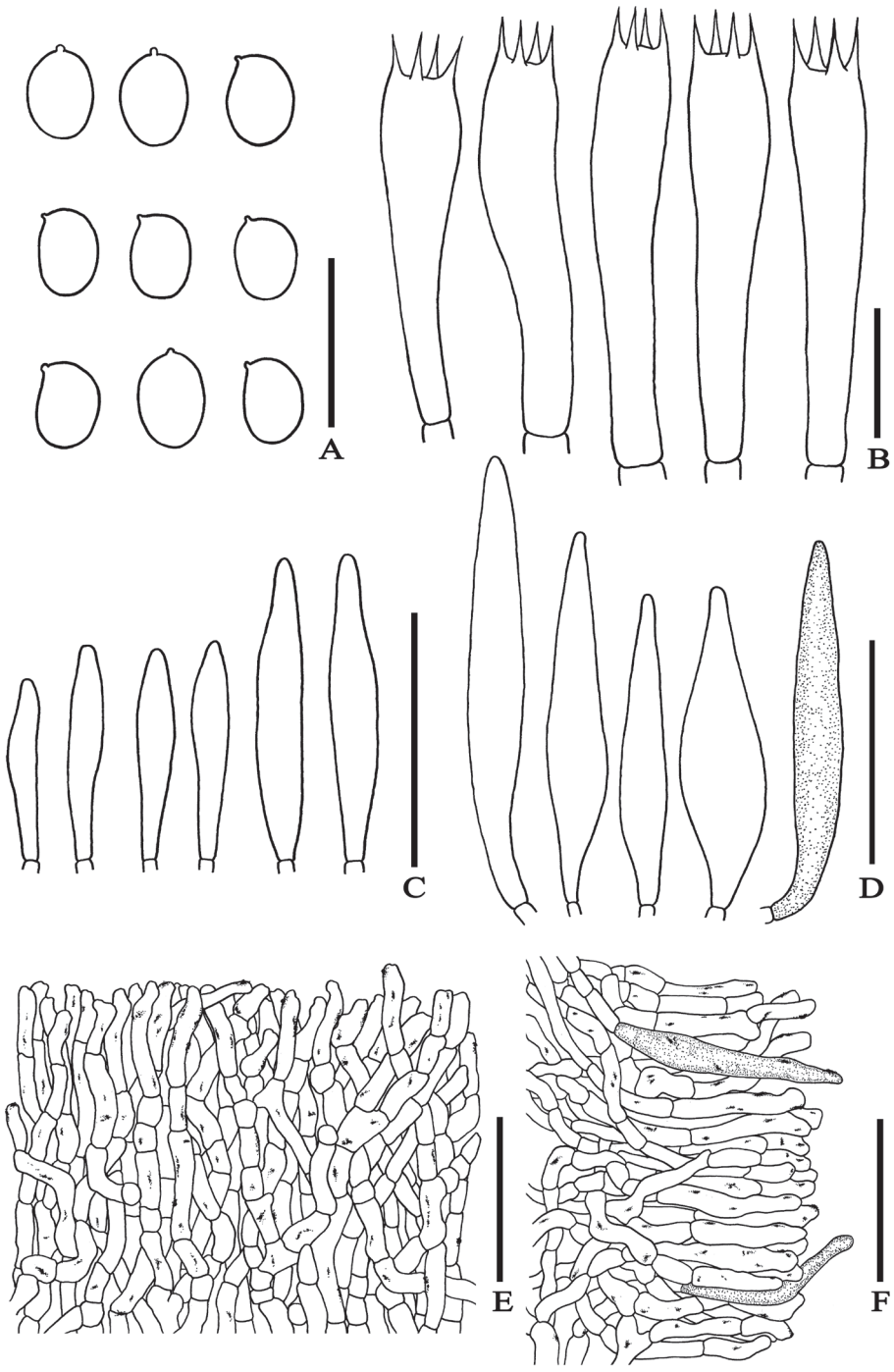

Figure 6. Microscopic features of *Erythrophylloporus suthepensis* **A** basidiospores **B** basidia **C** cheilocystidia **D** pleurocystidia **E** pileipellis **F** stipitipellis showing some dark caulocystidia mixed with slightly rough, cylindrical to irregular hyphae. – Scale bars: 10 µm (**A–B**); 50 µm (**C–F**). All drawings were made from the type (SV0236).

then paler to light yellow (4A5) near the base, unchanging when bruised. *Hymenophore* lamellate; lamellae decurrent, subdistant, slightly thick, with sinuate edge, of varying lengths, 26–34 lamellae, with 4–6 different lengths of lamellullae, 4–5 mm wide halfway to margin, brownish-orange (7C7–8) with deep yellow to orange (4–5A7–8) edge, bluish-grey when looking tangentially to the surface, bluing when bruised. *Odour* rubbery. *Taste* mild with rubbery texture. *Spore print* olivaceous brown (4F5).

Macrochemical reactions. KOH orange-brown on pileus and stipe surface; yellowish-brown on pileus and stipe context and hymenophore. NH_4OH yellowish-brown on pileus and stipe surface and hymenophore; yellowish on pileus and stipe context.

Basidiospores [218/4/2] (4.6–)4.8–5.2–5.7(–5.9) × (3.5–)3.6–4–4.3(–4.5) µm, *Q* = (1.15–)1.21–1.32–1.44(–1.57); from the type (SV0236) (4.6–)4.8–5.2–5.7(–5.9) × (3.5–)3.6–3.9–4.4(–4.5) µm, *Q* = (1.15–)1.21–1.32–1.43(–1.57), *N* = 80, broadly ellipsoid to subglobose, smooth under light microscope and SEM, yellowish to pale brown in water, hyaline in 5% KOH, thin-walled, inamyloid. *Basidia* 4-spored, (24.7–)25.3–31.1–35.8(–35.9) × (5.3–)5.3–6.6–7.5(–7.5) µm, narrowly clavate to subcylindrical, attenuated towards the base, clampless, hyaline to yellowish hyaline in water, Melzer's reagent and 5% KOH; *sterigmata* up to 4.5 µm long. *Cheilocystidia* (37.3–)37.9–51–63.8(–64.1) × (5.3–)5.4–8.5–12.4(–13.7) µm, narrowly conical to narrowly fusiform with obtuse apex, projecting up to 25 µm, thin-walled, smooth, yellowish-hyaline in water, hyaline in 5% KOH and NH_4OH, inamyloid, more or less forming a sterile edge . *Pleurocystidia* (46.5–)49.2–68.9–95.2(–99.3) × (9.3–)9.6–12.6–18.9(–20) µm, abundant, narrowly conical with obtuse apex, projecting up to 28 µm, thin-walled, mostly yellowish hyaline in water and hyaline in 5% KOH and NH_4OH, some containing yellowish-brown to dark brown pigments in water and yellowish-pale brown in 5% KOH and NH_4OH, inamyloid, arising more or less deeply in the subhymenium or from hymenophoral trama. *Hymenophoral trama* subregular near the pileus context becoming slightly divergent near the edge, 46–192 µm wide, widest near the pileus context then getting narrower when close to the edge, composed of clampless hyphae 2.5–7.5 µm wide, pinkish-red hyaline in water, especially at the centre of the trama, yellowish hyaline to hyaline in 5% KOH and NH_4OH. *Pileipellis* a palisadoderm to trichoderm 71–119 µm thick, composed of slightly thick-walled, cylindrical to irregular hyphae with fine encrustation on the wall, terminal cells 12–46 × 3.5–9 µm with pointed to notched apex or sometimes truncated apex, with 6–15(–28) µm short cells at the base, hyaline or yellowish-orange hyaline to orange hyaline hyphae with scattered fine encrustation on the wall when observed in water, hyaline to yellowish hyaline in 5% KOH and NH_4OH, inamyloid. *Pileus context* composed of slightly thick-walled, strongly interwoven hyphae, 5–8.5 µm wide, inamyloid. *Stipitipellis* a disrupted palisadoderm perpendicular to the stipe axis, 47–123 µm thick, composed of slightly thick-walled, cylindrical to irregular hyphae with fine encrustations on the wall, yellow to yellowish-orange, intermixed with mostly yellowish hyaline to yellowish-brown hyphae in 5% KOH and NH_4OH, terminal cells 14–47 × 4–8.5 µm with variously notched apex. *Caulocystidia* mixed in a group with the stipitipellis hyphae, same shape and size as the pleurocystidia, dark brown in water, paler in 5% KOH and NH_4OH. *Stipe context* composed of parallel,

densely packed, 4–9.5 µm wide hyphae, hyphae wall with scattered fine encrustations when observed in water. *Clamp connections* not seen in any tissue.

Habit and habitat. On soil, gregarious (up to 10 basidiomata) in dipterocarp forest dominated by *Dipterocarpus tuberculatus*, *D. obtusifolius*, *Shorea obtusa* and *S. siamensis*, mixed with scattered fagaceous trees.

Known distribution. Currently known only from Doi Suthep-Pui National Park, Chiang Mai Province, northern Thailand.

Additional specimens examined. – THAILAND, Chiang Mai Province, Meuang District, Doi Suthep-Pui National Park, 18°48'05"N, 98°55'40"E, elev. 800 m, 17 May 2015, *O. Raspé*, OR0615B (CMUB, BKF, BR).

Remarks. *Erythrophylloporus suthepensis* is characterised by the following combination of features: yellow to light orange to orange red to brownish-orange to dull red pileus; brownish-orange lamellae with deep yellow to orange edge; the colour of the lamellae appears more bluish-grey when observed from an oblique angle to the surface; pileus surface and lamellae turning blue when bruised; some pleurocystidia containing yellowish-brown to dark brown pigments in water; basidiospores that are smaller or shorter (4.6–5.9 × 3.5–4.5 µm) than the other *Erythrophylloporus* species (*E. aurantiacus* = 6.0–7.5 × 4–5.5µm; *E. cinnabarinus* = 5.5–7 × 4.5–5.5 µm; *E. fagicola* = 6.5–11 × 4–7.5 µm; *E. paucicarpus* = 5.9–8 × 4.1–6 µm) (Halling et al. 1999, Montoya and Bandala 2011, Zhang and Li 2018).

Morphologically, *E. suthepensis* is quite similar to *E. cinnabarinus* in that they have similar colours in pileus and lamellae; the lamellae in both species also turn more or less blue to dark blue when bruised. *Erythrophylloporus suthepensis* and *E. cinnabarinus* are also similar, based on some pleurocystidia containing yellowish-brown to dark brown pigments, but those features are not found in *E. paucicarpus* and in the two New World *Erythrophylloporus* species (Halling et al. 1999, Montoya and Bandala 2011). However, the pleurocystidia containing brown pigments seem to be more frequent in *E. cinnabarinus*, which also has, on average, larger basidiospores than *E. suthepensis* (Zhang and Li 2018).

The pinkish-red hymenophoral trama of *E. suthepensis* was not found in either *E. paucicarpus* or in the two American *Erythrophylloporus* species. In our observation of the two American specimens (*E. aurantiacus* voucher REH7271 and *E. fagicola* voucher Garay215), we found that the hymenophoral trama was yellowish hyaline when observed in water. The original description of *E. cinnabarinus* does not mention the colour of the hymenophoral trama and we could not obtain a specimen to observe this character. However, other morphological characters and phylogenetic evidence are enough to differentiate *E. suthepensis* from *E. cinnabarinus*.

Our phylogenetic analyses of a four-gene dataset revealed that *Phylloporus aurantiacus* from Costa Rica and *P. fagicola* from Mexico clustered in the *Erythrophylloporus* clade with high support (BS = 100% and PP = 1). Both species possess the distinctive morphological characters of *Erythrophylloporus*, which include yellowish-orange to reddish-orange basidiomata, orange to orange brown lamellae, bright yellow basal mycelium, ovoid or ellipsoid to broadly ellipsoid basidiospores with smooth surface and subcylindrical to subfusoid to ventricose cheilocystidia and pleurocystidia (Halling et al. 1999, Montoya and Bandala 2011). Therefore, the following two new combinations are proposed:

***Erythrophylloporus aurantiacus* (Halling & G.M. Muell.) Raspé & Vadthanarat, comb. nov.**
MycoBank: MB823607

Basionym. *Phylloporus aurantiacus* Halling & G.M. Mueller, Mycotaxon 73: 64 (1999)

Specimen examined. – COSTA RICA. Near town of Palo Verde, elev. 1600 m, 11 June 1994, Halling 7271 (NY).

***Erythrophylloporus fagicola* (Montoya & Bandala) Raspé & Vadthanarat, comb. nov.**
MycoBank: MB823608

Basionym. *Phylloporus fagicola* Montoya & Bandala, Mycotaxon 117: 10 (2011)

Specimen examined. – MEXICO. Veracruz: Mpio. Acatlán, Acatlán Volcano, 29 September 2009, Garay 215 (XAL).

Key to the species in ***Erythrophylloporus***

1	Growing in North or Central America **2**
–	Growing in Southeast Asia or in tropical to subtropical China **3**
2	Bluing of the context when exposed; basidiospores ellipsoid to oblong, obtuse, 6.5–11 × 4–7.5 µm; pleurocystidia somewhat thick-walled (0.8–3.5 µm thick) ..... ***E. fagicola***
–	Context unchanging when exposed; basidiospores ovoid to subellipsoid, 6.0–7.5 × 4–5.5 µm; pleurocystidia thin-walled ..... ***E. aurantiacus***
3	Yellowish-orange lamellae slightly reddening when bruised; context slowly or slightly reddening when exposed ..... ***E. paucicarpus***
–	Brownish-orange or orange, deep orange, reddish-orange to orange red lamellae bluing to greyish-green when bruised; context unchanging to gradually turning dark violet, blackish to dark blue **4**
4	Basidiospores 4.6–5.9 × 3.5–4.5 µm, broadly ellipsoid to subglobose; cystidia mostly hyaline, only some containing yellowish-brown to dark brown pigments ..... ***E. suthepensis***
–	Basidiospores 5.5–7 × 4.5–5.5 µm, broadly ellipsoid, ellipsoid to nearly ovoid; cystidia usually containing yellowish-brown pigments ..... ***E. cinnabarinus***

Discussion

Both phylogeny and morphology support the placement of the two new species from Thailand, *E. paucicarpus* and *E. suthepensis* in the genus *Erythrophylloporus*. Phylogenetically, both species were highly supported in the *Erythrophylloporus* clade

close to *E. cinnabarinus* (typus generis). Morphologically, they are characterised by having yellowish-orange to reddish- to brownish-orange basidiomata with bright yellow basal mycelium and smooth, ellipsoid, broadly ellipsoid to subglobose basidiospores. The other lamellate Boletaceae in *Phylloporus*, *Phylloboletellus* and *Phylloporopsis* are solely similar to the new species by having a lamellate hymenophore instead of a poroid hymenophore. However, *Phylloporus* differs from *Erythrophylloporus* species by having whitish- to yellowish-pale brown basidiomata with yellow to golden-yellow lamellae, with off-white to whitish to yellow basal mycelium and most species in the genus have basidiospores with more or less bacillate ornamentation under SEM (Neves & Halling 2010, Neves et al. 2012, Zeng et al. 2013). The single *Phylloboletellus* species, *Ph. chloephorus* Singer differs from *Erythrophylloporus* by having longitudinally ridged basidiospores (Bandala et al. 2004). The sole species of *Phylloporopsis*, *Phy. boletinoides*, differs by having beige to olive-cream or olive buff lamellate to subporoid hymenophore, with anastomosing and interveined gills and basal mycelium whitish to yellowish (Farid et al. 2018). Moreover, those genera are phylogenetically distant from *Erythrophylloporus*. (Bandala et al. 2004, Neves & Halling 2010, Neves et al. 2012, Zeng et al. 2013, Farid et al. 2018).

Interestingly, *Phylloporus coccineus* Corner, described from Singapore (Corner 1970), is similar to *Erythrophylloporus* species, in that it produces crimson to scarlet, lamellate basidiomata with orange to orange-red lamellae and yellow basal mycelium, broadly ellipsoid to subglobose and smooth basidiospores. It probably should also be transferred to *Erythrophylloporus,* but we refrain from doing so until specimens become available for molecular study. According to the protologue of *P. coccineus*, it differs from the newly described Asian species of *Erythrophylloporus* by having larger basidiospores (7.5–10 × 6.5–8 μm), larger cheilocystidia (70–120 × 10–18 μm) and larger caulocystidia (up to 200 × 10–16 μm) (Corner 1970).

Erythrophylloporus species formed two clades, an Asian species clade (BS = 65% and PP = 1) and a New World species clade (BS = 100% and PP = 1) (Fig. 1). The Asian one contains three species, *E. cinnabarinus*, *E. paucicarpus* and *E. suthepensis*, while the American clade contains the remaining two species *E. aurantiacus* and *E. fagicola*. *Erythrophylloporus aurantiacus* and *E. fagicola* seem to be genetically very close to each other, much closer than the species in the Asian clade. Only morphological differences between the two species were used to separate them from each other. *Erythrophylloporus fagicola* produces larger basidiospores than *E. aurantiacus* and pleurocystidia are somewhat thick-walled (0.8–3.5 μm thick) in *E. fagicola*, whereas they are thin-walled in *E. aurantiacus* and the latter has non-staining context, whereas the former has a cyanescent context. However, the descriptions were based on a limited number of collections and more samples are desirable to verify whether the morphological traits observed are good characters differentiating the two species or merely extremes of a continuum in morphological variation within a single species.

Regarding the phylogenetic affinities of *Erythrophylloporus*, Zhang and Li (2018) reported that it was likely close to the genus *Rugiboletus* G. Wu & Zhu L. Yang and *Lanmaoa* G. Wu & Zhu L. Yang, based on a multilocus dataset of nrLSU, *tef*1, *rpb*1

and *rpb*2, although this relationship was not supported in their phylogram. In our phylogeny, based on a multilocus dataset of *atp*6, *tef*1, *rpb*2 and *cox*3, with wider taxon sampling, *Erythrophylloporus* also clustered within the *Pulveroboletus* group, but was sister to *Singerocomus* with high bootstrap support (96%) but relatively weak posterior probability support (0.86). *Singerocomus* contains three species, *S. atlanticus* A.C. Magnago, *S. inundabilis* (Singer) T.W. Henkel and *S. rubriflavus* T.W. Henkel & Husbands that have some similar morphological characters to *Erythrophylloporus*, including red-orange to red pileus and light yellow basal mycelium. The three existing *Singerocomus* species are clearly different from all known *Erythrophylloporus* species by having a poroid, non-cyanescent hymenophore (Henkel et. al. 2016, Magnago et al. 2018). However, the hymenophore structure (lamellate vs. poroid) is not sufficient to separate genera in Boletaceae. *Phylloporus* currently contains both lamellate and poroid species, although some poroid species have already been transferred to another genus, *Hourangia* (Zhu et al. 2015). Phylogenetic analyses, including the remaining poroid *Phylloporus* species, are needed to verify their taxonomic position.

Erythrophylloporus putatively forms ectomycorrhizal associations with trees in family Fagaceae, including the genera *Fagus*, *Lithocarpus* and *Quercus* (Neves and Halling 2010, Montoya and Bandala 2011, Zhang and Li 2018). The two Thai *Erythrophylloporus* species were found in forests dominated by Dipterocarpaceae trees, mainly *Dipterocarpus*, including *D. tuberculatus*, *D. obtusifolius* and *Shorea*, including *S. obtusa* and *S. siamensis*. However, some *Quercus* and *Lithocarpus* trees (Fagaceae) were also observed in the vicinity and could also be the ectomycorrhizal partners. Further study is needed to confirm the ectomycorrhizal relationships of *Erythrophylloporus*.

Acknowledgements

Financial support from the Graduate School, Chiang Mai University, is appreciated. The work was partly supported by a TRF Research Team Association Grant (RTA5880006) to SL and OR. OR is grateful to the Fonds National de la Recherche Scientifique (Belgium) for travel grants. Authors are grateful for the permit number 0907.4/4769 granted by the Department of National Parks, Wildlife and Plant Conservation, Ministry of Natural Resources and Environment for collecting in Doi Suthep-Pui National Park.

References

Bandala VM, Montoya L, Jarvio D (2004) Two interesting records of boletes found in coffee plantations in eastern Mexico. Persoonia 18: 365–380.

Binder M, Hibbett DS (2006) Molecular systematics and biological diversification of Boletales. Mycologia 98: 971–981. https://doi.org/10.1080/15572536.2006.11832626

Binder M, Larsson KH, Matheny PB, Hibbett DS (2010) Amylocorticiales ord. nov. and Jaapiales ord. nov.: early diverging clades of agaricomycetidae dominated by corticioid forms. Mycologia 102: 865–880. https://doi.org/10.3852/09-288

Chuankid B, Vadthanarat S, Hyde KD, Thongklang N, Zhao R, Lumyong S, Raspé O (2019) Three new *Phylloporus* species from tropical China and Thailand. Mycological Progress 18(5): 603–614. https://doi.org/10.1007/s11557-019-01474-6

Corner EJH (1970) *Phylloporus* Quél. and *Paxillus* Fr. in Malaya and Borneo. Nova Hedwigia 20: 793–822.

Darriba D, Taboada GL, Doallo R, Posada D (2012) jModelTest 2: more models, new heuristics and parallel computing. Nature Methods 9: 772. https://doi.org/10.1038/nmeth.2109

Doyle JJ, Doyle JL (1990) Isolation of plant DNA from fresh tissue. Focus 12: 13–15. https://doi.org/10.2307/2419362

Farid A, Gelardi M, Angelini C, Franck AR, Costanzo F, Kaminsky L, Ercole E, Baroni TJ, White AL, Garey JR, Smith ME, Vizzini A (2018) *Phylloporus* and *Phylloboletellus* are no longer alone: *Phylloporopsis* gen. nov. (Boletaceae), a new smooth-spored lamellate genus to accommodate the American species *Phylloporus boletinoides*. Fungal Systematics and Evolution 2: 341–359. https://doi.org/10.3114/fuse.2018.02.10

Halling RE, Mueller GM, Dallwitz MJ (1999) A new *Phylloporus* (Basidiomycetes, Boletaceae) with a key to species in Colombia and Costa Rica. Mycotaxon 73: 63–67.

Halling RE, Nuhn M, Fechner NA, Osmundson TW, Soytong K, Arora D, Hibbett DS, Binder M (2012a) *Sutorius*: a new genus for *Boletus eximius*. Mycologia 104(4): 951–961. https://doi.org/10.3852/11-376

Halling RE, Nuhn M, Osmundson T, Fechner N, Trappe JM, Soytong K, Arora D, Hibbett DS, Binder M (2012b) Affinities of the *Boletus chromapes* group to *Royoungia* and the description of two new genera, *Harrya* and *Australopilus*. Australian Systematic Botany 25: 418–431. https://doi.org/10.1071/SB12028

Henkel TW, Obase K, Husbands D, Uehling JK, Bonito G, Aime MC, Smith ME (2016) New Boletaceae taxa from Guyana: *Binderoboletus segoi* gen. and sp. nov., *Guyanaporus albipodus* gen. and sp. nov., *Singerocomus rubriflavus* gen. and sp. nov., and a new combination for *Xerocomus inundabilis*. Mycologia 108(1): 157–173. https://doi.org/10.3852/15-075

Hosen MI, Feng B, Wu G, Zhu XT, Li YC, Yang ZL (2013) *Borofutus*, a new genus of Boletaceae from tropical Asia: phylogeny, morphology and taxonomy. Fungal Diversity 58: 215–226. https://doi.org/10.1007/s13225-012-0211-8

Katoh K, Standley DM (2013) MAFFT Multiple sequence alignment software version 7: improvements in performance and usability. Molecular Biology and Evolution 30: 772–780. https://doi.org/10.1093/molbev/mst010

Kornerp A, Wanscher JH (1978) Methuen Handbook of Colour (3rd edn). Eyre Methuen Ltd, London, 252 pp.

Kretzer AM, Bruns TD (1999) Use of *atp*6 in fungal phylogenetics: an example from the Boletales. Molecular Phylogenetics and Evolution 13: 483–492. https://doi.org/10.1006/mpev.1999.0680

Li YC, Feng B, Yang ZL (2011) *Zangia*, a new genus of Boletaceae supported by molecular and morphological evidence. Fungal Diversity 49: 125–143. https://doi.org/10.1007/s13225-011-0096-y

Li YC, Li F, Zeng NK, Cui YY, Yang ZL (2014) A new genus *Pseudoaustroboletus* (Boletaceae, Boletales) from Asia as inferred from molecular and morphological data. Mycological Progress 13: 1207–1216. https://doi.org/10.1007/s11557-014-1011-1

Magnago AC, Henkel T, Neves MA, Borges da Silveira RM (2018) *Singerocomus atlanticus* sp. nov., and a first record of *Singerocomus rubriflavus* (Boletaceae, Boletales) for Brazil. Acta Botanica Brasilica 32(2): 222–231. https://doi.org/10.1590/0102-33062017abb0320

Matheny PB (2005) Improving phylogenetic inference of mushrooms with RPB1 and RPB2 nucleotide sequences (*Inocybe*; Agaricales). Molecular Phylogenetics and Evolution 35: 1–20. https://doi.org/10.1016/j.ympev.2004.11.014

Miller MA, Holder MT, Vos R, Midford PE, Liebowitz T, Chan L, Hoover P, Warnow T (2009) The CIPRES portals. CIPRES. http://www.phylo.org/portal2/home

Montoya L, Bandala VM (2011) A new *Phylloporus* from two relict *Fagus grandifolia* var. *mexicana* populations in a montane cloud forest. Mycotaxon 117: 9–18. https://doi.org/10.5248/117.9

Neves MA, Binder M, Halling R, Hibbett D, Soytong K (2012) The phylogeny of selected *Phylloporus* species inferred from NUC-LSU and ITS sequences, and descriptions of new species from the Old World. Fungal Diversity 55(1): 109–123. https://doi.org/10.1007/s13225-012-0154-0

Neves MA, Halling RE (2010) Study on species of *Phylloporus* I: Neotropics and North America. Mycologia 102(4): 923–943. https://doi.org/10.3852/09-215

Nuhn ME, Binder M, Taylor AFS, Halling RE, Hibbett DS (2013). Phylogenetic overview of the Boletineae. Fungal Biology 117: 479–511. https://doi.org/10.1016/j.funbio.2013.04.008

Orihara T, Lebel T, Ge Z-W, Smith ME, Maekawa N (2016) Evolutionary history of the sequestrate genus *Rossbeevera* (Boletaceae) reveals a new genus *Turmalinea* and highlights the utility of ITS minisatellite-like insertions for molecular identification. Persoonia 37: 173–198. https://doi.org/10.3767/003158516X691212

Orihara T, Smith ME, Shimomura N, Iwase K, Maekawa N (2012) Diversity and systematics of the sequestrate genus *Octaviania* in Japan: two new subgenera and eleven new species. Persoonia 28: 85–112. https://doi.org/10.3767/003158512X650121

Phookamsak R, Hyde KD, Jeewon R, Bhat DJ, Jones EBG, Maharachchikumbura SSN et al. (2019) Fungal diversity notes 929–1035: taxonomic and phylogenetic contributions on genera and species of fungi. Fungal Diversity. https://doi.org/10.1007/s13225-019-00421-w

Raspé O, Vadthanarat S, De Kesel A, Degreef J, Hyde KD, Lumyong S (2016) *Pulveroboletus fragrans*, a new Boletaceae species from Northern Thailand, with a remarkable aromatic odor. Mycological Progress 15: 38. https://doi.org/10.1007/s11557-016-1179-7

Rehner SA, Buckley E (2005) A *Beauveria* phylogeny inferred from nuclear ITS and EF1-α sequences: evidence for cryptic diversification and links to *Cordyceps* teleomorphs. Mycologia 97: 84–98. https://doi.org/10.3852/mycologia.97.1.84

Ronquist F, Teslenko M, Van Der Mark P, Ayres DL, Darling A, Höhna S, Larget B, Liu L, Suchard MA, Huelsenbeck JP (2012) MrBayes 3.2: Efficient Bayesian phylogenetic inference and model choice across a large model space. Systematic Biology 61: 539–542. https://doi.org/10.1093/sysbio/sys029

Stamatakis A (2006) Raxml-vi-hpc: maximum likelihood-based phylogenetic analyses with thousands of taxa and mixed models. Bioinformatics 22: 2688–2690. https://doi.org/10.1093/bioinformatics/btl446

Thiers B (continuously updated) Index Herbariorum: A Global Directory of Public Herbaria and Associated Staff. New York Botanical Garden's Virtual Herbarium. http://sweetgum.nybg.org/science/ih/

Vadthanarat S, Lumyong S, Raspé O (2019) *Cacaoporus*, a new Boletaceae genus, with two new species from Thailand. MycoKeys 54: 1–29. https://doi: 10.3897/mycokeys.54.35018

Vadthanarat S, Raspé O, Lumyong S (2018) Phylogenetic affinities of the sequestrate genus *Rhodactina* (Boletaceae), with a new species, *R. rostratispora* from Thailand. MycoKeys 29: 63–80. https://doi.org/10.3897/mycokeys.29.22572

Wu G, Feng B, Xu J, Zhu XT, Li YC, Zeng NK, Hosen MI, Yang ZL (2014) Molecular phylogenetic analyses redefine seven major clades and reveal 22 new generic clades in the fungal family Boletaceae. Fungal Diversity 69: 93–115. https://doi.org/10.1007/s13225-014-0283-8

Wu G, Li YC, Zhu XT, Zhao K, Han LH, Cui YY, Li F, Xu JP, Yang ZL (2016) One hundred noteworthy boletes from China. Fungal Diversity 81: 25–188. https://doi.org/10.1007/s13225-016-0375-8

Wu G, Zhao K, Li YC, Zeng NK, Feng B, Halling RE, Yang ZL (2015) Four new genera of the fungal family Boletaceae. Fungal Diversity 81: 1–24. https://doi.org/10.1007/s13225-015-0322-0

Zhang M, Li TH (2018) *Erythrophylloporus* (Boletaceae, Boletales), a new genus inferred from morphological and molecular data from subtropical and tropical China. Mycosystema 37(9): 1111–1126.

Zhao K, Wu G, Feng B, Yang ZL (2014a) Molecular phylogeny of *Caloboletus* (Boletaceae) and a new species in East Asia. Mycological Progress 13: 1127–1136. https://doi.org/10.1007/s11557-014-1001-3

Zhao K, Wu G, Yang ZL (2014b) A new genus, *Rubroboletus*, to accommodate *Boletus sinicus* and its allies. Phytotaxa 188: 61–77. https://doi.org/10.11646/phytotaxa.188.2.1

Zeng NK, Tang LP, Li YC, Tolgor B, Zhu XT, Zhao Q, Yang ZL (2013) The genus *Phylloporus* (Boletaceae, Boletales) from China: morphological and multilocus DNA sequence analyses. Fungal Diversity 58: 73–101. https://doi.org/10.1007/s13225-012-0184-7

Zhu XT, Wu G, Zhao K, Halling RE, Yang ZL (2015) *Hourangia*, a new genus of Boletaceae to accommodate *Xerocomus cheoi* and its allied species. Mycological Progress 14: 37. https://doi.org/10.1007/s11557-015-1060-0

MycoKeys 55: 59–86 (2019)
doi: 10.3897/mycokeys.55.35682
http://mycokeys.pensoft.net

RESEARCH ARTICLE

A peer-reviewed open-access journal
MycoKeys
Launched to accelerate biodiversity research

Extensive sampling and high-throughput sequencing reveal *Posidoniomyces atricolor* gen. et sp. nov. (Aigialaceae, Pleosporales) as the dominant root mycobiont of the dominant Mediterranean seagrass *Posidonia oceanica*

Martin Vohník[1,2], Ondřej Borovec[1,2], Zuzana Kolaříková[1], Radka Sudová[1], Martina Réblová[3]

1 *Department of Mycorrhizal Symbioses, Institute of Botany, Czech Academy of Sciences, Lesní 322, 252 43 Průhonice, Czech Republic* **2** *Department of Experimental Plant Biology, Faculty of Science, Charles University, Viničná 5, 128 44 Prague, Czech Republic* **3** *Department of Taxonomy, Institute of Botany, Czech Academy of Sciences, Zámek 1, 252 43 Průhonice, Czech Republic*

Corresponding author: *Martin Vohník* (vohnik@ibot.cas.cz)

Academic editor: *Huzefa Raja* | Received 23 April 2019 | Accepted 6 June 2019 | Published 26 June 2019

Citation: Vohník M, Borovec O, Kolaříková Z, Sudová R, Réblová M (2019) Extensive sampling and high-throughput sequencing reveal *Posidoniomyces atricolor* gen. et sp. nov. (Aigialaceae, Pleosporales) as the dominant root mycobiont of the dominant Mediterranean seagrass *Posidonia oceanica*. MycoKeys 55: 59–86. https://doi.org/10.3897/mycokeys.55.35682

Abstract

Seagrasses provide invaluable ecosystem services yet very little is known about their root mycobiont diversity and distribution. Here we focused on the dominant Mediterranean seagrass *Posidonia oceanica* and assessed its root mycobiome at 32 localities covering most of the ecoregions in the NW Mediterranean Sea using light and scanning electron microscopy and tag-encoded 454-pyrosequencing. Microscopy revealed that the recently discovered dark septate endophytic association specific for *P. oceanica* is present at all localities and pyrosequencing confirmed that the *P. oceanica* root mycobiome is dominated by a single undescribed pleosporalean fungus, hitherto unknown from other hosts and ecosystems. Its numerous slow-growing isolates were obtained from surface-sterilised root segments at one locality and after prolonged cultivation, several of them produced viable sterile mycelium. To infer their phylogenetic relationships we sequenced and analysed the large (LSU) and small (SSU) subunit nrDNA, the ITS nrDNA and the DNA-directed RNA polymerase II (*RPB2*). The fungus represents an independent marine biotrophic lineage in the Aigialaceae (Pleosporales) and is introduced here as *Posidoniomyces atricolor* **gen. et sp. nov.** Its closest relatives are typically plant-associated saprobes from marine, terrestrial and freshwater habitats in Southeast Asia and Central America. This study expands our knowledge and diversity of the Aigialaceae, adds a new symbiotic lifestyle to this family and provides a formal name for the dominant root mycobiont of the dominant Mediterranean seagrass.

Keywords
dark septate endophytes, Dothideomycetes, marine fungi, root endophytes, seagrasses

Introduction

Although the occurrence of marine saprobic and endophytic fungi on mangroves and salt marsh plants is well-documented (e.g. Jones 1963; Jones and Pang 2012; Kohlmeyer and Kohlmeyer 1971; Gessner and Kohlmeyer 1976; Kohlmeyer and Volkmann-Kohlmeyer 1991, 2001, 2002), the mycobiota of seagrasses is generally neglected and relatively little understood (e.g. Kohlmeyer 1963; Kohlmeyer and Kohlmeyer 1979; Cuomo et al. 1985; Alva et al. 2002; Gnavi et al. 2014). Seagrasses are perennial flowering plants represented by several genera inhabiting shore environments practically everywhere outside the Arctic and Antarctic, but mainly in temperate, subtropical and especially tropical littoral zones. All seagrass genera are accommodated in various families of a single order, the Alismatales (Monocotyledons). Unlike most terrestrial and many aquatic plants, seagrasses seem to be devoid of mycorrhizae (Nielsen et al. 1999) and a specific root-fungus association has been so far reported only for a single seagrass species (Vohník et al. 2015).

Posidonia (Posidoniaceae) is the evolutionary oldest seagrass genus with the earliest fossil record from the Cretaceous (den Hartog 1970). It has a uniquely discontinuous distribution with eight of its nine species occurring in the Southern Hemisphere along the coast of Australia (Green and Short 2003). In our study, we focused on root mycobionts of the only non-Australian species, i.e. the dominant and endemic Mediterranean seagrass *Posidonia oceanica*. In the Mediterranean Sea, *P. oceanica* forms extensive clonal meadows which can be hundreds to thousands of years old and spread over one to several (up to 15) kilometres (Arnaud-Haond et al. 2012). These vast meadows are the primary source of carbon for the coastal ecosystems and, additionally, they play an important role in defining the coastal line and supply biogenic detritus made of seagrass roots, rhizomes and leaf debris entangling other living organisms like molluscs, algae or foraminifera (De Falco et al. 2017). Unlike other seagrasses, *P. oceanica* typically forms extensive branched root systems (Figure 1a) which support formation of "matte" (Figure 1b, c), i.e. a peat-like seabed layer which is exceptionally resistant to microbiological decay and may be up to several metres thick (Hemminga and Duarte 2000; Serrano et al. 2012).

The mycobiota of *P. oceanica* only recently gained appropriate attention; from the few available reports it seems to be predominated by fungi belonging to three classes and five orders of Ascomycota, i.e. Dothideomycetes (Pleosporales, Capnodiales), Leotiomycetes (Helotiales) and Sordariomycetes (Lulworthiales, Microascales and *Papulaspora* incertae sedis). These include obligate marine lignicolous fungi, ubiquitous surface-dwelling saprobes and endophytic fungi colonising roots, rhizomes and leaves, thus forming tighter (symbiotic) relationships with the host plant. Typically, they were growing on living or decaying plant parts (Kohlmeyer 1963; Cuomo et al. 1985) or were isolated as sterile mycelia and identified only by DNA sequence analysis (Panno et al. 2013; Gnavi et al. 2014; Vohník et al. 2016, 2017). They either belong to well-studied genera (e.g. *Corollospora*, *Halotthia*, *Lulworthia* and *Papulaspora*) or represent new marine lineages.

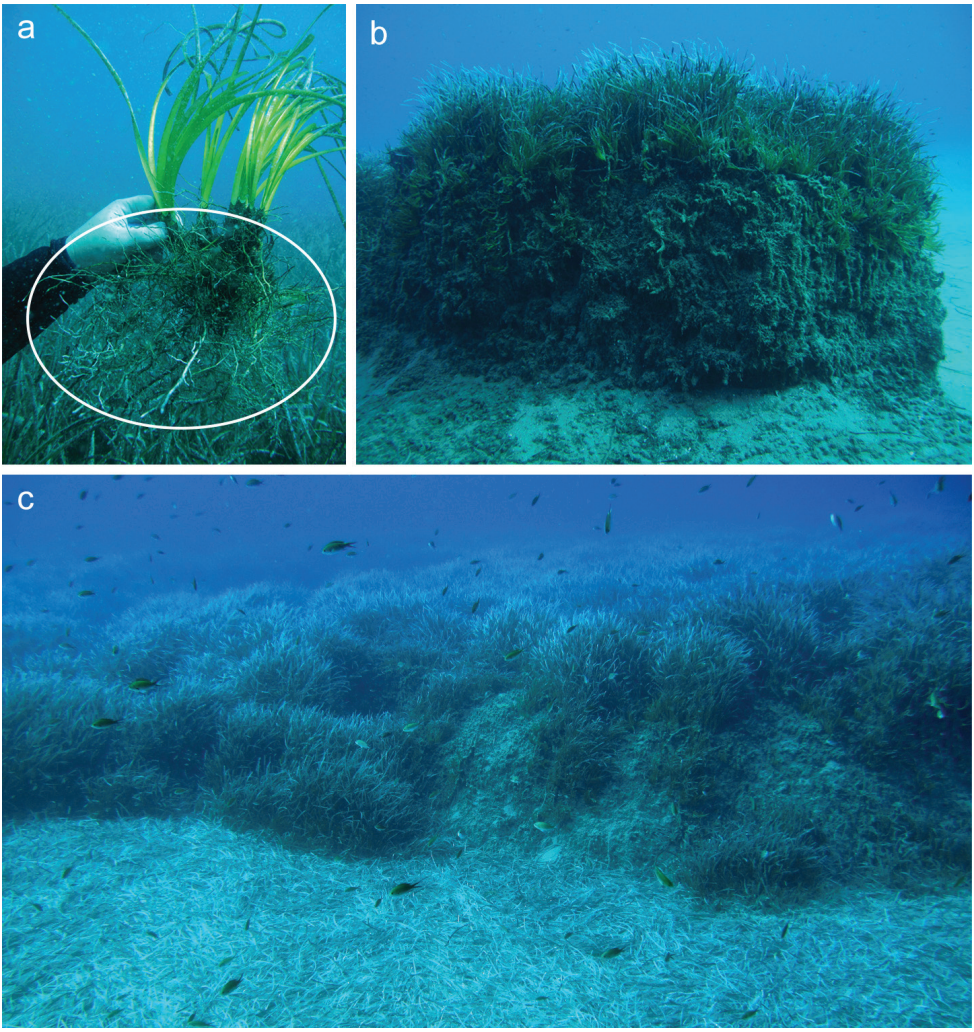

Figure 1. The dominant Mediterranean seagrass *Posidonia oceanica*. **a** Overall appearance, note dense branched root system of the seagrass (encircled) **b** *Posidonia oceanica* growing on an approx. 1.5 m thick layer of matte **c** typical habitat of the dominant Mediterranean seagrass, note the layer of shed seagrass leaves on the seabed.

Our previous microscopic observations revealed that living terminal roots of *P. oceanica*, particularly their surface and the thick-walled hypodermis, are regularly colonised by an unknown fungus with dark septate hyphae (Vohník et al. 2015). The resulting association resembles colonisation by the so-called dark septate endophytes (DSE) which regularly occur in the roots of most terrestrial plants (e.g. Jumpponen and Trappe 1998; Vohník and Albrechtová 2011; Lukešová et al. 2015) but seemed to be absent in the marine environment. The association is characterised by the formation of sparse, dark pigmented hyphae, dense finger-like pseudoparenchymatous nets

or loose hyphal sheaths on the root surface and melanised intracellular microsclerotia in the hypodermis. However, in contrast to typical terrestrial DSE, although the dark septate hyphae were also infrequently observed inside rhizodermal cells, they never colonised vascular tissues of the host roots. Interestingly, this association was absent in the roots of *Cymodocea nodosa*, a widely distributed seagrass in the Mediterranean Sea which sometimes accompanies *P. oceanica* (Vohník et al. 2015).

In our previous work focused on the diversity and distribution of *P. oceanica* root mycobionts, cultivations and 454-pyrosequencing of fungal DNA from surface-sterilised root segments from a few localities in the NW Mediterranean Sea revealed a relatively narrow fungal community lacking typical terrestrial and freshwater endophytes and mycorrhizal fungi (Vohník et al. 2016, 2017). This unusually limited fungal spectrum (cf. Kohout et al. 2012, 2013; Bruzone et al. 2017) was dominated by a single dark-pigmented mycobiont tentatively named "Pleosporales sp. MV-2012" (Vohník et al. 2016). Interestingly, this symbiotic fungus has not been documented in any of the other studies on *P. oceanica* mycobiota (see above) and to our knowledge it is not known from any other hosts and environments. Its extremely slow growth and characteristic colony morphology enable unequivocal identification already during the isolation stage but spore formation has never been observed (Vohník et al. 2016). Consequently, despite the striking DSE root colonisation pattern in vivo (Vohník et al. 2015), the absence of sexual characters and the lack of formation of conidia and conidiophores in axenic culture, either on agar media (standard or containing salt water) or on surface-sterilised root segments placed on nutrient media, pose a difficulty in estimating precise phylogenetic relationships of this dominant *P. oceanica* root mycobiont. Nevertheless, its preliminary position in the Aigialaceae (Pleosporales, Dothideomycetes), based on sequences of the partial nuclear large subunit (nucLSU) 28S rDNA gene, was discussed in Vohník et al. (2016).

The present study was motivated by the need to confirm the presence/dominance of the pleosporalean DSE fungus in the *P. oceanica* root mycobiota at a much larger scale than previously studied as well as the need for circumscription and precise phylogenetic placement of this mycobiont into the fungal system. Thus, we characterised *P. oceanica* root mycobionts using tag-encoded 454-pyrosequencing at 32 localities in the NW Mediterranean Sea (covering the distribution of *P. oceanica* from its westernmost localities to the boundary between the Western and Eastern Mediterranean basins). We also isolated and characterised *P. oceanica* root mycobionts at the locality where the specific DSE association has been observed for the first time (Vohník et al. 2015). Subsequently, characteristic strains of the Pleosporales sp. MV-2012 were selected for its circumscription based on morphological characters and an analysis of a molecular data set consisting of sequences of the following nuclear markers: nucLSU, nuclear small subunit (nucSSU) 18S rDNA gene and the second largest subunit of the RNA polymerase II (*RPB*2) gene. Additionally, an analysis of the unusually divergent ITS region of nuclear rDNA was performed to screen the possible geographical variability of the dominant *P. oceanica* root mycobiont.

Materials and methods

Sampling

Posidonia oceanica root samples were collected at 32 localities in seven states in the NW Mediterranean (Figure 2) representing four out of the eight Mediterranean Sea ecoregions (Table 1; see Notarbartalo di Sciara and Agardy 2010 in Giacoumi et al. 2013) at various depths using snorkelling and scuba diving. The samples for tag-encoded 454-pyrosequencing were collected in June, July and September 2012 whereas the samples for mycobiont isolation were collected in September 2016 (Table 1). Each locality was represented by a pooled sample consisting of five subsamples taken at least 3 meters apart (see Vohník et al. 2016).

Characterisation of *P. oceanica* root mycobionts by 454-pyrosequencing

For 454-pyrosequencing, root samples of the same weight representing individual localities were pooled into six sample sets (Figure 2, Table 1). DNA extraction, PCR amplification and sequencing was conducted as in Vohník et al. (2017). Briefly, after DNA extraction from surface-sterilised *P. oceanica* fine roots conducted using DNeasy Plant Mini Kit (Qiagen), the ITS region of the nrDNA was amplified in a two-step PCR with primers ITS1F/ITS4 (White et al. 1990; Gardes and Bruns 1993) in the first step. One negative control was included in the PCR analyses. From each DNA extract, two independent PCR reactions were run to avoid PCR bias. The obtained PCR products were then pooled, purified and used as a template for the second PCR with tagged ITS1/ITS4 primers. The resulting six samples and one negative control were purified, quantified, equimolarly mixed with other samples from the same 454-pyrosequencing plate and sequenced on the GS Junior platform (Roche).

In total, pyrosequencing yielded 32127 raw sequences which were subsequently processed in the pipeline SEED 2.0.4 (Větrovský and Baldrian 2013). Quality check (min. quality score 25) and denoising yielded 30935 sequences. Sequences shorter than 500 bp were excluded and the data set was trimmed to the 500 bp sequence length. The obtained 15951 sequences were then clustered to molecular OTUs (MOTUs) using UPARSE implementation in USEARCH 8.1.1861 (Edgar 2013) with 97% similarity threshold. Chimeric sequences identified in this step (198) were deleted to prevent diversity overestimation. Also 81 global singletons were removed from the data set. The consensus sequences were constructed for each MOTU using MAFFT v.7.222 alignments (Katoh et al. 2009), based on the most abundant nucleotide at each position. These consensus sequences were then checked for their closest hits by BLAST algorithm using UNITE (Kõljalg et al. 2013) and GenBank (Sayers et al. 2019) as reference databases. Main MOTUs obtained in this study are listed in Table 2.

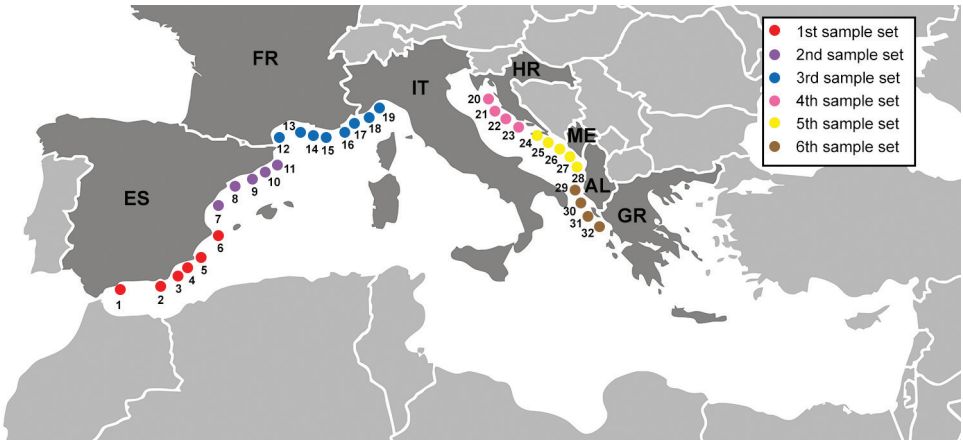

Figure 2. Map of the Mediterranean Sea with location of our 32 sampling sites. For further details see Table 1.

Isolation and characterisation of *P. oceanica* root mycobionts at the original locality

Root mycobionts were isolated from surface-sterilised terminal fine roots as described in Vohník et al. (2016) except that ten different media, amended with Novobiocin sodium salt (50 mg/L; Sigma-Aldrich, Germany) to prevent growth of bacteria, were used. These included glucose peptone yeast agar (GPYA; glucose 40 g, peptone 5 g, yeast extract 5 g and agar 15 g dissolved in 1 L of deionized water), GPYA + *Posidonia* extract, malt extract (MEA; HiMedia Pvt. Ltd., India), MEA + *Posidonia* extract, MEA with mycological peptone (MEAP; HiMedia), MEAP + *Posidonia* extract, modified Melin-Norkrans medium (MMN; Marx 1969), MMN + *Posidonia* extract, potato dextrose agar (PDA; HiMedia) and PDA + *Posidonia* extract. The *Posidonia* extract was prepared by soaking 200 g of *P. oceanica* leaves, roots, rhizomes and matte at 60 °C in 1 L of seawater for 30 min (Panno et al. 2013), filtrated and 100 mL of the filtrate was mixed with 900 mL of the respective media.

Segments of the surface-sterilised terminal fine roots (ca. 3–5 mm long) were incubated on the surface of the abovementioned solidified media at room temperature in the dark and periodically checked for mycelial growth. There were 50 segments per each medium in two square 25-compartment plastic Petri dishes, i.e. 500 segments in total. The incubation was terminated after ca. 10 months (28th September 2016 – 3rd July 2017) and the obtained isolates were conservatively grouped into several morphotypes using stereomicroscopy and colony characteristics according to Vohník et al. (2016).

DNA extraction, amplification and Sanger sequencing

DNA was extracted from multiple isolates of each morphotype/medium combination using Extract-N-Amp Plant Kits (Sigma-Aldrich, Germany) following manufacturer's instructions. Primers used for the amplification of genes and gene regions included: 1)

Table 1. List of the *Posidonia oceanica* localities sampled in this study.

Sample set[1]	Locality #[2]	Locality code[3]	Locality name	Locality ecoregion[4]	GPS coordinates	Sampling time
1st	1	ES-21	Bahía de la Plata, Estepona	Alboran Sea	36.42749N, 5.12923W	VII/2012
	2	ES-22	Cabo de Gata	dtto	36.72595N, 2.19537W	VII/2012
	3	ES-23	Villaricos	Algero-Provencal Basin	37.26676N, 1.75151W	VII/2012
	4	ES-27	Cope, Calabardina	dtto	37.43672N, 1.48422W	VII/2012
	5	ES-24	Cabo de Palos	dtto	37.63355N, 0.68996W	VII/2012
	6	ES-25	Calp, Cala el Racó	dtto	38.63556N, 0.07124E	VII/2012
2nd	7	ES-28	Platja de Capicorb, Torreblanca	dtto	40.20711N, 0.25956E	VII/2012
	8	ES-26	Platja dels Muntanyans, Torredembarra	dtto	41.14475N, 1.41552E	VII/2012
	9	ES-11	Platja de Llafranc, Callela de Palafrugell	dtto	41.89343N, 3.19391E	VI/2012
	10	ES-10	Platja de Tamariu	dtto	41.91756N, 3.20761E	VI/2012
	11	ES-9	Cala Montgó, L'Escala	dtto	42.10744N, 3.16892E	VI/2012
	12	FR-8	Anse de Paulilles, Paulilles	dtto	42.50236N, 3.12456E	VII/2012
3rd	13	FR-20	Les Arnettes	dtto	43.32922N, 5.03849E	VI/2012
	14	FR-7	Baie de Cousse, Sanary-sur-Mer	dtto	43.12054N, 5.77545E	VI/2012
	15	FR-19	Cabasson	dtto	43.09926N, 6.32504E	VI/2012
	16	FR-6	Cap Roux, Saint-Raphaël	dtto	43.45026N, 6.91951E	VI/2012
	17	FR-5	Antibes	dtto	43.55726N, 7.12209E	VI/2012
	18	IT-4	Finale Ligure	dtto	44.17337N, 8.36765E	VI/2012
	19	IT-3	Mulinetto Beach, Cogoleto	dtto	44.38016N, 8.63467E	VI/2012
4th	20	HR-37	Neviđane	Adriatic Sea	43.98368N, 15.33831E	IX/2012
	21	HR-38	Dobropoljana	dtto	43.98713N, 15.33295E	IX/2012
	22	HR-39	Žman	dtto	44.00308N, 15.05930E	IX/2012
	23	HR-2	Kukuljar	dtto	43.75960N, 15.63410E	IX/2012
5th	24	HR-1	Borak	dtto	42.92236N, 17.34685E	IX/2012 & IX/2016
	25	ME-36	Krimovica	dtto	42.27985N, 18.78738E	IX/2012
	26	ME-35	Sveti Stefan I	dtto	42.25022N, 18.89463E	IX/2012
	27	ME-34	Petrovac	dtto	42.19762N, 18.93726E	IX/2012
	28	ME-33	Crni Rt, Sutomore	dtto	42.13595N, 19.01549E	IX/2012
6th	29	AL-31	Orikum I	dtto	40.34226N, 19.40898E	IX/2012
	30	AL-32	Orikum II	dtto	40.35723N, 19.40926E	IX/2012
	31	GR-30	Kalamionas Beach, Kassiopi	Ionian Sea	39.78941N, 19.91542E	IX/2012
	32	GR-29	Kalami	dtto	39.74227N, 19.93443E	IX/2012

[1] grouping for pyrosequencing, see Materials and Methods

[2] sequential numbering corresponding to Figure 2 (along the coast from west to east)

[3] continues from Vohník et al. 2015, 2016 and 2017. AL = Albania, ES = Spain, FR = France, GR = Greece, HR = Croatia, IT = Italy, ME = Montenegro

[4] according to Notarbartalo di Sciara and Agardy (2010) in Giacoumi et al. (2013)

NS7, ITS1F, ITS2 and ITS4 (White et al. 1990; Gardes and Bruns 1993) for the ITS nrDNA, 2) LR0R and LR5 (Vilgalys and Hester 1990; Vilgalys unpublished: www.botany.duke.edu /fungi/mycolab) for the partial nucLSU (D1 and D2 domains), 3) NSSU131 and NS24 (Gargas and Taylor 1992; Kauff and Lutzoni 2002) for the whole

Table 2. List of main MOTUs (with at least 10 sequences) obtained in this study by tag-encoded 454-pyrosequencing.

MOTU #	Number of sequences in each sample set[1]						Total sequences	Closest match in GenBank/UNITE[2]	Identity of the closest match (species hypothesis in UNITE)	Origin/country of the closest match
	1	2	3	4	5	6				
1*	1566	1661	3279	2757	2131	2447	13841	KC412712	Pleosporales sp. MV-2012 (SH215217.07FU)	*Posidonia oceanica* root/France
2*	59	88	244	0	19	1	411	KC412712	Pleosporales sp. MV-2012 (SH215217.07FU)	*P. oceanica* root/France
5	80	16	0	0	13	12	121	KY859194	*Alternaria alternata*	Black Spot on *Rhodiola rosea*/China
6	0	101	0	0	0	0	101	JX974800	fungal sp. (SH482095.07FU)	polluted estuarine sediment/China
7	17	0	0	30	0	0	47	KY977441	*Pseudopithomyces chartarum*	endophytic in *Sophora moorcroftiana*/China(?)
10	2	27	0	0	0	0	29	KU869767	*Lobulomyces* sp.	endophytic in *Gracilariopsis lemaneiformis*/China(?)
11	0	23	0	0	0	0	23	KX449413	*Lepista nuda* (SH218331.07FU)	fruitbody/France
12	0	0	0	22	0	0	22	GU062266	*Phlebia tremellosa* (SH175372.07FU)	wood of *Alnus incana*/Latvia
13	15	0	0	0	7	0	22	MF435073	*Epicoccum nigrum*	leaves of *Physalis peruviana*/Ecuador
16	7	3	0	9	0	0	19	KF719965	*Lulwoana* sp. (SH174303.07FU)	*P. oceanica* root/Italy
17	5	0	0	14	0	0	19	KY977441	*Pseudopithomyces chartarum*	endophytic in *Sophora moorcroftiana*/China(?)
18	0	18	0	0	0	0	18	JF449459	Pezizomycotina sp. (SH208929.07FU)	*Fagus sylvatica* leaf litter/Austria
19	0	0	0	16	0	0	16	HQ436045	*Malassezia* sp. (SH176394.07FU)	*Axonopus compressus* soil/Singapore
21	0	0	13	0	0	0	13	KF639790	Pezizomycotina sp. (SH220055.07FU)	photographic material/Slovakia(?)
22	0	0	13	0	0	0	13	KY582119	*Cladosporium* sp.	root of *Nicotiana benthamiana*/Australia
23*	0	0	1	8	1	2	12	KC412712	Pleosporales sp. MV-2012 (SH215217.07FU)	*P. oceanica* root/France
24	0	11	0	0	0	0	11	KC965614	Chytridiomycota sp. (SH486050.07FU)	arctic soil/USA
25	11	0	0	0	0	0	11	UDB019799	*Rhodocollybia butyracea* (SH209203.07FU)	fruitbody/Estonia

[1] There were six sample sets representing different parts of the northwest Mediterranean Sea, see Materials and methods, Figure 2 and Table 1

[2] For details see Suppl. material 1

* MOTUs with closest sequence similarity to the Pleosporales sp. MV-2012 (SH215217.07FU in UNITE) (= *Posidoniomyces atricolor*)

nucSSU and 4) fRPB2-5F and fRPB2-7cR (Liu et al. 1999) for the segments 5–7 of the *RPB*2. PCR amplifications were carried out according to the methods described in Vohník et al. (2012). Primers used to sequence the purified PCR products included the amplification primers and nested primers: 1) NSSU897R, NSSU1088 and NS6 (White et al. 1990; Kauff and Lutzoni 2002) for the nucSSU and 2) RPB2-980F and RPB2-1014R (Reeb et al. 2004) for segments 5–7 of the *RPB*2 gene. Automated sequencing was carried out by Macrogen Europe Laboratory (Macrogen Inc., The Netherlands).

The obtained sequences were screened in Finch TV v.1.4.0 (https://digitalworld-biology.com/FinchTV) for possible machine errors, manually edited when needed and subjected to BLAST searches (BLASTn) in GenBank (Altschul et al. 1997). Sequences similar to identical to those previously deposited in GenBank as "Pleosporales sp. MV-2012" (Vohník et al. 2016, 2017) were aligned using ClustalW implemented in BioEdit v.7.1.8 (Hall 1999) to further screen their heterogeneity.

Sequence alignment and phylogenetic analyses

GenBank accession numbers for ITS, nucLSU, nucSSU and *RPB*2 sequences generated in this study and previously published sequences of the Aigialaceae (Pleosporales, Dothideomycetes) are listed in Suppl. material 2. Homologous nucLSU, nucSSU and *RPB*2 sequences of members of the Aigialaceae were selected from the top-scoring matches using BLASTn and retrieved from GenBank.

The nucLSU, nucSSU and *RPB*2 sequences were manually aligned in BioEdit. The *RPB*2 sequences were transformed into protein sequences maintaining a correct reading frame using the BioEdit programme. This alignment was improved by taking into account the exchangeability of amino acids with similar chemical properties at certain positions. The protein alignment was converted back into a DNA alignment. Single locus data sets for Aigialaceae (nucLSU: 46 sequences/876 characters including gaps; nucSSU: 40/1044; *RPB*2: 24/940) were assessed for conflicts using the 70% reciprocal bootstrap criterion (Mason-Gamer and Kellogg 1996) based on the comparison of the trees obtained with 1000 bootstrap (BS) replicates with RAxML-HPC v.7.0.3 (Stamatakis 2006). Conflict-free datasets were concatenated into a multi-locus alignment (deposited as TreeBASE 24210) that was subjected to a phylogenetic analysis.

Phylogenetic relationships of the Pleosporales sp. MV-2012 were inferred based on the analysis of the combined nucLSU-nucSSU-*RPB*2 sequences of 42 representatives of the Aigialaceae. Four Botryosphaeriales (*Lasiodiplodia lignicola*, *Neofusicoccum ribis*, *Phyllosticta ampelicida* and *Saccharata kirstenboschensis*) were used as an outgroup to root the tree. The first 49, 103 and 123 nt of nucLSU, nucSSU and *RPB*2 at the 5'-end and 480 and 595 nt of nucLSU and nucSSU at the 3'-end, respectively, were excluded from the alignment because of the incompleteness of the majority of sequences. Ambiguous regions were excluded from the alignment. To examine intraspecific variability, a phylogenetic analysis of 17 ITS sequences of the Pleosporales sp. MV-2012 strains and four other members of the Aigialaceae was conducted, with *Astrosphaeriella bambusae* (Pleosporales) selected

as an outgroup to root the tree. Due to a long insertion in the ITS1 in all isolates of the Pleosporales sp. MV-2012, a larger part of this sequence was not homologous with the rest of ITS1 sequences of the Aigialaceae. Therefore, the first 334 nt at the 3'-end of ITS1 were excluded and only the remaining 115 nt of ITS1, whole 5.8S and ITS2 were analysed.

The combined dataset was partitioned into three subsets of nucleotide sites (nucLSU, nucSSU, *RPB*2) for which we assumed rate heterogeneity. Maximum Likelihood (ML) and Bayesian Inference (BI) analyses were used to estimate phylogenetic relationships. ML analyses were performed with RAxML-HPC v.7.0.3 with a GTRCAT approximation. Nodal support was determined by non-parametric BS analysis with 1 000 replicates. BI analyses were performed in a likelihood framework as implemented in MrBayes v.3.2.6 (Huelsenbeck and Ronquist 2001) through the CIPRES Science Gateway v.3.3 (http://www.phylo.org) (Miller et al. 2010). For the BI approach, MrModeltest2 v.2.3 (Nylander 2008) was used to infer the appropriate substitution model that best fit the model of DNA evolution. The SYM+G model was selected according to the Akaike information criterion for ITS and all partitions of the Aigialaceae data sets. Two Bayesian searches were performed using default parameters. The B-MCMCMC analyses lasted until the average standard deviation of split frequencies was below 0.01 with trees saved every 1000 generations. The first 25% of saved trees, representing the burn-in phase of the analysis, were discarded. The remaining trees were used for calculating posterior probabilities (PP) of recovered branches. The illustration of phylogenetic relationships is a ML tree.

Results

Characterisation of *P. oceanica* root mycobionts by 454-pyrosequencing

The obtained sequences clustered into 61 MOTUs. Read numbers of 13 MOTUs detected in the negative control were subtracted from the read numbers of these particular MOTUs in each of the six samples (if present there), resulting in 14917 sequences in total remaining in the dataset. The most frequent MOTU 1 (13841 sequences in total) was present in all six sample sets (min. 1566, max. 3279 and avg. 2307 sequences per set) and matched with 99.8% similarity and 95.2% coverage with the sequence KC412712 (see Table 2) derived from the Pleosporales sp. MV-2012 (UNITE species hypothesis SH215217.07FU) isolate P15 previously obtained from *P. oceanica* surface-sterilized root segment collected at one of the localities also investigated in this study (France, Baie de Cousse, Sanary-sur-Mer; Table 1) (Vohník et al. 2016). Twenty one other MOTUs, including the second most frequent MOTU 2 (411 sequences in total) present in five sample sets (min. 1, max. 244 and avg. 69 sequences per set) matched with sequences representing the same species hypothesis SH215217.07FU (Suppl. material 1). When counting all these 22 MOTUs together, they comprised 14334 sequences, i.e. 96% of all sequences. In contrast, the two MOTUs (MOTU 16 and MOTU 48) with a close match to mycobionts from the family Lulworthiaceae were represented only by 19 and four sequences and found only in three and two sample sets, respectively (Table 2, Suppl. material 1). The third most frequent MOTU

5 represented the ubiquitous ascomycete *Alternaria alternata* and the sequences of the fourth most frequent MOTU 6 matched with an undescribed fungus (UNITE species hypothesis SH482095.07FU) from Chinese polluted estuarine sediment. All other MOTUs had each less than 100 sequences in total and represented various Ascomycota, Basidiomycota and Chytridiomycota from mostly terrestrial habitats (many as plant endophytes) of worldwide distribution (see Table 2, Suppl. material 1).

Isolation and characterisation of *P. oceanica* root mycobionts at the original locality

In total, we obtained 130 fungal mycelial isolates, i.e. 26% of the original 500 surface-sterilised root segments yielded mycelial isolates. There were no obvious effects of the isolation media on the mycelial isolate recovery except that the most isolates (i.e. 26) were obtained on PDA + *Posidonia* extract followed by PDA (23 isolates). With respect to recovery of the Pleosporales sp. MV-2012, the most efficient media were MMN and PDA + *Posidonia* extract with 55.6% and 53.8%, respectively. MMN and PDA were the two isolation media used in the first study to report the Pleosporales sp. MV-2012 from *P. oceanica* roots (Vohník et al. 2016).

Most of the obtained isolates were conservatively grouped into two dominant morphotypes, i.e. "Black" (62 isolates) and "Yellow" (38), where the former was morphologically identical to the Pleosporales sp. MV-2012 and the latter roughly corresponded to the Lulworthiales sp. MV-2012 described in Vohník et al. (2016, 2017). Approximately one third of the Black isolates, all the Yellow isolates and all remaining isolates were subjected to DNA extraction, amplification and sequencing which led to identification of 91 isolates. Since all sequenced Black isolates yielded high-quality sequences matching the Pleosporales sp. MV-2012, it was likely that also the rest of the Black isolates (i.e. those that were not selected for sequencing) belonged to this species, i.e. in total 112 isolates (ca. 86 %) were identified. Out of the identified isolates, the Pleosporales sp. MV-2012 represented 54.5%. All the Yellow isolates belonged to the Lulworthiales and matched the Lulworthiales sp. MV-2012, the Lulworthiales sp. MV-2012B (see Vohník et al. 2017) and *Lulwoana* sp. The remaining unidentified isolates either failed to amplify or produced mixed sequences suggesting their non-axenic status (data not shown).

After prolonged cultivation, several Pleosporales sp. MV-2012 isolates started to produce submerged mycelium and two of them were successfully transferred and maintained on potato carrot agar (PCA). These isolates were used for the phylogenetic analysis and the formal description of the dominant *P. oceanica* root mycobiont (see below).

Phylogenetic analysis

A previous phylogenetic analysis of nucLSU sequences of members of nine families of the Pleosporales (Vohník et al. 2016) positioned the Pleosporales sp. MV-2012 in the Aigialaceae. In line with these results, we performed a subsequent analysis and phylogenetic relationships were inferred based on the combined nucLSU-nucSSU-*RPB2* sequences of

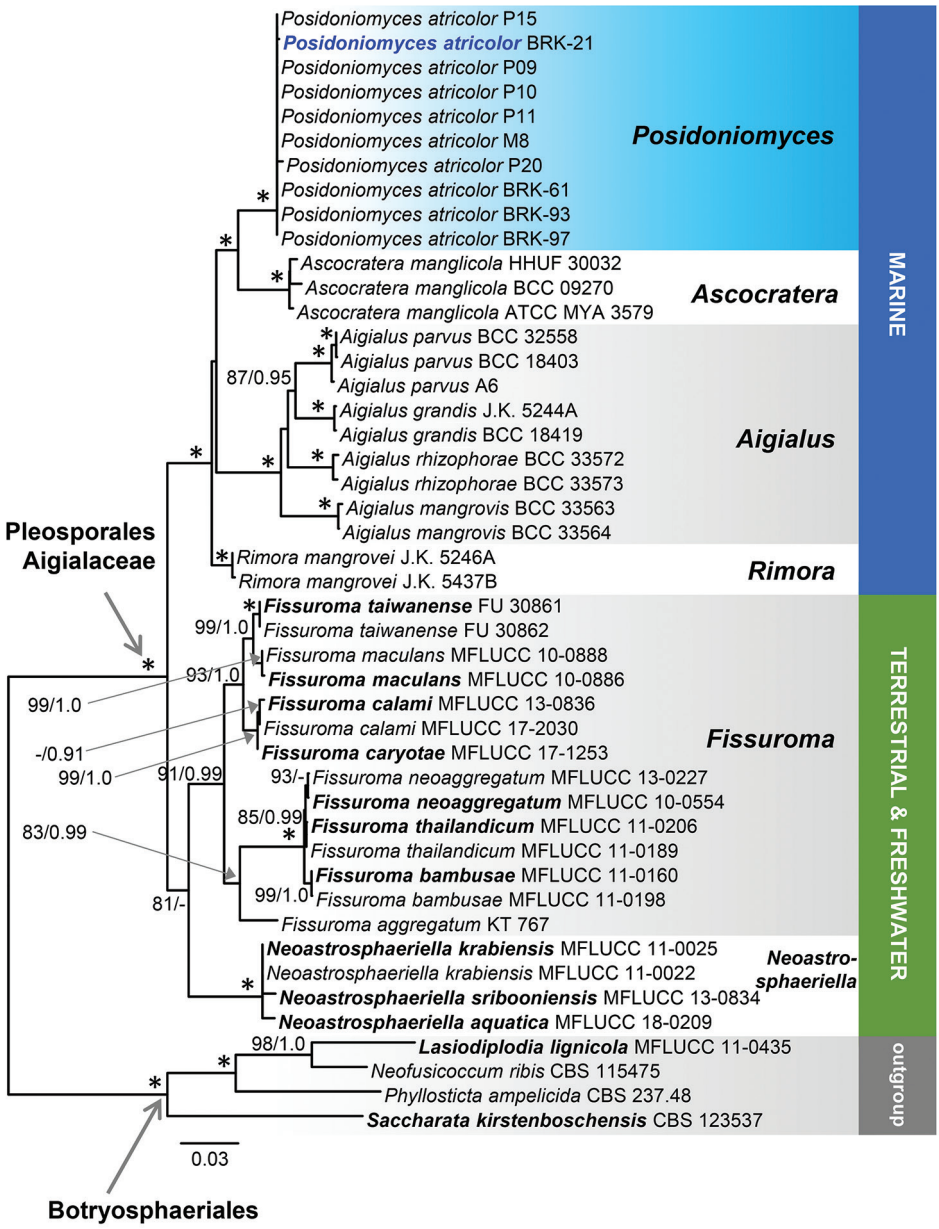

Figure 3. Phylogram generated from maximum likelihood analysis based on combined nucLSU, nucSSU and *RPB2* sequence data for *Posidoniomyces atricolor* and the Aigialaceae. Species names given in bold are type species. The ex-type of the taxonomic novelty is in bold and blue. An asterisk (*) indicates branches with ML BS = 100% and PP values = 1.0. Branch support of nodes ≥ 70 % ML BS and ≥ 0.90 PP is indicated above or below branches.

10 isolates of the Pleosporales sp. MV-2012 and 32 additional isolates representing 17 species of five genera (*Ascocratera*, *Aigialus*, *Rimora*, *Fissuroma* and *Neoastrosphaeriella*) of the Aigialaceae. The full data set consisted of 2860 characters and 936 unique char-

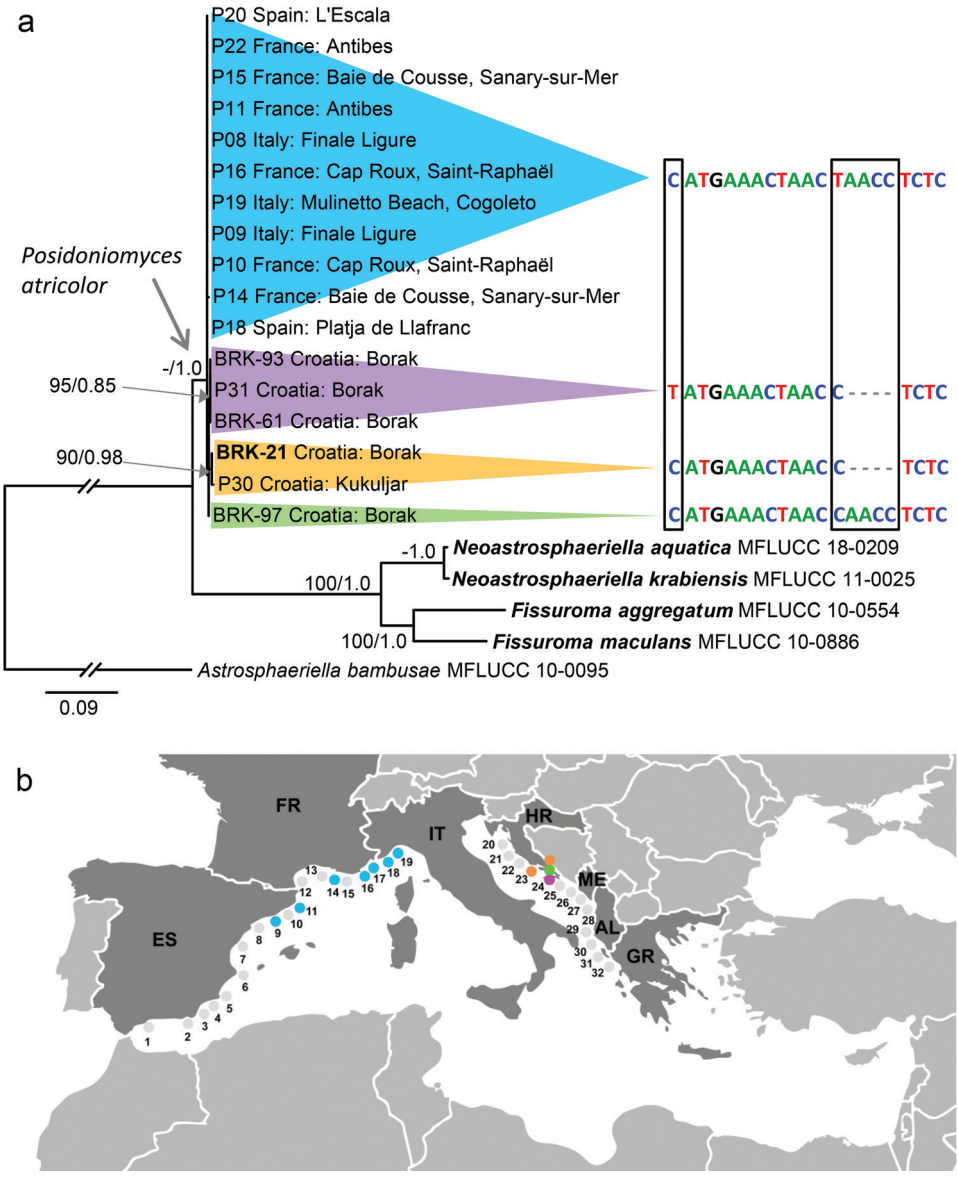

Figure 4. Phylogram and map showing a distribution pattern of *Posidoniomyces atricolor*. **a** Phylogram generated from maximum likelihood analysis based on ITS sequence data for *Posidoniomyces atricolor* and representatives of the Aigialaceae **b** map of the Mediterranean Sea with our 32 sampling sites. Sites in blue, orange, violet and green colour indicate locations of *P. atricolor* strains with corresponding mutations in ITS2 sequences.

acter sites. There were no differences in the topologies of trees generated from BI and ML analyses. In the ML tree (Figure 3), members of the Aigialaceae (100% ML BS/1.0 PP) formed two subclades defined by ecology. One subclade (81/0.84) contained taxa known only from terrestrial and freshwater habitats, i.e. *Fissuroma* and *Neoastrosphaeriella*. The other subclade (100/1.0) contained marine saprobic species of *Ascocratera*,

Aigialus and *Rimora* occurring on mangroves growing in estuarine environments and also a new marine lineage represented by the Pleosporales sp. MV-2012 associated with the roots of the seagrass *P. oceanica* and described as a new genus *Posidoniomyces* below.

The second analysis was based on ITS (partial ITS1, 5.8S and ITS2) sequences of 17 isolates of *P. atricolor* from nine localities in Croatia, France, Italy and Spain and additional four and only available ITS sequences of representatives of the Aigialaceae, *Fissuroma* and *Neoastrosphaeriella*. The data set consisted of 494 characters and 194 unique character sites. The topologies of trees from BI and ML analyses were identical. The ML tree is shown in Figure 4. *Posidoniomyces* forms monophyletic clade (49/1.0) with four subclades, which correspond to several indels in the ITS2. These changes in the primary sequence characterise populations of *P. atricolor* and their distribution pattern on the north-west coast of France and Spain and north-central part of the Adriatic coast of Croatia.

Taxonomy

***Posidoniomyces* Vohník & Réblová, gen. nov.**
MycoBank MB 830266

Diagnosis. In vivo, colonisation pattern of host roots resembles colonisation by the so-called dark septate endophytes (DSE) ubiquitous in the roots of most terrestrial plants. However, the dark septate hyphae and microsclerotia of *Posidoniomyces* never colonise vascular tissues of the host roots and are mostly confined to the hypodermis.

Type species. *Posidoniomyces atricolor* Vohník & Réblová

Etymology. Named after the host seagrass *Posidonia oceanica* and *myces* (Greek), meaning fungus.

Description. Root mycobiont of the dominant and endemic Mediterranean seagrass *Posidonia oceanica*. In vivo, hyphae brown, septate, forming intracellular microsclerotia in the hypodermis of the terminal fine roots and finger-like pseudoparenchymatous net on the surface of these roots, i.e. a colonisation pattern resembling the DSE association ubiquitous in the roots of terrestrial plants. In vitro, two distinct colonial morphotypes named compact and mycelial (often with aerial hyphae) are consistently formed. Colonies brown, mycelium composed of septate, hyaline, subhyaline to pigmented hyphae with intercalary, terminal, rarely lateral, one-celled globose, subglobose to ellipsoidal swellings that are prominent especially on the surface of the compact colonies. Sexual state unknown.

***Posidoniomyces atricolor* Vohník & Réblová, sp. nov.**
MycoBank MB 830267
Figs 5, 6

Typification. CROATIA. Dubrovnik-Neretva County: Potomje, Borak (42.92236N, 17.34685E), isolated from a surface-sterilised healthy-looking terminal root of *Posidonia oceanica*, 28 Sep 2016, M.Vohník & O.Borovec BRK-21 (holotype: PRA-15294!, dried

culture – compact morphotype from a surface-sterilised root segment; isotype: PRA-15295!, dried culture – mycelial morphotype derived from the original compact colony).

Etymology. *Atricolor* (L), meaning black, dark coloured, referring to the dark pigmented hyphae.

Description in culture. *Mycelial colonial morphotype*: Colonies on PCA 6–8 mm in diameter in 3 mo, circular, convex, appearing woolly, margin entire, aerial mycelium abundant, densest at the centre, cobwebby towards the margin, white to grey with a pale brown zone at the margin, colony surface with a dark brown hue formed by substrate mycelium and released pigment; reverse brown. *Compact colonial morphotype*: Colonies on PCA 5–6 mm in diameter in 8 mo, irregular, pulvinate, deeply furrowed, appearing mucoid-waxy to faintly floccose, of a "cartilage" consistency, become hollow upon aging, margin lobate, aerial mycelium scant, hyaline to pale brown, colony surface dark brown; reverse dark brown. Compact colonies, which are formed in vitro on sterilised roots of *P. oceanica*, become irregular in shape, folded and furrowed in an almost cerebriform pattern, cacao brown, ca. 5–6 mm long on the longest side after several months of cultivation. *Hyphae* hyaline to pale brown, septate, smooth-walled and 2–3(–3.5) µm wide, often with terminal, intercalary, rarely with lateral, one-celled, thick-walled globose, subglobose to ellipsoidal swellings 10–14 µm wide; hyphae frequently protrude from these swellings and continue growing. Surface of the compact colonies covered by hyaline to subhyaline, smooth-walled hyphae with terminal, capitate swellings. Chlamydospores, conidiogenous cells or conidia, ascomatal initials and ascomata not observed.

Description in vivo. In vivo *hyphae* pigmented, septate, smooth-walled and (2–)3–4(–5) µm wide, colonising root cells of the host and/or forming an extraradical hyphal sheath, i.e. a finger-like pseudoparenchymatous net on the root surface. *Microsclerotia* intracellular, melanised, round or elongated and 8–10(–17) µm wide, present in the *P. oceanica* root hypodermis. Intracellular hyphae also infrequently occur in the rhizodermis.

Specimens examined. Croatia. Dubrovnik-Neretva County: Potomje, Borak (42.92236N, 17.34685E), isolated from surface-sterilised healthy-looking terminal roots of *P. oceanica*, 28 Sep 2016, M.Vohník & O.Borovec BRK-11 (PRA-15296); ibid., BRK-25 (PRA-15298); BRK-34 (PRA-15297); BRK-60 (PRA-15300); BRK-61 (PRA-15293); BRK-76 (PRA-15302); BRK-87 (PRA-15299); BRK-93 (PRA-15301), BRK-97 (PRA-15303). Croatia. Split-Dalmatia County: Palagruža archipelago, Gangaro Island I (43.8639N, 15.4341E), isolated from a surface-sterilised healthy-looking terminal root of *P. oceanica*, 3 September 2012, M.Vohník & O.Borovec M8. France. Provence-Alpes-Côte d'Azur Region: Var Department, Saint-Raphaël, Cap Roux (43.45026N, 6.91951E), isolated from a surface-sterilised healthy-looking terminal root of *P. oceanica*, 17 June 2012, M.Vohník P10. France. Provence-Alpes-Côte d'Azur Region: Alpes-Maritimes Department, Antibes (43.55726N, 7.12209E), isolated from a surface-sterilised healthy-looking terminal root of *P. oceanica*, 18 June 2012, M.Vohník P11. France. Provence-Alpes-Côte d'Azur Region: Var Department, Sanary-sur-Mer (43.12054N, 5.77545E), isolated from a surface-sterilised healthy-looking terminal root of *P. oceanica*, 19 June 2012, M.Vohník P15. Italy. Liguria Region: Savona Province, Gulf of Genoa, Finale Ligure (44.17337N, 8.36765E), isolated from a sur-

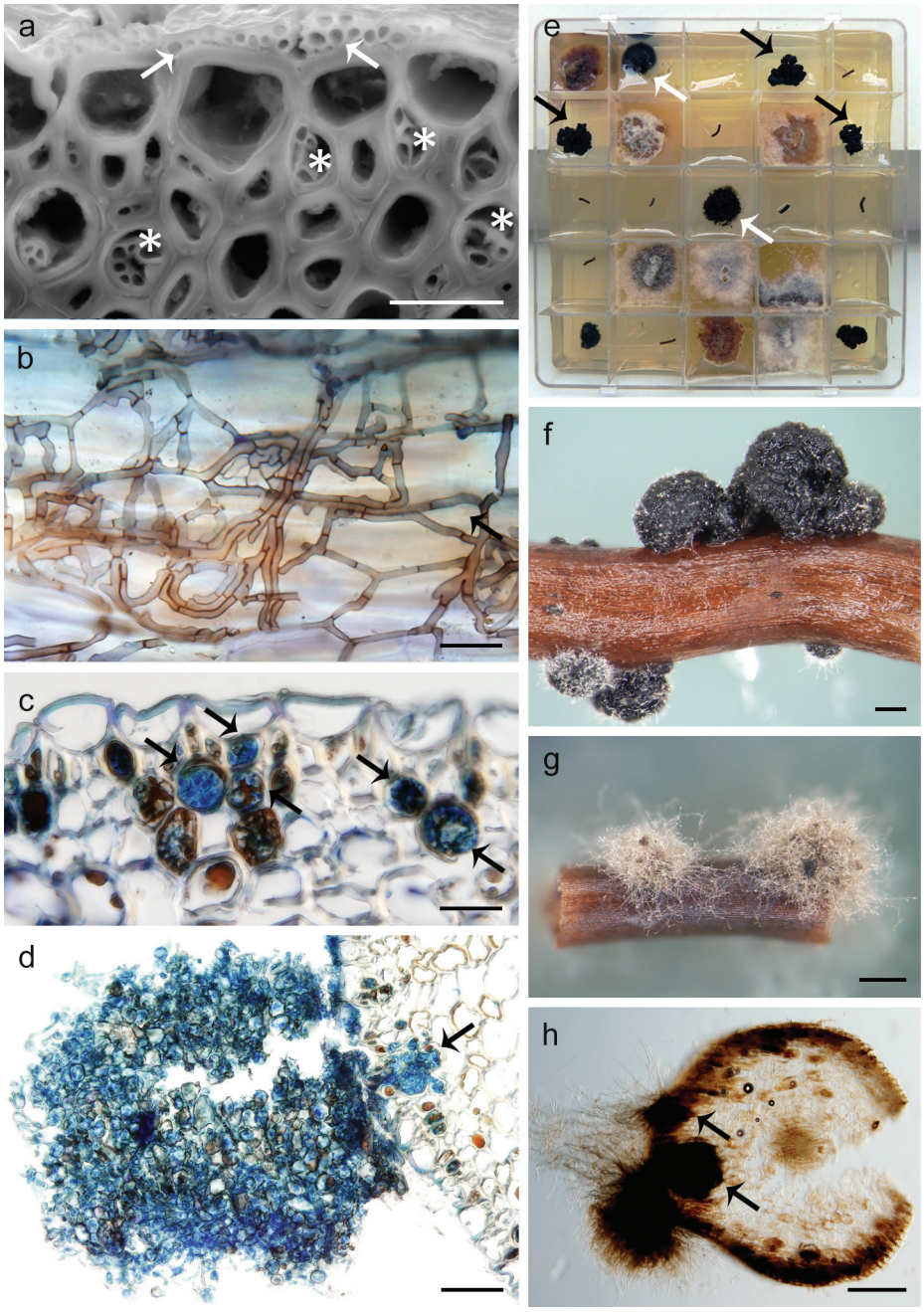

Figure 5. In vivo root colonisation pattern and in vitro cultural aspects of *Posidoniomyces atricolor*. **a** In vivo colonisation on the root surface (arrows) and in the hypodermis (asterisks) of *P. oceanica* **b** DSE colonisation on the root surface **c** germinating microsclerotia stained with trypan blue (arrows) **d** compact colony developed from microsclerotia (arrow) **e** surface-sterilised root segments yielding *P. atricolor* compact colonies (black arrows), sometimes with substrate mycelium (white arrows) **f** compact colonial morphotype **g** mycelial colonial morphotype **h** mycelial morphotype developing from microsclerotia (arrows) in transversal section. Scale bars: 20 µm (**a, b**), 50 µm (**c**), 100 µm (**d**), 200 µm (**f, h**), 500 µm (**g**).

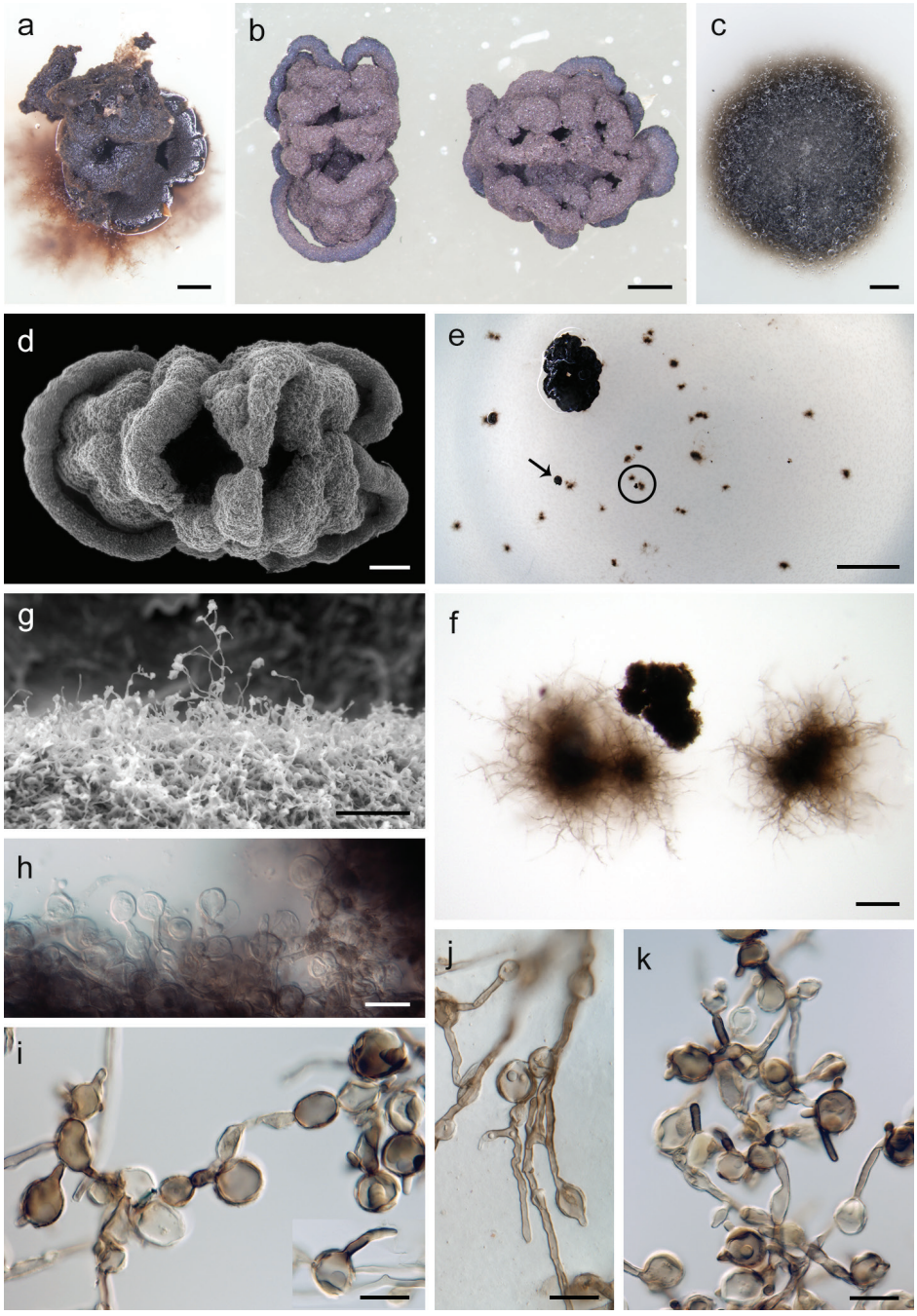

Figure 6. Colonial morphotypes of *Posidoniomyces atricolor* in vitro (type isolate BRK-21). **a** Compact morphotype with substrate mycelium **b, d** compact colonies with a cerebriform pattern **c** colony of *P. atricolor* on PCA **e** rhizoidal and compact (arrow) daughter colonies on PCA washed with sterile tap water **f** detail of the colonies encircled in **e**; **g, h** terminal capitate swellings on the surface of compact colonies **i–k** conspicuous swellings on aerial mycelium. Scale bars: 500 µm (**a, d**), 1000 µm (**b, c**), 5 mm (**e**), 200 µm (**f**), 100 µm (**g**), 20 µm (**h**).

face-sterilised healthy-looking terminal root of *P. oceanica*, 17 June 2012, M.Vohník P09. Spain. Girona Province: L'Escala (42.10744N, 3.16892E), isolated from a surface-sterilised healthy-looking terminal root of *P. oceanica*, 18 June 2012, M.Vohník P20.

Habitat and distribution. Root mycobiont of the dominant and endemic Mediterranean seagrass *Posidonia oceanica*. So far known only from the NW Mediterranean Sea.

Notes. Both colonial morphotypes, named compact and mycelial, appeared on surface-sterilised root segments of *P. oceanica* and after inoculation also on solid agar media but the compact colonies with the cerebriform pattern formed only on the original root segments. All examined colonies of *P. atricolor* emerging from the original root segments developed from melanised microsclerotia formed exclusively intracellularly in the *P. oceanica* hypodermis (Figure 5d, h). The mycelial morphotype was observed on MMN and PCA, while compact colonies were formed on PDA and PCA (Vohník et al. 2016; this study). When the surface of a colony exhibiting the compact colonial morphotype was washed regularly with sterile tap water, fragments of hyphae were released to form minute daughter colonies (Figure 6e). These daughter colonies were either of a rhizoidal form composed of substrate mycelium and continued to develop the mycelial morphotype or they assumed the compact colony character from the beginning (Figure 6f). A new hypha was often formed through the globose swelling, regardless of its position on the hypha (Figures 6i–k).

Discussion

The microscopic screening of *Posidonia oceanica* root fungal colonisation confirms that the recently described DSE association (Vohník et al. 2015) formed by the Pleosporales sp. MV-2012 (Vohník et al. 2016) and introduced as *Posidoniomyces atricolor* in this study, is present at all investigated localities. The tag-encoded 454-pyrosequencing of fungal DNA extracted from surface-sterilised *P. oceanica* root segments confirms the dominance of this fungus in the root mycobiota of the dominant seagrass in the NW Mediterranean Sea. Our analysis of combined DNA sequences of nuclear ribosomal and protein-coding loci confirms the placement of *P. atricolor* in the Aigialaceae (Pleosporales, Dothideomycetes) and suggests an independent marine biotrophic lineage.

The root-symbiotic *Posidoniomyces* is related to mostly saprobic lignicolous marine fungi from estuarine environments colonising wood and roots of mangroves growing in tropical regions of both Eastern and Western Hemispheres, a situation resembling, at least to some extent, the relationship of the ubiquitous terrestrial root-symbiotic *Rhizoscyphus ericae* aggregate to saprobic fungi from the genus *Hyaloscypha* (Fehrer et al. 2019). Because mycorrhizal fungi from the *R. ericae* aggregate have significant saprobic abilities (Martino et al. 2018), they can decompose recalcitrant peat and exchange mineral nutrients (especially nitrogen) for the host photosynthetically bound carbon. Since *P. oceanica* often grows on thick layers of recalcitrant peat-like matte (Figure 1b, c), which typically stores large amounts of organically-bound nutrients (Fourqurean et

al. 2012) directly unavailable to plants (Read 1991), it is tempting to speculate about the possible role of *P. atricolor* in mineral nutrition of the dominant Mediterranean seagrass (also see Borovec and Vohník 2018; Kolátková and Vohník 2019). On the other hand, genomes of DSE fungi typically combine saprobic and pathogenic traits (Schlegel et al. 2016; Knapp et al. 2018) and effects of root endophytes on host plant fitness vary along the parasitism-mutualism continuum (Newsham 2011; Mayerhofer et al. 2013). Thus, although the specific association with *P. atricolor* is omnipresent in *P. oceanica* at all so far investigated localities, to date there is no solid proof that it is of any benefit to the seagrass.

The Aigialaceae (Suetrong et al. 2009) was erected for marine ascomycetes characterised by fisstunicate asci with a non-amyloid apex and a ring-like apical apparatus containing septate or muriform ascospores with a gelatinous sheath or cap, trabeculate hamathecium and non-stromatic, carbonatious to coriaceous, non-papillate ascomata. Additionally, *Fissuroma* and *Neoastrosphaeriella* occurring on bamboo, palms and flowering plants in terrestrial and freshwater environments were added to the family by Liu et al. (2011). The asexual morphs of marine species are generally unknown. The asexual morph of *Fissuroma* was reported as coelomycetous, pleurophomopsis-like (Tanaka and Harada 2005; Liu et al. 2011). Axenic cultures of *P. atricolor* remained sterile and two colonial morphotypes, named compact and mycelial, were consistently formed originating from the primary source. Although the presence of both morphotypes on PCA, a low sugar content medium, would suggest that the mode of nutrition does not influence the colony appearance, the absence of one or the other morphotype on MMN and PDA may indicate that the nutrition mode could play a role to some extent. When a compact colony was regularly washed with sterile tap water, a number of daughter colonies were formed all over the agar plate (Figure 6e), suggesting that liquid culture might be an efficient way for producing larger quantities of *P. atricolor* mycelium. These colonies usually assumed the form of a miniature rhizoidal-like colony (Figure 6f) formed mainly by submerged mycelium or they formed the well-distinguishable compact colonial morphotype directly. It is probable that the capitate swellings protruding above the surface of the compact colonies (Figure 6g, h) together with hyphal fragments act as propagules in the absence of conidia and ensure the dispersal of the fungus in a simulated environment. These terminal, intercalary and sometimes lateral mostly globose swellings resemble intercalary conidia of species of *Knufia*, e.g. *K. perforans*, formed on elongated and monilioid hyphae (Tsuneda et al. 2011). However, *P. atricolor* compact colonies have never been observed in vivo directly on *P. oceanica* roots and it is thus unknown whether the capitate swellings form and act as propagules also under natural conditions.

The Dothideomycetes include several marine genera that usually do not form an asexual state and are distributed in several orders, i.e. Capnodiales, Dothideales, Hysteriales, Jahnulales, Patellariales and Pleosporales, or *incertae sedis* lineages (Suetrong et al. 2009). They include mainly taxa thriving in intertidal zone on a variety of substrates of mangroves in tropics or less frequently on salt marsh plants in temperate regions. Other marine Dothideomycetes can occur as parasites or possible endophytes

of seagrasses or marine macroalgae and are completely submerged. The omnipresence and dominance of *P. atricolor* in the roots of *P. oceanica* suggests a close symbiotic relationship with the dominant Mediterranean seagrass, a trait so far unparalleled in other Dothideomycetes. At the same time, to our knowledge, the characteristic DSE colonisation pattern of *P. atricolor* has never been observed in any other seagrass species, suggesting its specificity for *P. oceanica* (also see Discussion in Vohník et al. 2015).

The analysis of all available *P. atricolor* ITS sequences (Vohník et al. 2016, 2017; this study) revealed several aspects that may connect with their geographic distribution and possibly also the symbiotic lifestyle. The ITS1 region of *P. atricolor* contains ca. 294 nt long insertion near the 5'-end when compared to ITS1 of other members of the Aigialaceae. Only four species of the whole family have their ITS sequences available; the ITS1 varies between 151–168 nt in *Fissuroma* (*F. maculans*, *F. neoaggregatum*) and between 186–201 nt in *Neoastrosphaeriella* (*N. aquatica*, *N. krabiensis*), compared to 445 nt in *P. atricolor*. When the ITS1, 5.8S and ITS2 of *P. atricolor* were checked for closest hits by the BLAST search in GenBank, the closest relatives for the 5.8S region were members of the Aigialaceae and other taxa of the Pleosporales; however, no close hits were revealed for ITS1 and ITS2. Since the ITS region was amplified and sequenced as a part of the whole nuc18S region with several forward and reverse primers, it is unlikely that this divergence was caused by PCR or sequencing errors. ITS is a rapidly evolving region where numerous insertions and deletions occur. Considering the probably obligate symbiotic lifestyle of *P. atricolor* in the host roots, the long insertion in ITS1 and high divergence in ITS2 sequences may be a result of co-evolution of both partners, higher gene flow rate and possibly horizontal gene transfer resulting in genetic mismatches in the fungal partner (Saikkonen et al. 2004, 2010; also see Kolařík and Vohník 2018). However, outside the Aigialaceae, the ITS1 region can be much longer, for example in *Astrosphaeriella bambusae*, the outgroup, it is 445 nt long. On the other hand, the length of the ITS2 region is comparable between *P. atricolor* (188–192 nt) and other members of the Aigialaceae (156–163 nt).

Although the ITS sequences of all *P. atricolor* isolates are nearly identical (99.87–98.99% identity between the type strain BRK-21 and other isolates), they differ in up to six indels near the 5'-end of the ITS2. These site mutations can be used to some extent to characterise different populations of *P. atricolor* (Figure 4). Only strains which could be compared morphologically, i.e. those successfully derived from *P. oceanica* surface-sterilised root segments into axenic culture (Vohník et al. 2016; this study), were analysed. Their colony characters and colonisation pattern in the roots of the host were identical. At the ITS2 sequence level, we could distinguish populations from the north-west regions of the Mediterranean (France, Spain) and those from the north-central part of the Adriatic coast (Croatia). Moreover, the Croatian population from Borak (locality HR-1; Table 1) seems to be a source of several mutations. Further screening of *P. oceanica* root mycobiota outside the NW Mediterranean is apparently needed to fully elucidate the usefulness of ITS sequences for distinguishing geographically different populations of *P. atricolor*.

Although it is a significant producer of biomass and an important source of decomposing organic matter in the sea and adjacent habitats, the mycobiota of *P. oceanica* has

been studied only by a few authors (e.g. Kohlmeyer 1963; Cuomo et al. 1985; Panno et al. 2013; Gnavi et al. 2014; Vohník et al. 2016, 2017; this study), with differing results. Most significantly, no study prior to Vohník et al. (2016) reported *P. atricolor* in the mycobiota of the dominant Mediterranean seagrass. This is probably due to the manner of material sampling and isolation procedure, i.e. direct isolation from decaying plant matter vs. serially washed or surface-sterilised parts of living plants, the former often leading to detection of fast-growing surface-dwelling saprobes in contrast to isolation of true endophytes (Sieber 2002; also see Discussion in Vohník et al. 2016, 2017). Indeed, apart from *P. atricolor* and the obligate marine Sordariomycetes (*Corollospora marina* and *C. intermedia* in Microascales, *Lulwoana* sp. and *Lulworthia* sp. in Lulworthiales and *Papulaspora halima* incertae sedis) and Dothideomycetes (*Halotthia posidoniae*, *Pontoporeia biturbinata* and several other genera in Pleosporales), majority of the fungi reported from *P. oceanica* are asexually reproducing ubiquitous fungi (Panno et al. 2013).

The distribution pattern of *P. oceanica* mycobiota in leaves, rhizomes, roots and matte is affected by various environmental parameters, presence of growth-inhibiting substances in leaves or antagonistic organisms and may be also influenced by the season (Cuomo et al. 1985; Panno et al. 2013; Gnavi et al. 2014). However, no detailed data are yet available for the dominant root mycobiont *P. atricolor*, except that it seems to be restricted to *P. oceanica* roots. Mycorrhizal fungi form often vigorous extraradical mycelium penetrating the substrate far beyond the rhizosphere, thus forming the mycorrhizosphere (i.e. a volume of soil under a combined influence of the root and the emerging fungal hyphae) (Linderman 1988). The mycorrhizosphere significantly enlarges the volume of the substrate available for mycorrhizal nutrient uptake and in a way defines individual mycorrhizal types. It would therefore be interesting to screen the volume and enzymatic activity of the *P. atricolor* extraradical mycelium (if existing) to decide more precisely about the mode of the interaction between the dominant Mediterranean seagrass and its dominant root mycobiont.

Conclusions

This study confirms at an unprecedented scale that the diversity of the root mycobiota of the dominant Mediterranean seagrass is relatively narrow and dominated by a single pleosporalean fungus so far not known from any other hosts or environments. This fungus is introduced here as a new genus and species *Posidoniomyces atricolor* and resides as an independent marine biotrophic lineage in the Aigialaceae. The characteristic colonisation pattern of *P. atricolor* in *P. oceanica* roots has not been reported in any other seagrass and resembles colonisation by DSE fungi which are ubiquitous in terrestrial roots. Further research is needed on the distribution and genetic variability (especially ITS sequences) of *P. atricolor* in the rest of the Mediterranean Sea (i.e. Eastern Mediterranean Basin, the coast of North Africa). Additionally, given the uniquely discontinuous distribution area of the genus *Posidonia* (Green and Short 2003), targeted research on the root mycobiota of its Australian species would be of a special evolutionary significance.

Acknowledgments

This study constitutes a part of long-term research projects of the Czech Academy of Sciences, Institute of Botany (RVO 67985939) and Charles University, Faculty of Science (MŠMT LO1417). Judith Fehrer stimulated the cooperation between MV and MR from the outset, Jiří Machač helped with the photo documentation, Mirka Opičková helped with the DNA isolations (all Inst. of Botany, Průhonice), David Vondrášek (Charles Uni., Prague, CZ) helped with the sampling in France, Italy and Spain, Miroslav Kolařík helped with preliminary phylogenetic analyses and Jana Voříšková performed the pyrosequencing (both Inst. of Microbiology, Prague, CZ) and Ivan Župan (Zadar Uni., Zadar, HR) helped with obtaining a sampling permit issued by the Croatian Ministry of Environmental and Nature Protection (UP/I-612-07/13-48/48//517-07-1-1-1-13-2) as well as with the sampling in Croatia; all these contributions are greatly appreciated. The authors thank Conrad L. Schoch and Kazuaki Tanaka (reviewers) and Huzefa Raja (editor) for the careful reading and suggestions which helped to improve this paper.

References

Altschul SF, Madden TL, Schäffer AA, Zhang Z, Zhang Z, Miller W, Lipman DJ (1997) Gapped BLAST and PSI-BLAST: a new generation of protein database search programs. Nucleic Acids Research 25: 3389–3402. https://doi.org/10.1093/nar/25.17.3389

Alva P, Mckenzire EHC, Pointing SP, Pena-Murala R, Hyde KD (2002) Do seagrasses harbour endophytes? In: Hyde KD (Ed.) Fungi in Marine Environments. Fungal Diversity Research Series. Hong Kong University Press, Hong Kong, 167–178.

Arnaud-Haond S, Duarte CM, Diaz-Almela E, Marbà N, Sintes T, Serrão EA (2012) Implications of extreme life span in clonal organisms: millenary clones in meadows of the threatened seagrass *Posidonia oceanica*. PLOS ONE 7: e30454. https://doi.org/10.1371/journal.pone.0030454

Bao D, Luo Z, Jeewon R, Nalumpang S, Su H, Hyde KD (2019) *Neoastrosphaeriella aquatica* sp. nov. (Aigialaceae), a new species from freshwater habitat in southern Thailand. Phytotaxa 391: 197–206. https://doi.org/10.11646/phytotaxa.391.3.3

Borovec O, Vohník M (2018) Ontogenetic transition from specialized root hairs to specific root-fungus symbiosis in the dominant Mediterranean seagrass *Posidonia oceanica*. Scientific Reports 8: 10773. https://doi.org/10.1038/s41598-018-28989-4

Bruzone MC, Fehrer J, Fontenla SB, Vohník M (2017) First record of *Rhizoscyphus ericae* in Southern Hemisphere´s Ericaceae. Mycorrhiza 27: 147–163. https://doi.org/10.1007/s00572-016-0738-8

Crous PW, Wood AR, Okada G, Groenewald JZ (2008) Foliicolous microfungi occurring on *Encephalartos*. Persoonia 21: 135–146. https://doi.org/10.3767/003158508X380612

Cuomo V, Vanzanella F, Fresi E, Cinelli F, Mazzella L (1985) Fungal flora of *Posidonia oceanica* and its ecological significance. Transactions of the British Mycological Society 84: 35–40. https://doi.org/10.1016/S0007-1536(85)80217-5

De Falco G, Molinaroli E, Conforti A, Simeone S, Tonielli R (2017) Biogenic sediments from coastal ecosystems to beach-dune systems: implications for the adaptation of mixed and carbonate beaches to future sea level rise. Biogeosciences 14: 3191–3205. https://doi.org/10.5194/bg-14-3191-2017

den Hartog C (1970) Seagrasses of the world. North-Holland Publishing, the Netherlands.

Edgar RC (2013) UPARSE: highly accurate OTU sequences from microbial amplicon reads. Nature Methods 10: 996–998. https://doi.org/10.1038/nmeth.2604

Fehrer J, Réblová M, Bambasová V, Vohník M (2019) The root-symbiotic *Rhizoscyphus ericae* aggregate and *Hyaloscypha* (Leotiomycetes) are congeneric: Phylogenetic and experimental evidence. Studies in Mycology 92: 195–225. https://doi.org/10.1016/j.simyco.2018.10.004

Fourqurean JW, Duarte CM, Kennedy H, Marbà N, Holmer M, Mateo MA, Apostolaki ET, Kendrick GA, Krause-Jensen D, McGlathery KJ, Serrano O (2012) Seagrass ecosystems as a globally significant carbon stock. Nature Geoscience 5: 505–509. https://doi.org/10.1038/ngeo1477

Gardes M, Bruns TD (1993) ITS primers with enhanced specificity for Basidiomycetes – application to the identification of mycorrhizae and rusts. Molecular Ecology 2: 113–118. https://doi.org/10.1111/j.1365-294X.1993.tb00005.x

Gargas A, Taylor JW (1992) Polymerase chain reaction (PCR) primers for amplifying and sequencing nuclear 18S rDNA from lichenized fungi. Mycologia 84: 589–592. https://doi.org/10.1080/00275514.1992.12026182

Gessner RV, Kohlmeyer J (1976) Geographical distribution and taxonomy of fungi from salt marsh *Spartina*. Canadian Journal of Botany 54: 2023–2037. https://doi.org/10.1139/b76-216

Giakoumi S, Sini M, Gerovasileiou V, Mazor T, Beher J, Possingham HP, Abdulla A, Çinar ME, Dendrinos P, Gucu AC, Karamanlidis AA (2013) Ecoregion-based conservation planning in the Mediterranean: dealing with large-scale heterogeneity. PLOS ONE 8: e76449. https://doi.org/10.1371/journal.pone.0076449

Gnavi G, Ercole E, Panno L, Vizzini A, Varese GC (2014) Dothideomycetes and Leotiomycetes sterile mycelia isolated from the Italian seagrass *Posidonia oceanica* based on rDNA data. SpringerPlus 3: 508. https://doi.org/10.1186/2193-1801-3-508

Green EP, Short FT (2003) World atlas of seagrasses. University of California Press, USA.

Hall TA (1999) BioEdit: a user-friendly biological sequence alignment editor and analysis program for Windows 95/98/NT. Nucleic Acids Symposium Series 41: 95–98.

Hemminga MA, Duarte CM (2000) Seagrass Ecology. Cambridge University Press, UK. https://doi.org/10.1017/CBO9780511525551

Huelsenbeck JP, Ronquist F (2001) MrBayes: Bayesian inference of phylogenetic trees. Bioinformatics 17: 754–755. https://doi.org/10.1093/bioinformatics/17.8.754

Jones EBG (1963) Marine fungi: II. Ascomycetes and deuteromycetes from submerged wood and drift *Spartina*. Transactions of the British Mycological Society 46: 135–144. https://doi.org/10.1016/S0007-1536(63)80015-7

Jones EBG, Pang KL (2012) Marine fungi and fungal-like organisms. de Gruyter, Germany. https://doi.org/10.1515/9783110264067

Jumpponen A, Trappe JM (1998) Dark septate endophytes: a review of facultative biotrophic root-colonizing fungi. New Phytologist 140: 295–310. https://doi.org/10.1046/j.1469-8137.1998.00265.x

Katoh K, Asimenos G, Toh H (2009) Multiple alignment of DNA sequences with MAFFT. Methods in Molecular Biology 537: 39–64. https://doi.org/10.1007/978-1-59745-251-9_3

Kauff F, Lutzoni F (2002) Phylogeny of the Gyalectales and Ostropales (Ascomycota, Fungi): among and within order relationships based on nuclear ribosomal RNA small and large subunits. Molecular Phylogenetics and Evolution 25: 138–156. https://doi.org/10.1016/S1055-7903(02)00214-2

Knapp DG, Németh JB, Barry K, Hainaut M, Henrissat B, Johnson J, Kuo A, Lim JH, Lipzen A, Nolan M, Ohm RA (2018) Comparative genomics provides insights into the lifestyle and reveals functional heterogeneity of dark septate endophytic fungi. Scientific Reports 8: 6321. https://doi.org/10.1038/s41598-018-24686-4

Kohlmeyer J (1963) Zwei neuen Ascomycetes Gattungen auf *Posidonia* rhizomen. Nova Hedwigia 6: 5–13.

Kohlmeyer J, Kohlmeyer E (1971) Marine fungi from tropical America and Africa. Mycologia 63: 831–861. https://doi.org/10.1080/00275514.1971.12019172

Kohlmeyer J, Kohlmeyer E (1979) Marine Mycology. The higher fungi. Academic Press, USA.

Kohlmeyer J, Volkmann-Kohlmeyer B (1991) Illustrated key to the filamentous marine fungi. Botanica Marina 34: 1–61. https://doi.org/10.1515/botm.1991.34.1.1

Kohlmeyer J, Volkmann-Kohlmeyer B (2001) The biodiversity of fungi on *Juncus roemerianus*. Mycological Research 105: 1411–1412. https://doi.org/10.1017/S095375620124547X

Kohlmeyer J, Volkmann-Kohlmeyer B (2002) Fungi on *Juncus* and *Spartina*: new marine species of *Anthostomella*, with a list of marine fungi known from *Spartina*. Mycological Research 106: 365–374. https://doi.org/10.1017/S0953756201005469

Kohout P, Sýkorová Z, Čtvrtlíková M, Rydlová J, Suda J, Vohník M, Sudová R (2012) Surprising spectra of root-associated fungi in submerged aquatic plants. FEMS Microbiology Ecology 80: 216–235. https://doi.org/10.1111/j.1574-6941.2011.01291.x

Kohout P, Malinová T, Roy M, Vohník M, Jersáková J (2013) A diverse fungal community associated with *Pseudorchis albida* (Orchideaceae) roots. Fungal Ecology 6: 50–64. https://doi.org/10.1016/j.funeco.2012.08.005

Kolařík M, Vohník M (2018) When the ribosomal DNA does not tell the truth: The case of the taxonomic position of *Kurtia argillacea*, an ericoid mycorrhizal fungus residing among Hymenochaetales. Fungal Biology 122: 1–18. https://doi.org/10.1016/j.funbio.2017.09.006

Kolátková V, Vohník M (2019) Adaptive traits in the seagrass *Posidonia oceanica*: Root hairs with spiral cell walls, not spiral root hairs. Aquatic Botany 155: 52–53. https://doi.org/10.1016/j.aquabot.2018.11.013

Kõljalg U, Nilsson RH, Abarenkov K, Tedersoo L, Taylor AF, Bahram M, Bates ST, Bruns TD, Bengtsson-Palme J, Callaghan TM, Douglas B (2013) Towards a unified paradigm for sequence-based identification of fungi. Molecular Ecology 22: 5271–5277. https://doi.org/10.1111/mec.12481

Linderman RG (1988) Mycorrhizal interactions with the rhizosphere microflora: the mycorrhizosphere effect. Phytopathology 78: 366–371.

Liu JK, Phookamsak R, Jones EG, Zhang Y, Ko-Ko TW, Hu HL, Boonmee S, Doilom M, Chukeatirote E, Bahkali AH, Wang Y (2011) *Astrosphaeriella* is polyphyletic with species in *Fissuroma* gen. nov., and *Neoastrosphaeriella* gen. nov. Fungal Diversity 51: 135–154. https://doi.org/10.1007/s13225-011-0142-9

Liu YJ, Whelen S, Hall BD (1999) Phylogenetic relationships among ascomycetes: evidence from an RNA polymerase II subunit. Molecular Biology and Evolution 16: 1799–1808. https://doi.org/10.1093/oxfordjournals.molbev.a026092

Lukešová T, Kohout P, Větrovský T, Vohník M (2015) The potential of Dark Septate Endophytes to form root symbioses with ectomycorrhizal and ericoid mycorrhizal middle European forest plants. PLOS ONE 10: e0124752. https://doi.org/10.1371/journal.pone.0124752

Martino E, Morin E, Grelet GA, Kuo A, Kohler A, Daghino S, Barry KW, Cichocki N, Clum A, Dockter RB, Hainaut M (2018) Comparative genomics and transcriptomics depict ericoid mycorrhizal fungi as versatile saprotrophs and plant mutualists. New Phytologist 217: 1213–1229. https://doi.org/10.1111/nph.14974

Marx DH (1969) Influence of ectotrophic mycorrhizal fungi on resistance of pine roots to pathogenic infections I. Antagonism of mycorrhizal fungi to root pathogenic fungi and soil bacteria. Phytopathology 59: 153–163.

Mason-Gamer RJ, Kellogg EA (1996) Testing for phylogenetic conflict among molecular data sets in the tribe Triticeae (Gramineae). Systematic Biology 45: 524–545. https://doi.org/10.1093/sysbio/45.4.524

Mayerhofer MS, Kernaghan G, Harper KA (2013) The effects of fungal root endophytes on plant growth: a meta-analysis. Mycorrhiza 23: 119–128. https://doi.org/10.1007/s00572-012-0456-9

Miller MA, Pfeiffer W, Schwartz T (2010) Creating the CIPRES Science Gateway for inference of large phylogenetic trees. Proceedings of the Gateway Computing Environments Workshop, USA. https://doi.org/10.1109/GCE.2010.5676129

Newsham KK (2011) A meta-analysis of plant responses to dark septate root endophytes. New Phytologist 10: 783–793. https://doi.org/10.1111/j.1469-8137.2010.03611.x

Nielsen SL, Thingstrup I, Wigand C (1999) Apparent lack of vesicular-arbuscular mycorrhiza (VAM) in the seagrasses *Zostera marina* L. and *Thalassia testudinum* Banks ex Konig. Aquatic Botany 63: 261–266. https://doi.org/10.1016/S0304-3770(98)00123-5

Notarbartolo di Sciara G, Agardy T (2010) Overview of scientific findings and criteria relevant to identifying SPAMIs in the Mediterranean open seas, including the deep sea. UNEP-MAP, Tunis.

Nylander JAA (2008) MrModeltest2 v. 2.3 (Program for selecting DNA substitution models using PAUP*). Evolutionary Biology Centre, Sweden.

Panno L, Bruno M, Voyron S, Anastasi A, Gnavi G, Miserere L, Varese GC (2013) Diversity, ecological role and potential biotechnological applications of marine fungi associated to the seagrass *Posidonia oceanica*. New Biotechnology 30: 685–694. https://doi.org/10.1016/j.nbt.2013.01.010

Phookamsak R, Norphanphoun C, Tanaka K, Dai DQ, Luo ZL, Liu JK, Su HY, Bhat DJ, Bahkali AH, Mortimer PE, Xu JC (2015) Towards a natural classification of *Astrosphaeriella*-like species; introducing Astrosphaeriellaceae and Pseudoastrosphaeriellaceae fam. nov. and *Astrosphaeriellopsis*, gen. nov. Fungal Diversity 74: 143–197. https://doi.org/10.1007/s13225-015-0352-7

Read DJ (1991) Mycorrhizas in ecosystems. Experientia 47: 376–391. https://doi.org/10.1007/BF01972080

Reeb V, Lutzoni F, Roux C (2004) Contribution of RPB2 to multilocus phylogenetic studies of the euascomycetes (Pezizomycotina, Fungi) with special emphasis on the lichen-forming

Acarosporaceae and evolution of polyspory. Molecular Phylogenetics and Evolution 32: 1036–1060. https://doi.org/10.1016/j.ympev.2004.04.012

Saikkonen K, Wäli PR, Helander M, Faeth SH (2004) Evolution of endophyte-plant symbioses. Trends in Plant Science 9: 275–280. https://doi.org/10.1016/j.tplants.2004.04.005

Saikkonen K, Wäli PR, Helander M (2010) Genetic compatibility determines endophyte-grass combinations. PLOS ONE 5: e11395. https://doi.org/10.1371/journal.pone.0011395

Sayers EW, Cavanaugh M, Clark K, Ostell J, Pruitt KD, Karsch-Mizrachi I (2019) GenBank. Nucleic Acids Research 47: D94–D99. https://doi.org/10.1093/nar/gky989

Schlegel M, Münsterkötter M, Güldener U, Bruggmann R, Duò A, Hainaut M, Henrissat B, Sieber CM, Hoffmeister D, Grünig CR (2016) Globally distributed root endophyte *Phialocephala subalpina* links pathogenic and saprophytic lifestyles. BMC Genomics 17: 1015. https://doi.org/10.1186/s12864-016-3369-8

Crous PW, Schoch CL, Hyde KD, Wood AR, Gueidan C, De Hoog GS, Groenewald JZ (2009a) A class-wide phylogenetic assessment of Dothideomycetes. Studies in Mycology 64: 1–15. https://doi.org/10.3114/sim.2009.64.02

Schoch CL, Sung GH, López-Giráldez F, Townsend JP, Miadlikowska J, Hofstetter V, Robbertse B, Matheny PB, Kauff F, Wang Z, Gueidan C (2009b) The Ascomycota tree of life: a phylum-wide phylogeny clarifies the origin and evolution of fundamental reproductive and ecological traits. Systematic Biology 58: 224–239. https://doi.org/10.1093/sysbio/syp020

Serrano O, Mateo MA, Renom P, Julià R (2012) Characterization of soils beneath a *Posidonia oceanica* meadow. Geoderma 185–186: 26–36. https://doi.org/10.1016/j.geoderma.2012.03.020

Sieber TN (2002) Fungal root endophytes. In: Waisel Y, Eshel A, Kafkafi (Eds) Plant roots – the hidden half, 3rd edn. Marcel Dekker, USA. https://doi.org/10.1201/9780203909423.ch49

Slippers B, Boissin E, Phillips AJ, Groenewald JZ, Lombard L, Wingfield MJ, Postma A, Burgess T, Crous PW (2013) Phylogenetic lineages in the Botryosphaeriales: a systematic and evolutionary framework. Studies in Mycology 76: 31–49. https://doi.org/10.3114/sim0020

Stamatakis A (2006) RAxML-VI-HPC: maximum likelihood-based phylogenetic analyses with thousands of taxa and mixed models. Bioinformatics 22: 2688–2690. https://doi.org/10.1093/bioinformatics/btl446

Suetrong S, Schoch CL, Spatafora JW, Kohlmeyer J, Volkmann-Kohlmeyer B, Sakayaroj J, Phongpaichit S, Tanaka K, Hirayama K, Jones EB (2009) Molecular systematics of the marine Dothideomycetes. Studies in Mycology 64: 145–154. https://doi.org/10.3114/sim.2009.64.09

Tanaka K, Harada Y (2005) Bambusicolous fungi in Japan (4): a new combination, *Astrosphaeriella aggregata*. Mycoscience 46: 114–118. https://doi.org/10.1007/S10267-004-0223-7

Tanaka K, Hirayama K, Yonezawa H, Hatakeyama S, Harada Y, Sano T, Shirouzu T, Hosoya T (2009) Molecular taxonomy of bambusicolous fungi: Tetraplosphaeriaceae, a new pleosporalean family with *Tetraploa*-like anamorphs, and notes on the phylogeny of selected species from bamboo. Studies in Mycology 64: 175–209. https://doi.org/10.3114/sim.2009.64.10

Tennakoon DS, Phookamsak R, Kuo CH, Goh TK, Jeewon R, Hyde KD (2018) Morphological and phylogenetic evidence reveal *Fissuroma taiwanense* sp. nov. (Aigialaceae, Pleospo-

rales) from *Hedychium coronarium*. Phytotaxa 338: 265–275. https://doi.org/10.11646/phytotaxa.338.3.4

Tsuneda A, Hambleton S, Currah RS (2011) The anamorph genus *Knufia* and its phylogenetically allied species in *Coniosporium*, *Sarcinomyces*, and *Phaeococcomyces*. Botany 89: 523–536. https://doi.org/10.1139/b11-041

Větrovský T, Baldrian P (2013) Analysis of soil fungal communities by amplicon pyrosequencing: current approaches to data analysis and the introduction of the pipeline SEED. Biology and Fertility of Soils 49: 1027–1037. https://doi.org/10.1007/s00374-013-0801-y

Vilgalys R, Hester M (1990) Rapid genetic identification and mapping of enzymatically amplified ribosomal DNA from several Cryptococcus species. Journal of Bacteriology 172: 4238–4246. https://doi.org/10.1128/jb.172.8.4238-4246.1990

Vohník M, Albrechtová J (2011) The co-occurrence and morphological continuum between ericoid mycorrhiza and dark septate endophytes in roots of six European *Rhododendron* species. Folia Geobotanica 46: 373–386. https://doi.org/10.1007/s12224-011-9098-5

Vohník M, Sadowsky JJ, Kohout P, Lhotáková Z, Nestby R, Kolařík M (2012) Novel root-fungus symbiosis in Ericaceae: sheathed ericoid mycorrhiza formed by a hitherto undescribed basidiomycete with affinities to Trechisporales. PLOS ONE 7: e39524. https://doi.org/10.1371/journal.pone.0039524

Vohník M, Borovec O, Župan I, Vondrášek D, Petrtýl M, Sudová R (2015) Anatomically and morphologically unique dark septate endophytic association in the roots of the Mediterranean endemic seagrass *Posidonia oceanica*. Mycorrhiza 25: 663–672. https://doi.org/10.1007/s00572-015-0642-7

Vohník M, Borovec O, Kolařík M (2016) Communities of cultivable root mycobionts of the seagrass *Posidonia oceanica* in the northwest Mediterranean Sea are dominated by a hitherto undescribed pleosporalean dark septate endophyte. Microbial Ecology 71: 442–451. https://doi.org/10.1007/s00248-015-0640-5

Vohník M, Borovec O, Župan I, Kolařík M, Sudová R (2017) Fungal root symbionts of the seagrass *Posidonia oceanica* in the central Adriatic Sea revealed by microscopy, culturing and 454-pyrosequencing. Marine Ecology Progress Series 583: 107–120. https://doi.org/10.3354/meps12337

Wanasinghe DN, Jeewon R, Jones EG, Boonmee S, Kaewchai S, Manawasinghe IS, Lumyong S, Hyde KD (2018) Novel palmicolous taxa within Pleosporales: multigene phylogeny and taxonomic circumscription. Mycological Progress 17: 571–590. https://doi.org/10.1007/s11557-018-1379-4

White TJ, Bruns TD, Lee SB, Taylor JW (1990) Amplification and direct sequencing of fungal ribosomal RNA genes for phylogenetics. In: Innis N, Gelfand D, Sninsky J, White T (Eds) PCR - protocols and applications – a laboratory manual. Academic Press, USA. https://doi.org/10.1016/B978-0-12-372180-8.50042-1

Yang T, Groenewald JZ, Cheewangkoon R, Jami F, Abdollahzadeh J, Lombard L, Crous PW (2017) Families, genera, and species of Botryosphaeriales. Fungal Biology 121: 322–346. https://doi.org/10.1016/j.funbio.2016.11.001

Supplementary material 1

Characteristics of fungal MOTUs obtained from surface sterilized *Posidonia oceanica* roots in this study

Authors: Martin Vohník, Ondřej Borovec, Zuzana Kolaříková, Radka Sudová, Martina Réblová

Data type: species data

Link: https://doi.org/10.3897/mycokeys.55.35682.suppl1

Supplementary material 2

A list of fungi, isolate information and new sequences determined for this study (in bold) and additional sequences retrieved from GenBank

Authors: Martin Vohník, Ondřej Borovec, Zuzana Kolaříková, Radka Sudová, Martina Réblová

Data type: species data

Link: https://doi.org/10.3897/mycokeys.55.35682.suppl2

MycoKeys 55: 87–99 (2019)
doi: 10.3897/mycokeys.55.33859
http://mycokeys.pensoft.net

RESEARCH ARTICLE

A peer-reviewed open-access journal
MycoKeys
Launched to accelerate biodiversity research

Three new species of *Dicephalospora* from China as revealed by morphological and molecular evidences

Huan-Di Zheng[1], Wen-Ying Zhuang[1]

1 *State Key Laboratory of Mycology, Institute of Microbiology, Chinese Academy of Sciences, Beijing 100101, China*

Corresponding author: *Wen-Ying Zhuang* (zhuangwy@im.ac.cn)

Academic editor: *N. Wijayawardene* | Received 14 February 2019 | Accepted 21 May 2019 | Published 1 July 2019

Citation: Zheng H-D, Zhuang W-Y (2019) Three new species of *Dicephalospora* from China as revealed by morphological and molecular evidences. MycoKeys 55: 87–99. https://doi.org/10.3897/mycokeys.55.33859

Abstract

Three new species of *Dicephalospora* are introduced based on morphological characters and DNA sequence analyses (maximum parsimony and neighbor-joining methods), viz. *D. albolutea*, *D. shennongjiana*, and *D. yunnanica*. All of them lack mucilaginous caps at ascospore poles. *Dicephalospora albolutea* is distinguished by cream to yellowish white apothecia and slightly curved ascospores. *Dicephalospora shennongjiana* is characterized by yellow apothecia, elliptical-fusoid ascospores 19–22 × 7–8.8 µm, and J+ asci 130–150 × 14–16.5 µm. *Dicephalospora yunnanica* is distinguished by orange apothecia and fusoid ascospores 16.5–25.3 × 3.3–3.5 µm. Descriptions and illustrations of the new species as well as a key to the known species in the genus are provided.

Keywords

Morphology, phylogeny, species diversity, taxonomy

Introduction

Dicephalospora Spooner is a small genus established by Spooner (1987) with *D. calochroa* (Syd. & P. Syd.) Spooner as the type species. The poles of ascospores with a mucilaginous cap and J+ asci were treated as two important features to delimitate the genus, but a later study proved they are not reliable features at the generic level (Zhuang et al. 2016). The emended diagnostic characters of the genus are that apothecia erumpent or superficial, stipitate, yellow, orange, red to blackish, ectal excipulum of textura prismatica with refractive walls, medullary excipulum of textura intricata, asci J+ or J- in Melzer's reagent, ascospores hyaline, subellipsoid to fusoid, guttulate, poles

either with a mucilaginous cap or not, paraphyses filiform, straight or slightly curved at apex, and occurring on rotten wood, twigs, and leaf petioles (Zhuang et al. 2016). The genus was once treated as a member of Rutstroemiaceae (Kirk et al. 2008), Helotiaceae (Wijayawardene et al. 2017, 2018), or Sclerotiniaceae (Index Fungorum 2019). Including *Dicephalospora* in Helotiaceae is more reasonable in view of the phylogenetic studies of related groups in recent years (Han et al. 2014; Zhao et al. 2016).

Zhuang et al. (2016) carried out a comprehensive study on taxonomy of *Dicephalospora* in China and provided a key to the known species of the genus. Approximately, 10 species are currently accepted in the genus and nine of them have been found in China (Zhuang 1995a, 1995b, 1999; Verkley 2004; Zhuang et al. 2016). Dicephalosterol was discovered from the culture of *D. rufocornea* (Hosoya et al. 1999). This compound is a new testosterone 5α-reductase inhibitor and has a potential to be developed as a drug to prevent and cure prostatic hypertrophy (Hosoya et al. 1999). Additional information about utilization of the *Dicephalospora* spp. was rarely published maybe due to the minimal biomass in nature, difficulty of getting pure culture, and slow-growth if cultured.

During the examinations of helotialean fungi from China, three species fit well with the emended generic concept of *Dicephalospora* (Zhuang et al. 2016). However, new collections are found to differ from hitherto known species of *Dicephalospora*. To confirm their affinities and investigate their relationships with other species, phylogenetic analyses were conducted based on the internal transcribed spacers and 5.8S of nuclear ribosomal DNA (ITS).The results support their placement within the genus and their distinctions from any known species.

Materials and methods

Specimens were collected, recorded, and photographed by a Canon PowerShot G16 digital camera in the field. Descriptions of gross morphology and substrate were according to field notes and photos. Dried apothecia were rehydrated with distilled water and sectioned at a thickness of 15–20 μm with a Yidi YD-1508A freezing microtome (Jinhua, China). Measurements were taken from longitudinal sections and squash mounts in lacto-phenol cotton blue solution using an Olympus BH-2 microscope (Tokyo, Japan). Iodine reactions of ascal apparatus were tested with or without 3% KOH solution pretreatment in Melzer's reagent and Lugol's solution (Baral 2009). Microscopic images were taken using a Canon G5 digital camera (Tokyo, Japan) attached to a Zeiss Axioskop 2 Plus microscope (Göttingen, Germany). Voucher specimens were deposited in the Herbarium Mycologicum Academiae Sinicae (**HMAS**). Names of the new species were formally registered in the database Fungal Names (http://www.fungalinfo.net/fungalname/fungalname.html).

Pure cultures were obtained from some specimens following the method provided by Webster and Weber (2001) and preserved in the State Key Laboratory of Mycology, Institute of Microbiology, Chinese Academy of Sciences.

Genomic DNA was extracted from dried apothecia or pure culture, using Plant Genomic DNA Kit (TIANGEN Biotech. Co., Beijing, China). ITS region was amplified

and sequenced using the primer pair ITS1/ITS4 (White et al. 1990). PCR reactions had a final volume of 30 µl, containing 15 µl 2×Taq MasterMix (Beijing CWBiotech, China), 1.5 µl of each primer (10 mM), 2 µl DNA, and 10 µl deionized water. PCR reactions were carried out in an Applied Biosystems 2720 thermocycler (Foster City, CA, USA) under the following conditions: 94 °C for 5 min, followed by 35 cycles of 94 °C for 30 s, 53 °C for 30 s and 30 s at 72 °C, and a final extension of 72 °C for 10 min. The PCR products were purified and sequenced at Beijing Tianyi Huiyuan Bioscience and Technology, China.

Newly generated sequences were assembled and edited using BioEdit 7.0.5.3 (Hall 1999) or SeqMan (DNASTAR, Lasergene 7.1.0). The new sequences were deposited in GenBank and additional sequences were downloaded from GenBank (Table 1).

Table 1. Sequences used in this study.

Species	Specimen/strain	ITS
Chlorosplenium chlora (Schwein.) M.A. Curtis	HMAS 266518	**MK425599**
	HMAS 279692	**MK425600**
Ciboria batschiana (Zopf) N.F. Buchw.	CBS 312.37	KF859931
Ciborinia foliicola (E.K. Cash & R.W. Davidson) Whetzel	1932.H	Z80892
Dicephalospora albolutea H.D. Zheng & W.Y. Zhuang	HMAS 279693	**MK425601**
Dicephalospora aurantiaca (W.Y. Zhuang) W.Y. Zhuang & Z.Q. Zeng	HMAS 61850	DQ986486
Dicephalospora chrysotricha (Berk.) Verkley	ICMP:19950	KF727410
	ICMP:19952	KF727411
Dicephalospora dentata Xiao X. Liu & W.Y. Zhuang	HMAS 266694	KP204263
Dicephalospora huangshanica (W.Y. Zhuang) W.Y. Zhuang & Z.Q. Zeng	HMAS 74836	DQ986485
	HMAS 81364	DQ986484
	HMAS 279694	**MK425602**
Dicephalospora rufocornea (Berk. & Broome) Spooner	HMAS 75518	DQ986480
	10106	KU668565
	HMAS 279695	**MK425603**
	HMAS 279696	**MK425604**
	HMAS 279697	**MK425605**
Dicephalospora shennongjiana H.D. Zheng & W.Y. Zhuang	HMAS 279698	**MK425606**
Dicephalospora yunnanica H.D. Zheng & W.Y. Zhuang	HMAS 279699	**MK425607**
	HMAS 279700	**MK425608**
	HMAS 279701	**MK425609**
Hymenoscyphus fructigenus (Bull.) Gray	CBS650.92	GU586933
	HMAS 75893	JX977144
Lachnum pygmaeum (Fr.) Bres.	ARON 2924.S	AJ430215
Lachnum spartinae S.A. Cantrel	SAP 138	AF422970
Lambertella corni-maris Höhn.	CLX 3892	KC958560
	CLX 4075	KC958562
Lanzia allantospora (Dennis) Spooner	PRJ D804	AY755334
Lanzia luteovirescens (Roberge ex Desm.) Dumont & Korf	1823	KC533545
Moellerodiscus lentus (Berk. & Broome) Dumont	7818	KU668564
	10544	KU668566
Monilinia fructicola (G. Winter) Honey	MO-3D	JN001480
	RS10	JF325841
Rutstroemia firma (Pers.) P. Karst.	2089.1	Z80893
	2089	KC533547
Sclerotinia sclerotiorum (Lib.) de Bary	2	KF148605
	6	KF148609

* Numbers in bold indicate sequences produced by this study.

Lachnum pygmaeum (Fr.) Bres. and *L. spartinae* S.A. Cantrel were chosen as outgroup taxa. The ITS sequence matrix was aligned and manually edited using BioEdit 7.0.5.3 (Hall 1999). Phylogenetic analyses were performed using maximum parsimony (MP) and neighbor-joining (NJ) methods with PAUP* 4.0b10 and parameters were set according to Zheng and Zhuang (2015). The topological confidence of the NJ and MP trees was assessed with bootstrap analysis using 1,000 replications, each with 10 replicates of random stepwise addition of taxa. The resulting trees were viewed via TreeView 1.6.6 (Page 1996).

Results

Phylogenetic analyses

The ITS dataset included 37 sequences from eight *Dicephalospora* species, 11 related fungi and two outgroup taxa. The final alignment resulted in 634 characters including gaps, of which 252 were parsimony-informative, 38 were variable and parsimony-uninformative, and 344 were constant. In the MP analysis, eight most parsimonious trees were generated (tree length = 790, consistency index = 0.5899, homoplasy index = 0.4101, retention index = 0.8126, rescaled consistency index = 0.4793) and one of them was shown in Figure 1. MP and NJ bootstrap proportions (BP) greater than 50% were labeled at the nodes.

From topology of the phylogenetic tree (Fig. 1), *Dicephalospora* species clustered together with a medium supporting value (56% MPBP). The three putative new species were clearly distinct from the known and sequenced species of the genus. *Dicephalospora albolutea* appeared as an independent lineage distinct from any other members of the genus. *Dicephalospora shennongjiana* was resolved as a sibling species of *D. huangshanica* (97% MPBP and 99% NJBP). ITS sequences of the three collections of *D. yunnanica* were identical and formed a well-supported group with *D. aurantiaca* (100% MPBP and 100% NJBP).

Taxonomy

Dicephalospora albolutea **H.D. Zheng & W.Y. Zhuang, sp. nov.**
Fungal Names FN570602
Figure 2

Etymology. The specific epithet refers to the color of apothecia.

Holotype. CHINA. Yunnan Province, Binchuan County, Jizu Mountain, alt. 2500 m, on rotten leaf veins, 21 September 2017, H.D. Zheng, X.C. Wang, Y.B. Zhang & Y. Zhang 11613 (HMAS 279693, ITS GenBank accession number: MK425601).

Description. *Apothecia* scattered, discoid, stipitate, with even margin, 1–2.5 mm in diameter; hymenium surface cream to yellowish white; receptacle surface concolorous.

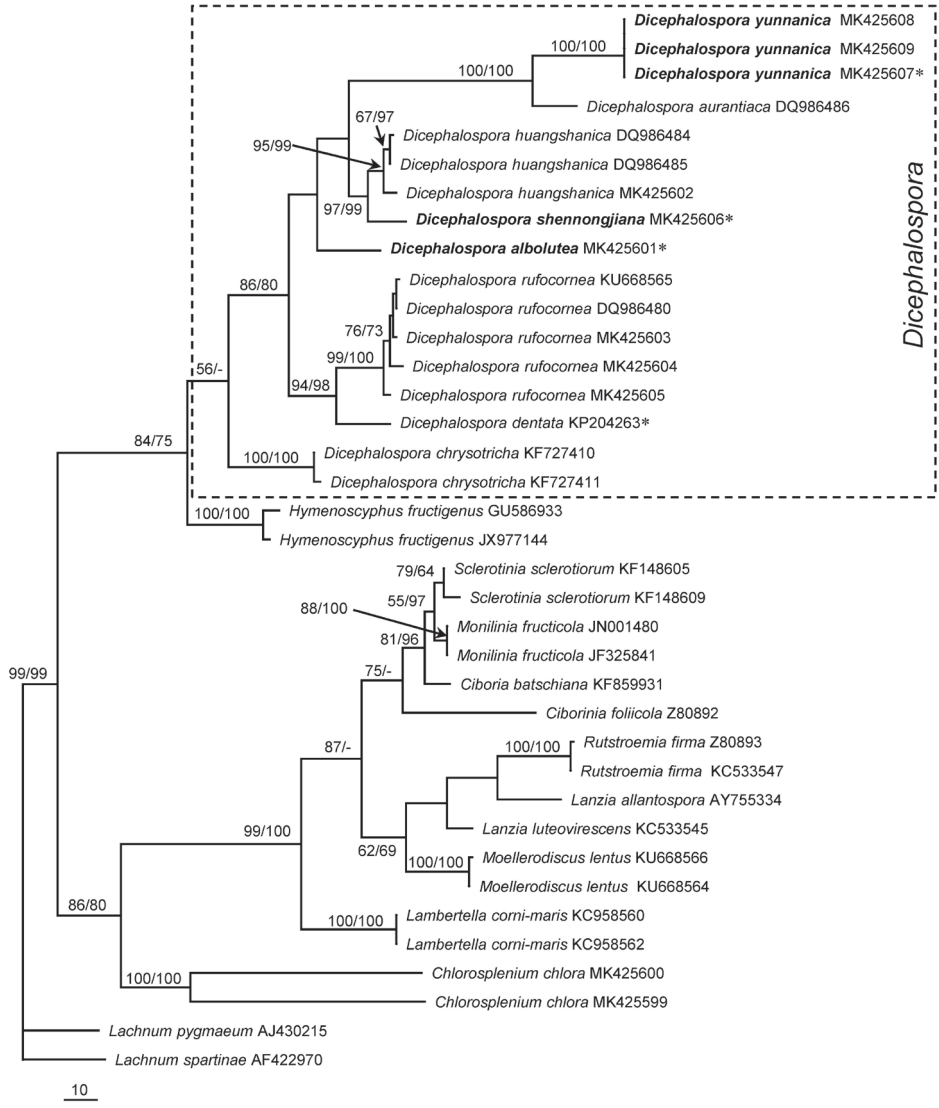

Figure 1. One of the MP trees inferred from ITS sequences. Bootstrap support values (≥50%) of MP and NJ are shown at nodes from left to right. New proposed species are shown in bold. New species are in bold. Sequences derived from holotypes are marked with an asterisk (*).

Ectal excipulum of textura prismatica, 20–70 μm thick, cells somewhat thick- and glassy-walled, 16.5–40 × 5.5–11 μm. *Medullary excipulum* of textura porrecta and textura intricata, 25–275 μm thick, hyphae hyaline, thin-walled, 2.5–5 μm wide. *Subhymenium* not distinguishable. *Hymenium* 165–175 μm thick. *Asci* unitunicate, arising from simple septa, 8-spored, cylindric-clavate, J+ in Melzer's reagent and Lugol's solution without KOH pretreatment, visible as two blue lines, 140–156 ×

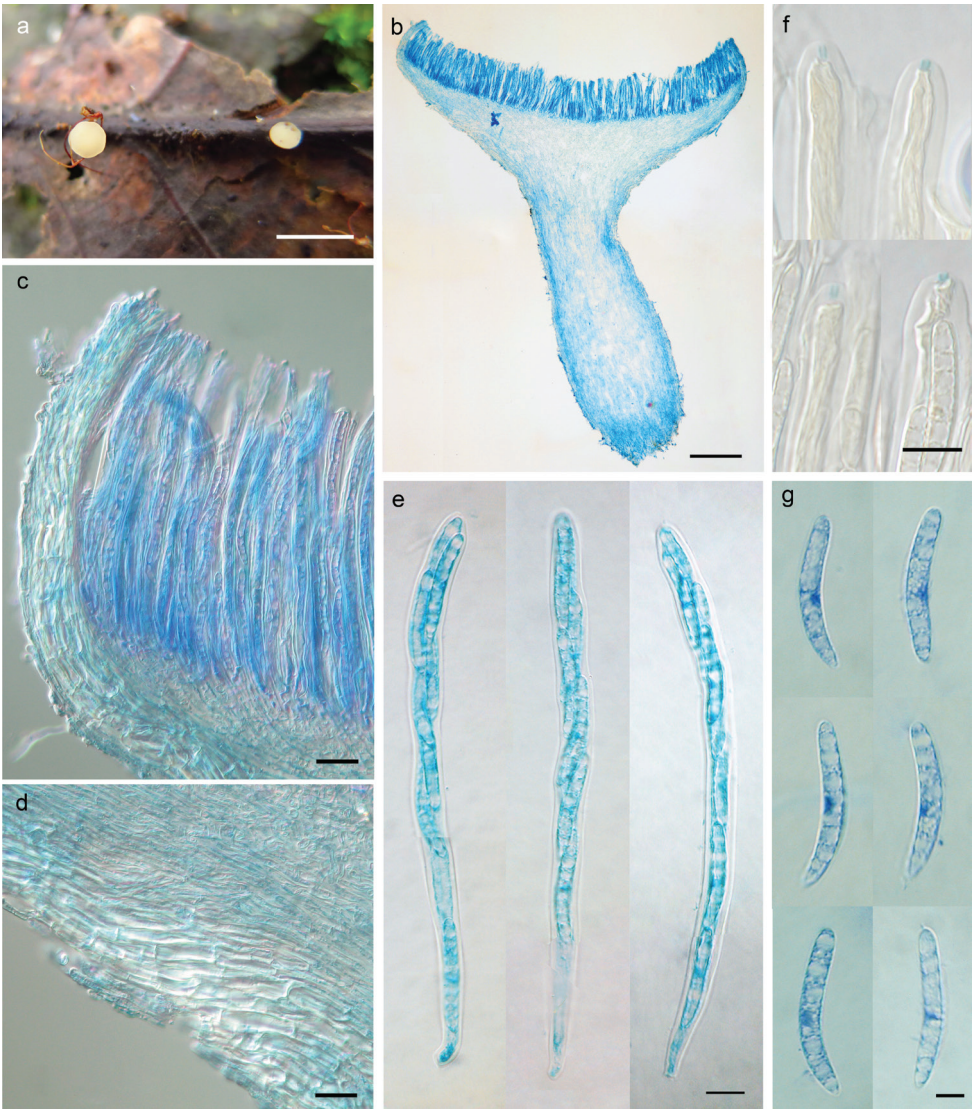

Figure 2. *Dicephalospora albolutea* (HMAS 279693, **holotype**). **a** fresh apothecia on natural substrate **b** longitudinal section of apothecium **c** structure of margin and hymenium **d** structure of flank **e** asci **f** IKI reaction of apical rings **g** ascospores. Mouting media: **b–e, g** lacto-phenol cotton **f** lugol's solution. Scale bars: 5 mm (**a**); 200 μm (**b**); 20 μm (**c, d**); 10 μm (**e, f**); 5 μm (**g**).

9.5–10.5 μm. *Ascospores* sausage-shaped to subfusoid, with anterior end rounded and posterior end narrower, slightly curved, aseptate, hyaline, smooth, lacking a gel cap at each end, multiguttulate, with a dark-stained area when mounted in cotton blue solution, biseriate, 26–31 × 3.8–5.0 μm. *Paraphyses* filiform, straight, slightly enlarged

at apex, hyaline, septate, 3–3.5 μm broad at upper portion and 1.5–2 μm below, equal to or very slightly exceeding the asci.

Notes. The diagnostic features of *D. albolutea* are cream to yellowish white apothecia and sausage-shaped ascospores. The apothecial color of earlier known *Dicephalospora* species varied from yellow, orange, red to dark, but never as pale as that in *D. albolutea*. *Dicephalospora calochroa* (Syd. & P. Syd.) Spooner is somewhat similar in length of asci and ascospores, but differs by vivid orange apothecia, wider asci (125–150 × 12–15 μm) and ascospores (20–25 × 6–8 μm), which are pointed at both ends (Spooner 1987). *Dicephalospora albolutea* differs from any investigated species by at least 45 bp in sequences of ITS region, and appeared as an independent lineage in the phylogenetic tree (Fig. 1), which further confirmed its distinction from others in the group.

Dicephalospora shennongjiana **H.D. Zheng & W.Y. Zhuang, sp. nov.**
Fungal Names FN570603
Figure 3

Etymology. The specific epithet refers to the type locality of the fungus.

Holotype. CHINA. Hubei Province, Shennongjia, Shennongyuan, alt. 2250 m, on stromatized dead vine, 15 Sept 2014, H.D. Zheng, Z.Q. Zeng, W.T. Qin & K. Chen 9589 (HMAS 279698, ITS GenBank accession number: MK425606).

Description. *Apothecia* scattered, discoid to flat, stipitate, with even margin, 0.5–0.8 mm in diameter; hymenium surface greenish yellow; receptacle surface slightly darker. *Ectal excipulum* of textura prismatica, 15–40 μm thick, cells hyaline to pale brownish, somewhat thick- and glassy-walled, 10–20 × 4–11 μm. *Medullary excipulum* of textura intricata, 25–110 μm thick, hyphae hyaline, thin-walled, 2–4 μm wide. *Subhymenium* about 15 μm thick. *Hymenium* 170–180 μm thick. *Asci* arising from simple septa, unitunicate, 8-spored, clavate, J+ in Melzer's reagent and Lugol's solution without KOH pretreatment, visible as two blue lines, 130–150 × 14–16.5 μm. *Ascospores* elliptical-subfusoid, aseptate, hyaline, smooth, lacking a gel cap at each end, multiguttulate, with a dark-stained area when mounted in cotton blue solution, uniseriate, 19–22 × 7–8.8 μm. *Paraphyses* filiform, slightly enlarged at apex, hyaline, septate, branched and tangled near apex, 3–3.5 μm broad at upper portion and 1.5–2 μm below, exceeding the asci by 10–20 μm.

Notes. The new species can be distinguished from other species by shape of ascospores and tangled paraphyses apices. *Dicephalospora damingshanica* has a similarly shaped ascospore, but larger (22–32 × 9–12.7 μm), and with a hyaline mucilaginous cap at both ends (Zhuang 1999). Phylogenetically, *D. shennongjiana* is closely related to *D. huangshanica*, but the latter differs by red apothecia, smaller asci (89–96 × 9.5–11 μm), fusoid ascospores (18–26 × 4–5 μm) (Zhuang 1995a), and 22 bp divergence in ITS region.

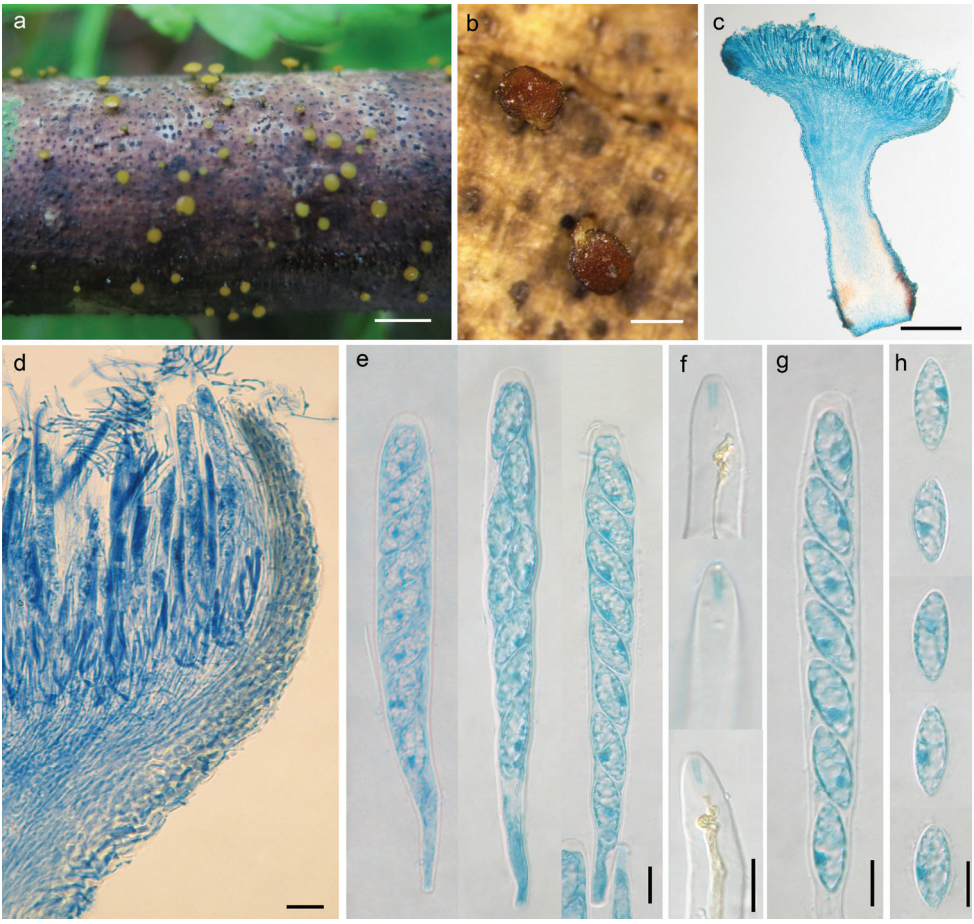

Figure 3. *Dicephalospora shennongjiana* (HMAS 279698, **holotype**) **a** fresh apothecia on natural substrate **b** dried apothecia **c** longitudinal section of apothecium **d** structure of margin, flank and hymenium **e** asci **f** IKI reaction of apical rings **g** ascospores in an ascus **h** ascospores. Mouting media: **c–e, g, h** lactophenol cotton **f** fugol's solution. Scale bars: 2 mm (**a**); 0.4 mm (**b**); 200 µm (**c**); 20 µm (**d**); 10 µm (**e–h**).

Dicephalospora yunnanica **H.D. Zheng & W.Y. Zhuang, sp. nov.**
Fungal Names FN570604
Figure 4

Etymology. The specific epithet refers to the type locality of the fungus.

Holotype. CHINA. Yunnan Province, Maguan County, Dabao Village, alt. 1565 m, on rotten leaf rachis, 13 August 2016, X.H. Wang, S.H. Li, H.D. Zheng & S.C. Li YN16-108 (HMAS279699, ITS GenBank accession number: MK425607).

Description. *Apothecia* scattered, discoid, stipitate, with even margin, 0.8–2.0 mm in diameter; hymenium surface bright yellow to orange; receptacle surface paler. *Ectal excipulum*

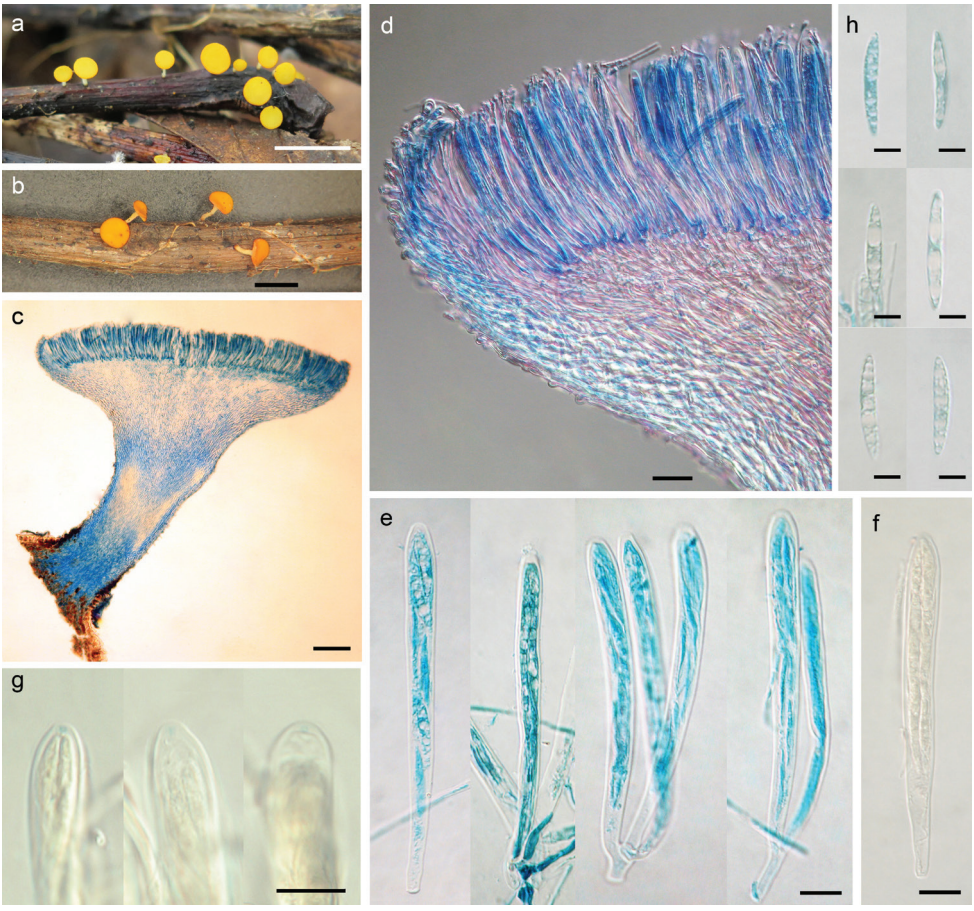

Figure 4. *Dicephalospora yunnanica* (HMAS 279699, **holotype**) **a** fresh apothecia on natural substrate **b** dried apothecia **c** longitudinal section of apothecium **d** structure of margin, flank and hymenium **e, f** asci **g** IKI reaction of apical rings **h** ascospores. Mouting media: **c–e, h** lacto-phenol cotton **f, g** lugol's solution. Scale bars: 5 mm (**a**); 2 mm (**b**); 200 μm (**c**); 20 μm (**d**); 10 μm (**e–g**); 5 μm (**h**).

of textura prismatica, 22–60 μm thick, cells hyaline, somewhat thick- and glassy-walled, 7–20 × 5–7 μm. *Medullary excipulum* of textura intricata, 30–230 μm thick, hyphae thin-walled, 2–5 μm wide. *Subhymenium* not distinguishable. *Hymenium* 100–115 μm thick. *Asci* arising from simple septa, unitunicate, 8-spored, cylindric-clavate, J+ in Melzer's reagent and Lugol's solution without KOH pretreatment, visible as two faint blue lines, 85–100 × 7.5–8.5 μm. *Ascospores* fusoid, aseptate, with one side very slightly flattened and pointed at ends, hyaline, smooth, lacking a gel cap at each end, multiguttulate, biseriate, 16.5–25.3 × 3.3–3.5 μm. *Paraphyses* filiform, slightly enlarged at apex, straight or sometimes slightly curved at the apical portion, hyaline, septate, 2.5–4 μm broad at upper portion and 1.5–2 μm below, slightly exceeding the asci by about 5 μm.

Additional specimens examined. CHINA. Yunnan Province, Maguan County, Xiaobaozi Town, alt. 1550 m, on rotten leaf rachis, 13 August 2016, X.H. Wang, S.H. Li, H.D. Zheng & S.C. Li YN16-135 (HMAS 279700); Maguan County, Pojiao Village, alt. 1450 m, on rotten leaf rachis, 14 August 2016, X.H. Wang, S.H. Li, H.D. Zheng & S.C. Li YN16-165 (HMAS 279700).

Notes. *Dicephalospora yunnanica* shares similar gross morphology with and appeared to be sister of *D. aurantiaca* in the phylogenetic tree (Fig. 1). However, *D. aurantiaca* has larger asci (93–103 × 9.7–10.5 μm) and ascospores (21–26 × 4–4.8 μm), as well as obviously curved paraphysis apices (Zhuang 1995a; Zhuang et al. 2016). Concerning the DNA sequence data, the three collections of *D. yunnanica* share exactly the same sequences, while the closest species *D. aurantiaca* showed 75 bp divergence (including 32 gaps) for ITS.

A taxonomic key to the known species of *Dicephalospora*

1	Receptacle surface covered with hairs	***D. chrysotricha***
–	Receptacle surface without hairs	**2**
2	Apothecial margin dentate	***D. dentata***
–	Apothecial margin even	**3**
3	Hymenium surface cream to yellowish white when fresh	***D. albolutea***
–	Hymenium surface darker in color	**4**
4	Hymenium surface red or dark red	***D. huangshanica***
–	Hymenium surface lacking of a red tint	**5**
5	Paraphyses with darkly pigmented contents	***D. phaeoparaphysis***
–	Paraphyses without darkly pigmented contents	**6**
6	Ascospores with a gel cap at each end	**7**
–	Ascospores lacking of a gel cap at each end	**10**
7	Ascospores 9–12.7 μm wide	***D. damingshanica***
–	Ascospores less than 9 μm wide	**8**
8	Asci J–, ascospores 20–28 × 4.5–5.7 μm	***D. pinglongshanica***
–	Asci J+	**9**
9	Ascospores 23–27(–29) × 6.5–7.5 μm	***D. calochroa***
–	Ascospores (27–)32–39 × 4–5.5(–6) μm	***D. rufocornea***
10	Ascospores constricted in the middle, 20–27 × 4–5 μm	***D. contracta***
–	Ascospores not constricted in the middle	**11**
11	Ascospores 19–22 × 7–8.8 μm	***D. shennongjiana***
–	Ascospores less than 7 μm wide	**12**
12	Ascospores 16.5–25.3 × 3.3–3.5 μm, paraphyses straight	***D. yunnanica***
–	Ascospores 21–26 × 4–4.8 μm, paraphyses curved at apex	***D. aurantiaca***

Discussion

Identification of *Dicephalospora* species is mainly based on morphological features, such as color of apothecia, anatomic structure, and characteristics of asci and ascospores. DNA sequence data are sometimes considered, which play an important role in the delineation of fungal species (Hibbett et al. 2016; Jeewon and Hyde 2016). In the present study, three new species were introduced based on morphology and ITS phylogeny. So far, the genus comprises 13 species, of which 12 have been reported from China. *Dicephalospora chrysotricha* (Berk.) Verkley originally described from, and endemic to, New Zealand, is the only exception and known only from the type locality (Verkley 2004).

In the phylogenetic analyses, only some species possessing fusoid to sausage-shaped and elliptic-subfusoid ascospores were involved due to limitation of the available sequences. The ITS barcodes seem to be useful for distinguishing *Dicephalospora* species, as they grouped as well-separated clades (Fig. 1). Seven of the eight species were together receiving moderate statistic supports (86% MPBP and 80% BIPP) and formed the core group. However, *D. chrysotricha* joined them as a distantly separated lineage with very low support (Fig. 1, 56% MPBP). *Dicephalospora chrysotricha* is distinct from any other taxa of the genus in having hair-like projections on receptacle surface. *Dicephalospora chrysotricha* was previously treated as a member of *Trichopeziza* Fuckel (Saccardo 1889) and then *Chlorosplenium* Fr. (Dennis 1961). The transfer of this species to *Dicephalospora* might have been because of presence of polar mucilaginous caps of ascospores and the more or less similar ectal excipulum structure except for hairs (Verkley 2004). However, it does not fit well the generic concept of *Dicephalospora*. Further study is required to clarify the taxonomic position of this fungus.

As to the phylogenetic position of *Dicephalospora*, Figure 1 shows its close relationship with *Hymenoscyphus* Gray, which agrees with the treatment of Wijayawardene et al. (2017). Similar results were also achieved in other recent studies (Han et al. 2014; Zhao et al. 2016). In the phylogenetic study of Hyaloscyphaceae and related helotialean cup-fungi, *D. huangshanica* and *D. rufocornea* grouped together with some genera of Helotiaceae, such as *Hymenoscyphus*, *Crocicreas* Fr. and *Cudoniella* Sacc., as a highly supported clade in the maximum-likelihood tree inferred from combined sequence data of ITS, the large subunit nrDNA gene (LSU), the second largest subunit of RNA polymerase II gene (RPB2), and mitochondrial small subunit (mtSSU) (Han et al. 2014). Zhao et al. (2016) carried out phylogenetic analyses of *Lambertella* Höhn. and allied genera including *Dicephalospora* and *Hymenoscyphus*, as inferred from ITS, LSU and RPB2 sequence data. In their phylogenetic trees, *D. rufocornea* was also associated with the clade consisting of *Hymenoscyphus* species. In view of the above results, close relationship of *Dicephalospora* with genera of Helotiaceae is obvious. Comprehensive work containing more genera and more genes are required to obtain an accurate conclusion on phylogenetic placement of *Dicephalospora*.

Acknowledgements

This work was supported by the National Natural Science Foundation of China (nos. 31770019, 31570018). The authors thank all co-collectors of specimens examined in this study for their invaluable help during the field work.

References

Baral H-O (2009) Iodine reaction in Ascomycetes: why is Lugol's solution superior to Melzer'sreagent? http://www.gbif-mycology.de/HostedSites/Baral/IodineReaction.htm [Accessed on: 2011-3-18]

Dennis RWG (1961) Some inoperculate Discomycetes from New Zealand. Kew Bulletin 15: 293–320. https://doi.org/10.2307/4109373

Hall TA (1999) BioEdit: a user-friendly biological sequence alignment editor and analysis program for Windows 95/98/NT. Nucleic Acids Symposium Series 41: 95–98.

Han JG, Hosoya T, Sung GH, Shin HD (2014) Phylogenetic reassessment of Hyaloscyphaceae sensu lato (Helotiales, Leotiomycetes) based on multigene analyses. Fungal Biology 118: 150–167. https://doi.org/10.1016/j.funbio.2013.11.004

Hibbett D, Abarenkov K, Kõljalg U, Öpik M, Chai B, Cole J, Wang Q, Crous P, Robert V, Helgason T, Herr JR, Kirk P, Lueschow S, O'Donnell K, Nilsson RH, Oono R, Schoch C, Smyth C, Walker DM, Porras-Alfaro A, Taylor JW, Geiser DM (2016) Sequence-based classification and identification of Fungi. Mycologia 108: 1049–1068. https://doi.org/10.3852/16-130

Hosoya T, Hamano K, Sugano M, Ogura Y, Hatano E, Hamada T (1999) Discovery of dicephalosterol, a new testosterone 5a-reductase inhibitor, and some new mycological aspects of its producer, *Dicephalospora rufocornea* (Sclerotiniaceae, Discomycetes). Mycoscience 40: 525–529. https://doi.org/10.1007/BF02461030

Index Fungorum (2019) Index Fungorum. http://www.indexfungorum.org/names/Names.asp [Accessed on: 2019-2-12]

Jeewon R, Hyde KD (2016) Establishing species boundaries and new taxa among fungi: recommendations to resolve taxonomic ambiguities. Mycosphere 7: 1669–1677. https://doi.org/10.5943/mycosphere/7/11/4

Kirk PM, Cannon PF, Minter DW, Stalpers JA (2008) Dictionary of the Fungi (10th edn). CABI, Wallingford, 771 pp.

Page RDM (1996) Treeview: an application to display phylogenetic trees on personal computers. Computer Applications in the Biosciences 12: 357–358. https://doi.org/10.1093/bioinformatics/12.4.357

Saccardo PA (1889). Discomyceteae et Phymatosphaeriaceae. Sylloge Fungorum 8: 1–1143.

Spooner BM (1987) Helotiales of Australasia: Geoglossaceae, Orbiliaceae, Sclerotiniaceae, Hyaloscyphaceae. Bibliotheca Mycologica 116: 1–711.

Verkley GJM (2004) Redisposition of *Chlorosplenium chrysotrichum* to the genus *Dicephalospora* (Sclerotiniaceae, Ascomycota). Sydowia 56: 343–348.

Webster J, Weber RWS (2001) Teaching techniques for mycology: 15. Fertilization and apothecium development in *Pyronema domesticum* and *Ascobolus furfuraceus* (Pezizales). Mycologist 15: 126–131. https://doi.org/10.1016/S0269-915X(01)80035-5

White T, Bruns TD, Lee A, Taylor JW (1990) Amplification and direct sequencing of fungal ribosomal RNA genes for phylogenetics. In: Innis MA, Gelfand DH, Snisky JJ, White TJ (Eds) PCR Protocols: A Guide to Methods and Applications. Academic Press, San Diego, 315–322. https://doi.org/10.1016/B978-0-12-372180-8.50042-1

Wijayawardene NN, Hyde KD, Rajeshkumar KC, Hawksworth DL, Madrid H, Kirk PM, Braun U, Singh RV, Crous PW, Kukwa M, Lücking R, Kurtzman CP, Yurkov A, Haelewaters D, Aptroot A, Lumbsch HT, Timdal E, Ertz D, Etayo J, Phillips AJL, Groenewald JZ, Papizadeh M, Selbmann L, Dayarathne MC, Weerakoon G, Jones EBG, Suetrong S, Tian Q, Castañeda-Ruiz RF, Bahkali AH, Pang K-L, Tanaka K, Dai DQ, Sakayaroj J, Hujslová M, Lombard L, Shenoy BD, Suija A, Maharachchikumbura SSN, Thambugala KM, Wanasinghe DN, Sharma BO, Gaikwad S, Pandit G, Zucconi L, Onofri S, Egidi E, Raja HA, Kodsueb R, Cáceres MES, Pérez-Ortega S, Fiuza PO, Monteiro JS, Vasilyeva LN, Shivas RG, Prieto M, Wedin M, Olariaga I, Lateef AA, Agrawal Y, Fazeli SAS, Amoozegar MA, Zhao GZ, Pfliegler WP, Sharma G, Oset M, Abdel-Wahab MA, Takamatsu S, Bensch K, de Silva NI, De Kesel A, Karunarathna A, Boonmee S, Pfister DH, Lu Y-Z, Luo Z-L, Boonyuen N, Daranagama DA, Senanayake IC, Jayasiri SC, Samarakoon MC, Zeng X-Y, Doilom M, Quijada L, Rampadarath S, Heredia G, Dissanayake AJ, Jayawardana RS, Perera RH, Tang LZ, Phukhamsakda C, Hernández-Restrepo M, Ma X, Tibpromma S, Gusmao LFP, Weerahewa D, Karunarathna SC (2017) Notes for genera: Ascomycota. Fungal Diversity 86: 1–594. https://doi.org/10.1007/s13225-017-0386-0

Wijayawardene NN, Hyde KD, Lumbsch HT, Liu JK, Maharachchikumbura SSN, Ekanayaka AH, Tian Q, Phookamsak R (2018) Outline of *Ascomycota*: 2017. Fungal Diversity 88(1): 167–263. https://doi.org/10.1007/s13225-018-0394-8

Zhao YJ, Hosaka K, Hosoya T (2016) Taxonomic re-evaluation of the genus *Lambertella* (Rutstroemiaceae, Helotiales) and allied stroma-forming fungi. Mycological Progress 15: 1215–1228. https://doi.org/10.1007/s11557-016-1225-5

Zheng HD, Zhuang WY (2015) Five new species of *Hymenoscyphus* (Helotiaceae, Ascomycota) with notes on the phylogeny of the genus. Mycotaxon 130: 1017–1038. https://doi.org/10.5248/130.1017

Zhuang WY (1995a) A few petiole-inhabiting discomycetes in China. Mycosystema 7: 13–17.

Zhuang WY (1995b) Some new species and new records of discomycetes in China. V. Mycotaxon 56: 31–40.

Zhuang WY (1999) Discomycetes of tropical China. VI. Additional species from Guangxi. Fungal Diversity 3: 187–196.

Zhuang WY, Zeng ZQ, Liu XX (2016) Taxonomic revision of the genus *Dicephalospora* (Helotiales) in China. Mycosystema 35: 791–801. https://doi.org/10.13346/j.mycosystema.160047

MycoKeys 55: 101–120 (2019)
doi: 10.3897/mycokeys.55.34527
http://mycokeys.pensoft.net

RESEARCH ARTICLE

A peer-reviewed open-access journal
MycoKeys
Launched to accelerate biodiversity research

The genera *Rugonectria* and *Thelonectria* (Hypocreales, Nectriaceae) in China

Zhao-Qing Zeng[1], Wen-Ying Zhuang[1]

1 *State Key Laboratory of Mycology, Institute of Microbiology, Chinese Academy of Sciences, Beijing 100101, China*

Corresponding authors: *Zhao-Qing Zeng* (zengzq@im.ac.cn); *Wen-Ying Zhuang* (zhuangwy@im.ac.cn)

Academic editor: *Danny Haelewaters* | Received 14 March 2019 | Accepted 22 May 2019 | Published 1 July 2019

Citation: Zeng Z-Q, Zhuang W-Y (2019) The genera *Rugonectria* and *Thelonectria* (Hypocreales, Nectriaceae) in China. MycoKeys 55: 101–120. https://doi.org/10.3897/mycokeys.55.34527

Abstract

Recent collections and herbarium specimens of *Rugonectria* and *Thelonectria* from different regions of China were examined. Using combined analyses of morphological and molecular data, 17 species are recognised including three species of *Rugonectria* and 14 species in *Thelonectria*. Amongst them, *R. microconidia* and *T. guangdongensis* are new to science. *Rugonectria microconidia* on mossy bark is characterised by superficial, yellow to orange, pyriform to subglobose perithecia with a warted surface; ellipsoidal to broadly ellipsoidal, striate, uniseptate ascospores; and allantoid to rod-shaped, aseptate microconidia. *Thelonectria guangdongensis* possesses bright red perithecia with a slightly roughened surface and a prominently dark papilla; ellipsoidal, smooth, uniseptate ascospores; and subcylindrical, slightly curved, multiseptate macroconidia. Morphological distinctions and sequence divergences between the new species and their close relatives are discussed. Name changes for the previously recorded species in China are noted.

Keywords

Morphology, Multigene analyses, Taxonomy

Introduction

The family Nectriaceae was introduced in 1865 and circumscribed to accommodate the hypocrealean species having ascomata that are generally yellow, orange-red to purple and usually changing colour in potassium hydroxide (KOH) and lactic acid (LA) (Rossman et al. 1999). About 55 genera containing 900 species are included in the family (Lombard et al. 2015). A phylogenetic backbone for Nectriaceae was constructed based on DNA sequences of 10 loci by Lombard et al. (2015).

The genus *Rugonectria* P. Chaverri & Samuels, typified by *R. rugulosa* (Pat. & Gaillard) Samuels, P. Chaverri & C. Salgado, is characterised by perithecia solitary or in groups, seated on or partially immersed in a stroma. The perithecia are orange to red, globose to subglobose and non-papillate, with warted or rugose walls. Ascospores are ellipsoidal to oblong, striate, hyaline and 1-septate; and microconidia are ovoid to cylindrical (Chaverri et al. 2011). Currently, four species are recognised in the genus (Chaverri et al. 2011; Zeng et al. 2012). *Thelonectria* P. Chaverri & C. Salgado, typified by *T. discophora* (Mont.) P. Chaverri & C. Salgado, was established by Chaverri et al. (2011) to accommodate the nectriaceous fungi having superficial, globose to subglobose or pyriform to elongated perithecia which do not collapse when dry, with a prominent and darkened papilla; smooth, rarely spinulose or striate ascospores and curved macroconidia with rounded ends (Chaverri et al. 2011; Lombard et al. 2015; Salgado-Salazar et al. 2016). About 44 species are currently accepted in the genus (Chaverri et al. 2011; Salgado-Salazar et al. 2012, 2015, 2016; Zeng and Zhuang 2013; Crous et al. 2018). Species in the genera *Rugonectria* and *Thelonectria* are distributed in the tropics, subtropics and temperate regions and occur on early decaying bark, roots, branches, trunks and rarely in soil (Chaverri et al. 2011; Salgado-Salazar et al. 2015). A few species are plant pathogenic, such as *R. castaneicola* (W. Yamam. & Oyasu) Hirooka & P. Chaverri causing *Abies* and *Acer* cankers and *T. rubi* (Osterw.) C. Salgado & P. Chaverri causing *Rubus* cankers (Cedeño et al. 2004; Kobayashi et al. 2005; Chaverri et al. 2011; Salgado-Salazar et al. 2015).

The first record of *Rugonectria* from China dates back to 2000 when *R. rugulosa* (as *Nectria rugulosa* Pat. & Gaillard) was reported by Lu et al. (2000) based on a specimen collected on dead petioles of king palm. Research on *Thelonectria* in China was started by Teng (1936) when *T. discophora* (as *N. discophora* Mont.) was first reported on bark of fallen branches from Yunnan Province. In connection with our current work on the Chinese fungus flora, fresh materials and herbarium specimens of the two genera were examined. Based on morphology and phylogenetic analyses of the partial sequences of α-actin (ACT), internal transcribed spacer (ITS), nuclear ribosomal large subunit (LSU) rDNA and the largest subunit of RNA polymerase II (RPB1), 17 species were identified, including two undescribed species. Morphological and molecular diagnostic features between the new taxa and their closely related fungi are discussed.

Materials and methods

Sampling and morphological studies

Specimens were collected from Beijing, Fujian, Guangdong, Hainan, Henan, Hubei, Hunan and Yunnan provinces and are deposited in Herbarium Mycologicum Academiae Sinicae (HMAS) and cultures are kept in the State Key Laboratory of Mycology, Institute of Microbiology, Chinese Academy of Sciences. The methods used by Luo and Zhuang (2010) and Chaverri et al. (2011) were followed for morphological observations. The ascomatal wall reactions to 3% KOH and 100% LA were tested. To observe micro-

morphological characteristics of perithecial walls, sections were made with a freezing microtome (YD-1508-III, Jinhua, China) at a thickness of 6–8 μm. Lactophenol cotton blue solution was used as mounting medium for examination of anatomic structures and measurements of perithecia, asci and ascospores. Photographs were taken with a Leica DFC450 digital camera (Wetzlar, Germany) attached to a Leica M125 stereomicroscope (Milton Keynes, UK) for gross morphology and a Zeiss AxioCam MRc 5 digital camera (Jena, Germany) attached to a Zeiss Axio Imager A2 microscope (Göttingen, Germany) for microscopic features. Descriptive statistics of ascospores and conidia (minimum, maximum, mean and standard deviation) were calculated following the methods of Hirooka et al. (2012). Measurements of individual structures were based on 30 units, except as otherwise noted. Morphology of colonies were characterised using potato dextrose agar (PDA, 20% w/v potato + 2% w/v dextrose + 2% w/v agar) and synthetic nutrient-poor agar (SNA; Nirenberg 1976) at 25 °C in an incubator with alternating periods of light and darkness (12 h/12 h). Colony growth rates were measured after 7 d.

DNA extraction, PCR amplification and sequencing

Genomic DNA was extracted from fresh mycelium following the method of Wang and Zhuang (2004). Four primer pairs, act1-act2 (Samuels et al. 2006), ITS5-ITS4 (White et al. 1990), LR0R-LR5 (Vilgalys and Hester 1990; Rehner and Samuels 1994) and crpb1a-rpb1c (Castlebury et al. 2004) were used to amplify the ACT, ITS, LSU and RPB1 regions, respectively. PCR reactions were performed using an ABI 2720 Thermal Cycler (Applied Biosciences, Foster City, USA) with a 25 μl reaction system consisting of 12.5 μl Taq MasterMix, 1 μl each primer (10 μM), 1 μl template DNA and 9.5 μl ddH_2O, based on the procedures detailed in Chaverri et al. (2011). DNA sequencing was carried out in both directions on an ABI 3730XL DNA Sequencer (Applied Biosciences, Foster City, USA).

Sequence alignment and phylogenetic analyses

Newly obtained sequences and those retrieved from GenBank are listed in Table I. The sequences were assembled, aligned and the primer sequences were trimmed via BioEdit 7.0.5 (Hall 1999) and converted to NEXUS files by ClustalX 1.8 (Thompson et al. 1997). A partition homogeneity test was performed with 1,000 replicates in PAUP*4.0b10 (Swofford 2002) to evaluate statistical congruence amongst the four loci. The aligned ACT, ITS, LSU and RPB1 sequences were combined in BioEdit and analysed with Bayesian Inference (BI), Maximum Parsimony (MP) and Maximum Likelihood (ML) methods to determine the phylogenetic positions of the new species. The MP analysis was performed with PAUP 4.0b10 (Swofford 2002) using 1000 replicates of heuristic search with random addition of sequences and subsequent TBR (tree bisection and reconnection) branch swapping. Topological confidence of the resulting trees was tested by Maximum Parsimony bootstrap proportion (MPBP) with 1000

Table 1. List of species, herbarium/strain numbers and GenBank accession numbers of materials used in this study.

Species	Herbarium/strain numbers	GenBank Accession numbers			
		ACT	ITS	LSU	RPB1
Cosmospora coccinea Rabenh.	CBS 114050	GQ505967	FJ474072	GQ505990	GQ506020
Nectria cinnabarina (Tode) Fr.	AR 4302/AR 4477	HM484627	HM484548	HM484562	HM484577
Rugonectria castaneicola (W. Yamam. & Oyasu) Hirooka & P. Chaverri	CBS 128360	–	MH864901	MH876352	–
R. microconidia Z.Q. Zeng & W.Y. Zhuang	HMAS 254521	**MF669044**[a]	**MF669050**	**MF669052**	**MF669056**
R. neobalansae (Samuels) P. Chaverri & Samuels	CBS 125120	–	KM231750	HM364322	KM232146
R. rugulosa (Pat. & Gaillard) Samuels, P. Chaverri & C. Salgado	YH 1001	JF832515	JF832661	JF832761	JF832836
R. sinica W.Y. Zhuang, Z.Q. Zeng & W.H. Ho	HMAS 183542	**MF669046**	HM054141	HM042430	**MF669058**
Thelonectria asiatica C. Salgado & Hirooka	MAFF 241576	KC121436	KC153774	KC121500	KC153967
T. beijingensis Z.Q. Zeng, J. Luo & W.Y. Zhuang	HMAS 188498	**MF669047**	JQ836656	**MF669054**	**MF669059**
T. blattea C. Salgado & P. Chaverri	CBS 95268	KC121387	KC153725	KC121451	KC153918
T. brayfordii C. Salgado & Samuels	CBS 118612	KC121381	KC153719	KC121445	KC153912
T. conchyliata C. Salgado & P. Chaverri	GJS 8745	KC121401	KC153739	KC121465	KC153932
T. discophora (Mont.) P. Chaverri & C. Salgado	AR 4742	KC121376	KC153714	KC121440	KC153907
T. guangdongensis Z.Q. Zeng & W.Y. Zhuang	HMAS 254522	**MF669045**	**MF669051**	**MF669053**	**MF669057**
T. ianthina C. Salgado & Guu	GJS 10118	KC121393	KC153731	KC121457	KC153924
T. japonica C. Salgado & Hirooka	MAFF 241524	KC121428	KC153766	KC121492	KC153959
	HMAS 98327	**MK556799**	HM054140	HM042434	–
T. mammoidea (W. Phillips & Plowr.) C. Salgado & R.M. Sanchez	IMI 69361	KC121425	KC153763	KC121489	KC153956
T. ostrina C. Salgado & P. Chaverri	GJS 9623	KC121418	KC153756	KC121482	KC153949
T. phoenicea C. Salgado & P. Chaverri	GJS 85179	KC121398	KC153736	KC121462	KC153929
	HMAS 76856	**MK556800**	JQ836657	DQ119572	–
T. pinea (Dingley) C. Salgado & P. Chaverri	AR 4324	HM352875	HM364294	HM364307	HM364326
T. porphyria C. Salgado & Hirooka	MAFF 241515	KC121426	KC153764	KC121490	KC153957
	HMAS 98333	**MK556798**	HM054136	HM042433	–
T. purpurea C. Salgado & P. Chaverri	GJS 10131	KC121394	KC153732	KC121458	KC153925
T. rubi (Osterw.) C. Salgado & P. Chaverri	CBS 11312	KC121380	KC153718	KC121444	KC153911
T. sinensis (J. Luo & W.Y. Zhuang) Z.Q. Zeng & W.Y. Zhuang	HMAS 183186	**MF669048**	FJ560441	FJ560436	**MF669060**
T. tyrus C. Salgado & P. Chaverri	GJS 9046	KC121413	KC153751	KC121477	KC153944
T. violaria C. Salgado & R.M. Sanchez	AR 4766	KC121377	KC153715	KC121441	KC153908
T. yunnanica Z.Q. Zeng & W.Y. Zhuang	HMAS 183564	**MF669049**	FJ560438	**MF669055**	**MF669061**

[a] The GenBank numbers in bold type were newly generated in this study.

replications, each with 10 replicates of random addition of taxa. The BI analysis was conducted by MrBayes 3.1.2 (Ronquist and Huelsenbeck 2003) using a Markov chain Monte Carlo algorithm. Nucleotide substitution models were determined by MrModeltest 2.3 (Nylander 2004). Four Markov chains were run simultaneously for 1000000 generations with the trees sampled every 100 generations. A 50% majority rule consensus tree was computed after excluding the first 2500 trees as 'burn-in'. Bayesian Inference posterior probability (BIPP) was determined from the remaining trees. ML analysis was conducted with IQ-Tree 1.6.10 (Nguyen et al. 2015) using the best model for each locus chose by ModelFinder (Chernomor et al. 2016). Branch support measures were calculated with 1000 bootstrap replicates. Trees were examined by TreeView 1.6.6 (Page 1996). *Cosmospora coccinea* Rabenh. and *Nectria cinnabarina* (Tode) Fr. were used as outgroup taxa. Maximum Likelihood bootstrap proportion (MLBP) and MPBP greater than 50% and BIPP greater than 90% were shown at the nodes.

Results

The sequences of ACT, ITS, LSU and RPB1 from 25 representative taxa of *Rugonectria* and *Thelonectria* were analysed. The partition homogeneity test (P = 0.03) indicated that the individual partitions were not highly incongruent (Cunningham 1997), thus these four loci were combined for the phylogenetic analyses. In the MP analysis, the datasets included 2524 nucleotide characters, of which 1836 were constant, 198 were variable and parsimony-uninformative and 490 were parsimony-informative. The MP analysis resulted in three most parsimonious trees (tree length = 1415, CI = 0.6721, HI = 0.3279, RI = 0.6098, RCI = 0.5351). One of them is shown in Figure 1. The ML and BI trees were of similar topology. The final matrix was deposited in TreeBASE with accession no. S23994. The isolate HMAS 254521 grouped with other members of *Rugonectria* by receiving high bootstrap values (MLBP/MPBP/BIPP = 100%/100%/100%) and the isolate HMAS 254522 clustered with the representatives of *Thelonectria* (MLBP/MPBP/BIPP = 100%/100%/100%), which support the taxonomic placements of these new species.

Taxonomy

***Rugonectria microconidia* Z.Q. Zeng & W.Y. Zhuang, sp. nov.**
Fungal Names: FN570487
Figure 2

Holotype. CHINA. Hunan, Yizhang, Mangshan, (24°57'56.58"N, 112°57'34.63"E), alt. 700 m, on mossy bark, 26 October 2015, Z.Q. Zeng, X.C. Wang, K. Chen, Y.B. Zhang 10266 (HMAS 254521); ex-type culture: HMAS 247232.

Sequences. ACT (MF669044), ITS (MF669050), LSU (MF669052) and RPB1 (MF669056).

Etymology. The specific epithet refers to the microconidia produced in culture.

Description. Mycelium not visible around ascomata or on natural substrata. Ascomata superficial, gregarious, with basal stroma, pyriform to subglobose, non-papillate, yellow to orange, often with a darker red ostiolar area when dry, turning dark red in KOH, becoming slightly yellow in LA, 421–549 × 333–470 µm (n = 8). Perithecial surface warted, 30–93 µm thick, of textura globulosa to textura angularis, cells 10–27 × 8–18 µm, walls 1.5–2.5 µm thick. Perithecial wall of two layers, 45–70 µm thick, outer layer 25–45 µm thick, of textura globulosa to textura angularis; inner layer 7–25 µm thick, of textura prismatica. Asci unitunicate, clavate, 8-spored, 93–130 × (11–)15–25 µm (112.6 ± 12.6 × 18.9 ± 3.2 µm). Ascospores ellipsoid to broadly ellipsoid, 1-septate, striate, uniseriate or biseriate above and uniseriate below, hyaline, 20–28 × 8–12 µm (24.0 ± 2.0 × 10.1 ± 0.9 µm). Colony on PDA 42 mm diameter after 7 d under daylight at 25 °C, surface velvety, with white aerial mycelium, producing pale pinkish pigment in medium. Colony on SNA reaches 40 mm diameter after 7 d under daylight at 25 °C, surface with sparse whitish aerial mycelium. Conidiophores simply branched,

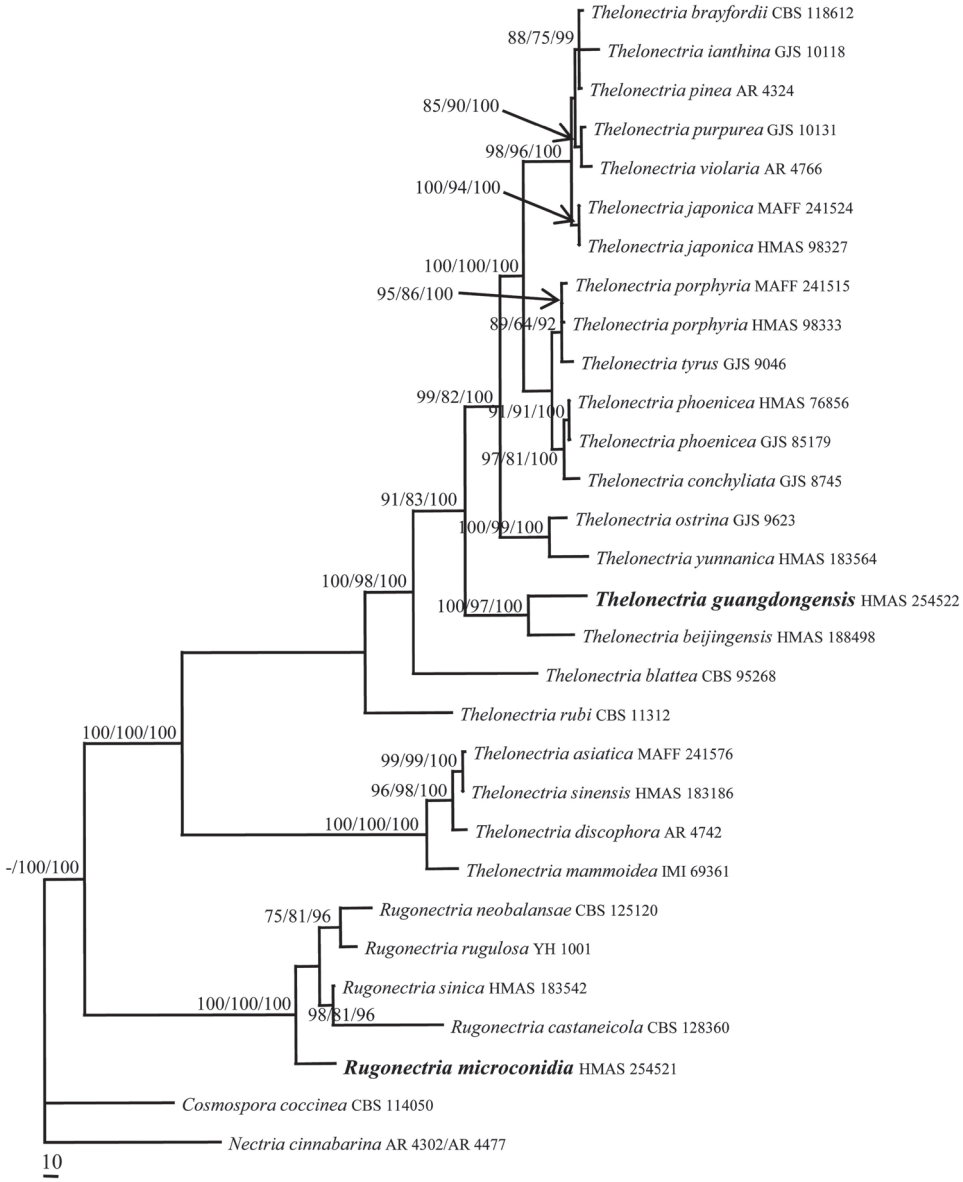

Figure 1. A Maximum Parsimony tree inferred from the combined ACT, ITS, LSU and RPB1 sequences. *Cosmospora coccinea* and *Nectria cinnabarina* were used as outgroup taxa. MLBP (left) and MPBP (middle) above 50%, BIPP (right) above 90% are indicated at nodes.

18–50 × 2–3 μm. Microconidia allantoid to rod shaped, slightly curved, 0(1–2)-septate, 3–14(–18) × 1.2–2.5(–3) μm (6.7 ± 3.1 × 1.6 ± 0.4 μm).

Habitat. On mossy bark.

Distribution. Asia (China).

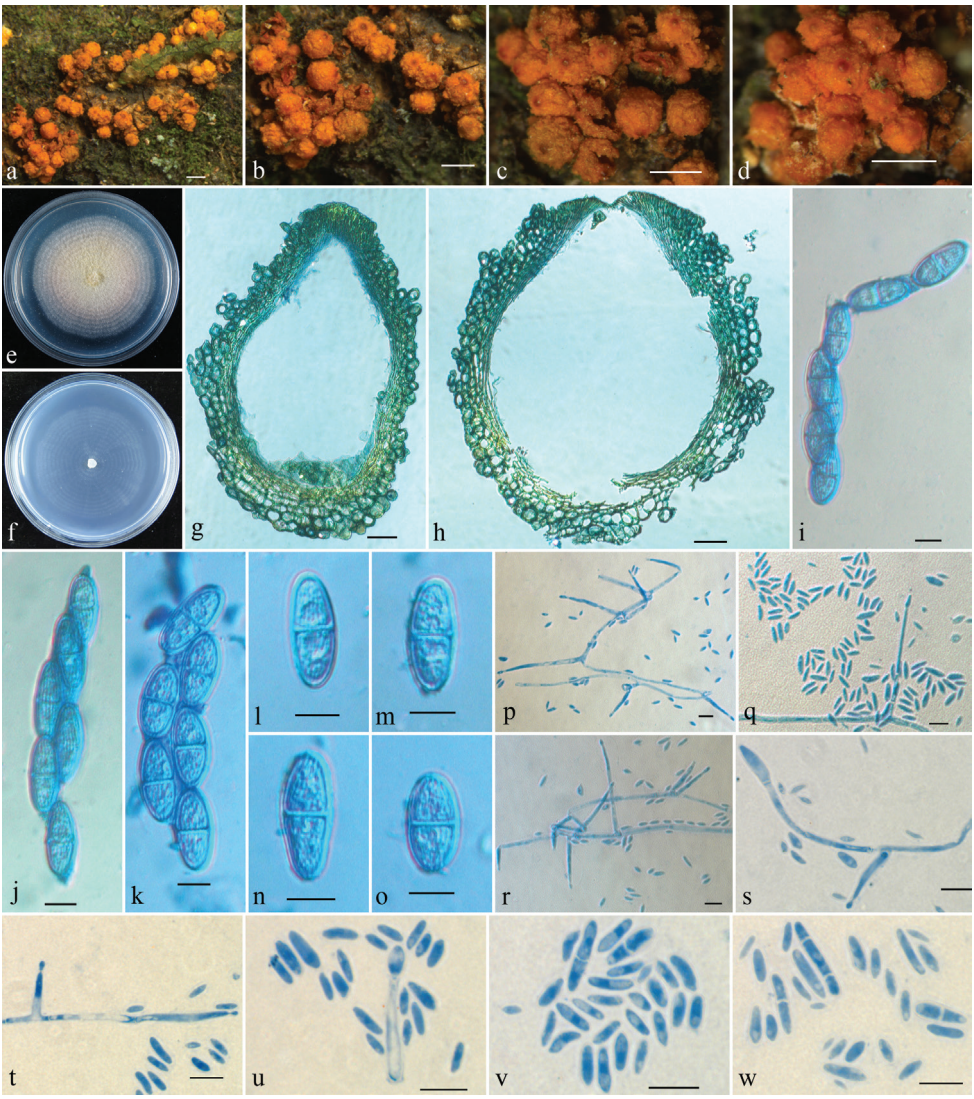

Figure 2. *Rugonectria microconidia* **a–d** ascomata on natural substratum **e** colony on PDA **f** colony on SNA **g, h** median section through perithecium **i–k** asci with ascospores **l–o** ascospores **p–s** conidiophores and conidia **t, u** conidiogenous cells and conidia **v, w** microconidia. Scale bars: 0.5 mm (**a–d**); 50 µm (**g, h**); 10 µm (**i–w**).

Notes. The non-papillate perithecia with warted surface, clavate asci with ellipsoidal to broadly ellipsoidal, uniseptate, striate ascospores, as well as our molecular data, suggest that this species belongs to *Rugonectria* (Chaverri et al. 2011). Amongst the known species of the genus, *R. microconidia* is morphologically most similar to the type species, *R. rugulosa*, in having gregarious, warted, orange perithecia often with a dark red ostiole when dry (Samuels et al. 1990; Samuels and Brayford 1994). The newly de-

scribed species differs in having asci that are 93–130 × (11–)15–25 μm and larger than those of *R. rugulosa* that are (53–)64–83(–95) × (7.5–)11.3–15.5(–17) μm. In addition, the ascospores of *R. microconidia* are also larger, 20–28 × 8–12 μm, while those of *R. rugulosa* are (10–)13.5–18(–24) × (3.3–)4.7–6.7(–10) μm. Unlike *R. microconidia*, *R. rugulosa* does not produce macroconidia in culture (Samuels et al. 1990; Samuels and Brayford 1994). Sequence comparisons reveal that there are 21 bp, 21 bp, 12 bp and 22 bp divergences in the ACT, ITS, LSU and RPB1 regions, respectively, between *R. microconidia* and *R. rugulosa* (YH1001). Both morphological and molecular data suggest that these species are distinct.

Rugonectria rugulosa (Pat. & Gaillard) Samuels, P. Chaverri & C. Salgado, in Chaverri, Salgado, Hirooka, Rossman & Samuels, Stud. Mycol. 68: 73, 2011

≡ *Nectria rugulosa* Pat. & Gaillard, Bull. Soc. Mycol. Fr. 5(4): 115, 1890.
≡ *Neonectria rugulosa* (Pat. & Gaillard) Mantiri & Samuels, in Mantiri, Samuels, Rahe & Honda, Can. J. Bot. 79(3): 339, 2001.
= *Cylindrocarpon rugulosum* Brayford & Samuels, in Samuels & Brayford, Sydowia 46(1): 148, 1994.

Specimens examined. CHINA. Henan, Jigongshan, alt. 400 m, on rotten twigs, 14 November 2003, W.Y. Zhuang, Y. Nong 5142 (HMAS 91774). Hainan, Changjiang, Bawangling, alt. 1100 m, on rotten twigs, 7 December 2000, W.Y. Zhuang, X.M. Zhang H25 (HMAS 83349); Ledong, Jianfengling, alt. 1100 m, on rotten twigs, 9 December 2000, W.Y. Zhuang, X.M. Zhang, Z.H. Yu H36, H41 (HMAS 83350, 83370); Qiongzhong, Limushan, alt. 700 m, on rotten twigs, 18 December 2000, W.Y. Zhuang, X.M. Zhang H124 (HMAS 76867); Tongzha, Wuzhishan, alt. 1000 m, on bark, 16 December 2000, W.Y. Zhuang, X.M. Zhang, Z.H. Yu, Y.H. Zhang H105 (HMAS 83371); on rotten twigs, W.P. Wu W7058 (HMAS 183161); Yunnan, Xichou, on rotten twigs, 11 November 1999, W.Y. Zhuang, Z.H. Yu 3407 (HMAS 183160).

Habitat. On rotten twigs, wood of recently dead and dying trees.

Distribution. Africa (Congo), Americas (Venezuela), Asia (China, Indonesia), possibly pantropical.

Notes. The species was formerly placed in *Nectria* (Fr.) Fr. and *Neonectria* Wollenw. until Chaverri et al. (2011) introduced *Rugonectria* with *R. rugosa* as the type species. The Chinese materials match well the description of the fungus (Samuels and Brayford 1994).

Rugonectria sinica W.Y. Zhuang, Z.Q. Zeng & W.H. Ho, in Zeng, Zhuang & Ho, Mycosystema 31(4): 467, 2013

Specimens examined. CHINA. Hainan, Changjiang, Bawanling, alt. 1100 m, on dead twigs of *Quercus* sp., 7 December 2000, W.Y. Zhuang, X.M. Zhang H22, H30

(HMAS 76854, 83369); Changjiang, Bawanling, alt. 1100 m, on dead twigs, 7 December 2000, W.Y. Zhuang, X.M. Zhang H28 (HMAS 76865); Lingshui, Diaoluoshan, alt. 1100 m, on bark, 13 December 2000, W.Y. Zhuang, X.M. Zhang, Z.H. Yu H70 (HMAS 76866); Henan, Jigongshan, alt. 400 m, on dead twigs, 14 November 2003, W.Y. Zhuang, Y. Nong 5099 (HMAS 91773); Fujian, Wuyishan, on dead twigs, 21 September 2006, W.Y. Zhuang, J. Luo, W.Y. Li 6846 (HMAS 183542).

Sequences. ACT (MF669046), ITS (HM054141), LSU (HM042430) and RPB1 (MF669058).

Habitat. On bark and dead twigs.

Distribution. Asia (China).

Notes. Morphologically *Rugonectria sinica* resembles *R. castaneicola* (W. Yamam. & Oyasu) Hirooka & P. Chaverri in having four-spored asci (Zeng et al. 2012). However, *R. castaneicola* differs in possessing perithecia that are 250–470 × 350–430 μm and larger than those of *R. sinica* that are 216–420 × 194–404 μm. In addition, the ascospores of *R. castaneicola* are larger, 18–28 × 7.5–11 μm, while those of *R. sinica* are 16–26 × 5.5–11 μm. The sequence analyses of the ITS and β-tubulin regions from type culture confirmed that they are different taxa (Zeng et al. 2012).

***Thelonectria guangdongensis* Z.Q. Zeng & W.Y. Zhuang, sp. nov.**
Fungal Names: FN570488
Figure 3

Holotype. CHINA. Guangdong, Shixing, Chebaling, (24°43'17.38"N, 114°16'39.50"E), alt. 600 m, on branches, 2 November 2015, Z.Q. Zeng, X.C. Wang, K. Chen, Y.B. Zhang 10627 (HMAS 254522); ex-type culture: HMAS 247233.

Sequences. ACT (MF669045), ITS (MF669051), LSU (MF669053) and RPB1 (MF669057).

Etymology. The specific epithet refers to the type locality of the fungus.

Description. Mycelium not visible around ascomata or on natural substrata. Ascomata perithecial, solitary to gregarious, up to 10 in a group, with a well–developed stroma, superficial, subglobose to globose, bright red with a prominently darkened papilla, turning dark red in KOH, becoming slightly yellow in LA, 235–382 × 245–412 μm (n = 8). Perithecial surface slightly roughened. Perithecial wall of two layers, 20–50 μm thick, outer layer 13–37 μm thick, of textura intricata; inner layer 7.5–13 μm thick, of textura prismatica. Asci not observed. Ascospores ellipsoid, 1-septate, smooth, 10–13 × 3–5 μm (11.6 ± 1.3 × 4.2 ± 0.7 μm). Colony on PDA 28 mm diameter after 7 d under daylight at 25 °C, surface velvety, with white aerial mycelium, producing purple pigment in medium. Colony on SNA 35 mm diameter after 7 d under daylight at 25 °C, surface with sparse whitish aerial mycelium. Phialides cylindrical or slightly swollen, 20–58 × 2–4 μm. Macroconidia cylindrical, slightly curved with rounded ends, 2–5-septate, 48–70 × 4.8–5.3 μm (58.9 ± 7.14 × 5.0 ± 0.2 μm). Microconidia and chlamydospores not observed in culture.

Habitat. On branches.

Distribution. Asia (China).

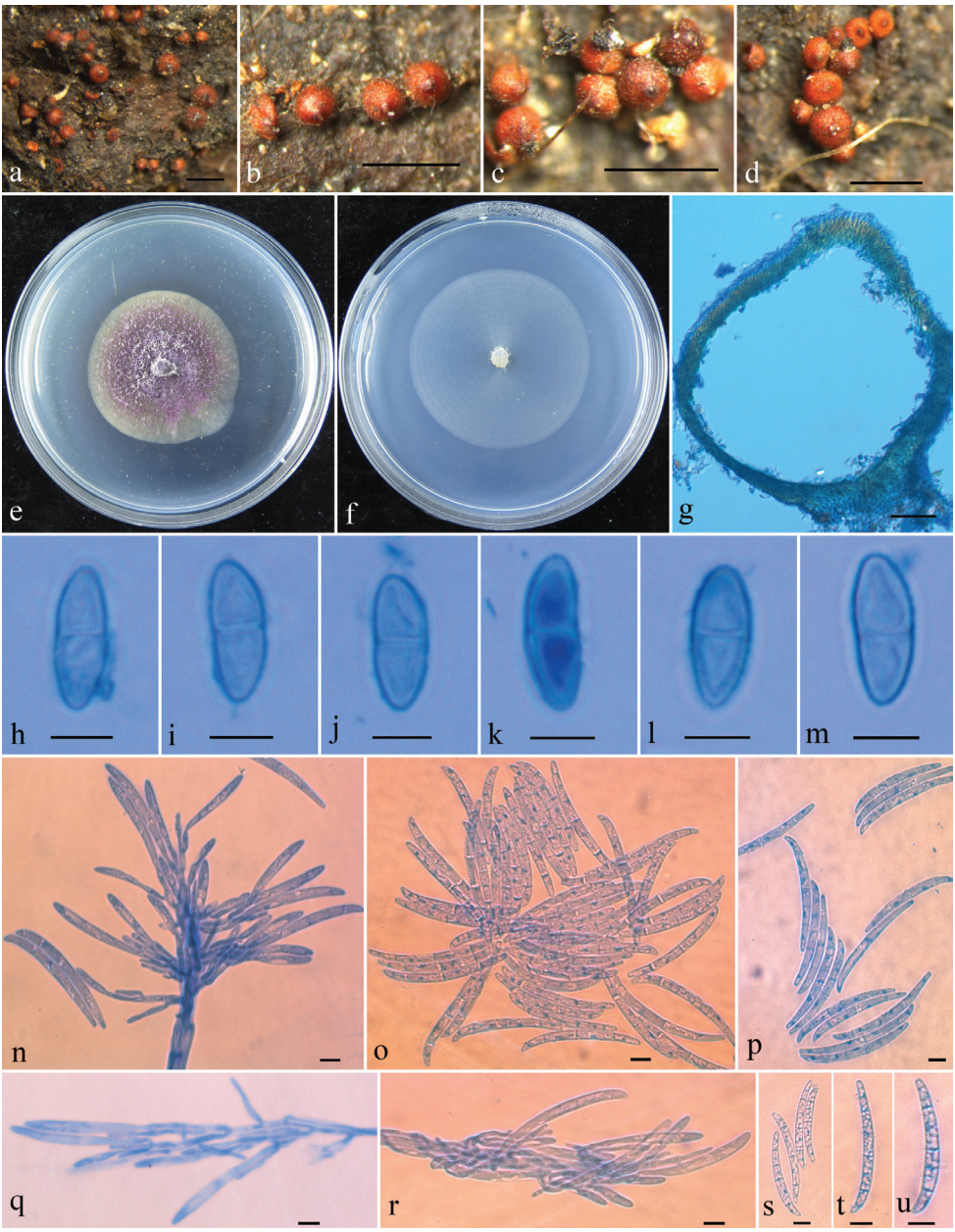

Figure 3. *Thelonectria guangdongensis* **a–d** ascomata on natural substratum **e** colony on PDA **f** colony on SNA **g** median section through perithecium **h–m** ascospores **n, q, r** conidiogenous cells and macroconidia **o, p, s–u** macroconidia. Scale bars: 0.5 mm (**a–d**); 50 µm (**g**); 10 µm (**h–u**).

Notes. Amongst species of *Thelonectria*, *T. guangdongensis* resembles *T. phoenicea* in having subglobose to globose perithecia with slightly roughened surface, purple colony, lack of microconidia and number of septa in macroconidia (Salgado-Salazar et al. 2015). However, *T. phoenicea* has much larger perithecia 300–600 × 200–350

μm, wider ascospores that are 4–5.5 μm wide, and wider phialides 3–6.5 μm wide (Salgado-Salazar et al. 2015). Moreover, there are 13 bp, 44 bp, 8 bp and 54 bp divergences in the ACT, ITS, LSU and RPB1 regions, respectively, between the type of *T. guangdongensis* (HMAS 254522) and that of *T. phoenicea* (G.J.S. 85–179).

Phylogenetically *T. guangdongensis* is closely related to *T. beijingensis* with strong statistical support (MLBP/MPBP/BIPP = 100%/97%/100%) (Figure 1). However, *T. beijingensis* differs in having larger ascospores that are 13–17 × 4–7 μm, while those of *T. guangdongensis* are 10–13 × 3–5 μm and form microconidia in culture in addition to macroconidia (Zeng and Zhuang 2013). There are 20 bp, 30 bp, 5 bp and 50 bp divergences in the ACT, ITS, LSU and RPB1 regions between the ex-type culture of *T. guangdongensis* and that of *T. beijingensis* (HMAS 188498). Both morphology and molecular data support the establishment of the new species.

Thelonectria beijingensis Z.Q. Zeng, J. Luo & W.Y. Zhuang, Phytotaxa 85(1): 18, 2013

Specimen examined. CHINA. Beijing, on bark of an unidentified tree, 1 September 2010, L. Cai 7604 (HMAS 188498), ex-type culture: HMAS 188566.

Sequences. ACT (MF669047), ITS (JQ836656), LSU (MF669054) and RPB1 (MF669059).

Habitat. On bark.

Distribution. Asia (China).

Notes. This species was introduced by Zeng and Zhuang (2013) and only known from the type locality. The phylogenetic analyses indicate that the species is associated with *T. guangdongensis* (Figure 1).

Thelonectria coronalis C. Salgado & Guu, in Salgado-Salazar, Rossman, Samuels, Capdet & Chaverri, Mycologia 104(6): 1339, 2012

Habitat. On bark of decaying shrubs and trees.

Distribution. Asia (China).

Notes. Salgado-Salazar et al. (2012) described *T. coronalis*, based on the specimens occurring on bark of decaying shrubs and trees. The fungus is only known from Taipei and Yilan of Taiwan Province.

Thelonectria coronata (Penz. & Sacc.) P. Chaverri & C. Salgado, in Chaverri, Salgado, Hirooka, Rossman & Samuels, Stud. Mycol. 68: 76, 2011

≡ *Nectria coronata* Penz. & Sacc., Malpighia 11(11–12): 510, 1897.

Specimen examined. CHINA. Hainan, Lingshui, Diaoluoshan, alt. 1050 m, on rotten twigs of *Pinus* sp., 15 December 2000, W.Y. Zhuang, X.M. Zhang H90 (HMAS 76855).

Habitat. On bark of shrubs and trees, sometimes associated with small cankers.

Distribution. Americas (Costa Rica), Asia (Indonesia, Taiwan), possibly pantropical.

Notes. The morphology and molecular data indicated that *T. coronata* is a species complex. Salgado-Salazar et al. (2012) divided it into five taxa on the basis of multigene phylogeny. The Chinese collection matches well the concept of *T. coronata* sensu stricto by Salgado-Salazar et al. (2012).

Thelonectria discophora (Mont.) P. Chaverri & C. Salgado, in Chaverri, Salgado, Hirooka, Rossman & Samuels, Stud. Mycol. 68: 76, 2011

≡ *Sphaeria discophora* Mont., Annls Sci. Nat., Bot., sér. 2 3: 353, 1835.
≡ *Neonectria discophora* (Mont.) Mantiri & Samuels, in Mantiri, Samuels, Rahe & Honda, Can. J. Bot. 79(3): 339, 2001.

Specimens examined. CHINA. Hainan, Changjiang, Bawangling, alt. 1100 m, 7 December 2000, on rotten twigs, W.Y. Zhuang, X.M. Zhang, Z.H. Yu H24 (HMAS 83351); Lingshui, Diaoluoshan, alt. 1050 m, 15 December 2000, on rotten twigs, W.Y. Zhuang, X.M. Zhang H83, H92-1 (HMAS 83353, 83352). Yunnan, Tengchong, 16 October 2003, W.P. Wu W7097 (HMAS 183180).

Habitat. On decaying bark of shrubs and trees.

Distribution. Americas (Chile), Asia (China), Europe (Scotland).

Notes. *Thelonectria discophora* is the type species of the genus *Thelonectria*. Many specimens identified as this species were determined to be species complex until Salgado-Salazar et al. (2015) separated them into at least 16 taxa, based on phylogenetic analyses of six nuclear loci and morphological evidences.

Thelonectria ianthina C. Salgado & Guu, in Salgado-Salazar, Rossman, Samuels, Hirooka, Sanchez & Chaverri, Fungal Diversity 70(1): 12, 2015

Habitat. On decaying bark of trees and shrubs.

Distribution. Americas (Costa Rica), Asia (China).

Notes. This species is known from Heredia Province of Costa Rica and Taiwan Province of China on decaying bark of trees and shrubs (Salgado-Salazar et al. 2015).

Thelonectria japonica C. Salgado & Hirooka, in Salgado-Salazar, Rossman, Samuels, Hirooka, Sanchez & Chaverri, Fungal Diversity 70(1): 14, 2015

Specimens examined. CHINA. Hubei, Wufeng, Houhe, alt. 800 m, 13 September 2004, on rotten twigs, W.Y. Zhuang, Y. Nong 5621 (HMAS 98327); Yunnan, Tengchong, on rotten twigs, W.P. Wu W7104a (HMAS 183155).

Sequences. ACT (MK556799), ITS (HM054140) and LSU (HM042434).

Habitat. On decaying bark of *Fagus crenata* and possibly on bark of other shrubs and trees.

Distribution. Asia (China, Japan).

Notes. Specimens of this fungus were treated as *T. discophora* sensu lato until *T. japonica* was introduced by Salgado-Salazar et al. (2015). The morphological characteristics of the Chinese materials fit the concept of *T. japonica*. The Hubei and Yunnan collections extend its distribution to China.

Thelonectria lucida (Höhn.) P. Chaverri & C. Salgado, in Chaverri, Salgado, Hirooka, Rossman & Samuels, Stud. Mycol. 68: 76, 2011

≡ *Nectria lucida* Höhn., Sber. Akad. Wiss. Wien, Math.-naturw. Kl., Abt. 1 118: 298, 1909.

≡ *Neonectria lucida* (Höhn.) Samuels & Brayford, in Brayford, Honda, Mantiri & Samuels, Mycologia 96(3): 590, 2004.

Habitat. On decaying bark of shrubs and trees.

Distribution. Africa (Cameroon), Americas (Costa Rica), Asia (China, Indonesia), possibly pantropical.

Notes. This is a relatively common species and recorded as *Neonectria lucida* by Guu et al. (2007) from Taiwan Province.

Thelonectria mamma C. Salgado & P. Chaverri, in Salgado-Salazar, Rossman & Chaverri, Fungal Diversity 80: 444, 2016

Habitat. On decaying bark of shrubs and trees.

Distribution. Americas (French Guiana), Asia (China).

Notes. The specimens of this species were filed under *T. lucida* (Guu et al. 2007). After re-examinations of the collections from China and French Guiana, Salgado-Salazar et al. (2016) stated that they represent a separate species related to *T. discophora* sensu stricto.

Thelonectria phoenicea C. Salgado & P. Chaverri, in Salgado-Salazar, Rossman, Samuels, Hirooka, Sanchez & Chaverri, Fungal Diversity 70(1): 16, 2015

Specimen examined. CHINA. Hainan, Lingshui, Diaoluoshan, alt. 1050 m, 15 December 2000, W.Y. Zhuang, X.M. Zhang H86 (HMAS 76856).

Sequences. ACT (MK556800), ITS (JQ836657) and LSU (DQ119572).

Habitat. On decaying *Acacia celsa* and other plants.

Distribution. Asia (China, Indonesia), Oceania (Australia).

Notes. Re-examination of HMAS 76856 indicated that *T. phoenicea* is the correct name for the specimen which was previously identified as *T. discophora*. It is distributed also in Taiwan Province (Salgado-Salazar et al. 2015).

Thelonectria porphyria C. Salgado & Hirooka, in Salgado-Salazar, Rossman, Samuels, Hirooka, Sanchez & Chaverri, Fungal Diversity 70(1): 19, 2015

Specimen examined. CHINA. Hubei, Wufeng, Houhe, alt. 800 m, on rotten twigs, 12 September 2004, W.Y. Zhuang, Y. Nong 5542 (HMAS 98333).

Sequences. ACT (MK556798), ITS (HM054136) and LSU (HM042433).

Habitat. On decaying bark of *Cryptomeria japonica* and other woody substrates.

Distribution. Asia (China, Japan).

Notes. The collection was previously treated as *T. discophora* sensu lato (Zhuang 2013). The sequence analyses (Figure 1) and morphological characteristics of HMAS 98333 indicate that the correct name for the collection is *T. porphyria*.

Thelonectria sinensis (J. Luo & W.Y. Zhuang) Z.Q. Zeng & W.Y. Zhuang, Phytotaxa 85(1): 18, 2013

≡ *Neonectria sinensis* J. Luo & W.Y. Zhuang, Mycologia 102(1): 147, 2010.

Specimen examined. CHINA. Hubei, Shennongjia, alt. 1700 m, on bark of a coniferous (?) tree, 17 September 2003, X.M. Zhang, Y.Z. Wang Z108 (HMAS 183186), ex-type culture: HMAS 173255.

Sequences. ACT (MF669048), ITS (FJ560441), LSU (FJ560436) and RPB1 (MF669060).

Habitat. On bark of a coniferous (?) tree.

Distribution. Asia (China).

Notes. The species was originally placed in *Neonectria* by Luo and Zhuang (2010). The anatomic structures and DNA data support its placement in *Thelonectria* (Zeng and Zhuang 2013).

Thelonectria veuillotiana (Sacc. & Roum.) P. Chaverri & C. Salgado, Stud. Mycol. 68: 77, 2011

≡ *Nectria veuillotiana* Sacc. & Roum., Rev. Mycol. 2: 189, 1880.
≡ *Neonectria veuillotiana* (Sacc. & Roum.) Mantiri & Samuels, Canda. J. Bot. 79: 339, 2001.

Specimens examined. CHINA. Anhui, Jinzhai, Tiantangzhai, alt. 1000 m, on bark, 24 August 2011, W.Y. Zhuang, H.D. Zheng, Z.Q. Zeng, S.L. Chen 7869 (HMAS

266577). Hubei, Shennongjia, alt. 1200 m, on rotten twigs associated with other fungi, 15 September 2004, W.Y. Zhuang, Y. Nong 5686 (HMAS 98332); Shennongjia, alt. 1700 m, on bark associated with other fungi, 15 September 2003, X.M. Zhang, Y. Z. Wang Z196 (HMAS 183188); Xingshan, Longmenhe, alt. 1800 m, on rotten twigs associated with other fungi, 18 September 2004, W.Y. Zhuang, Y. Nong 5832 (HMAS 99207). Jilin, Changbaishan, alt. 800 m, on rotten twigs, 27 July 2012, T. Bau, W.Y. Zhuang, H.D. Zheng, Z.Q. Zeng, Z.X. Zhu, F. Ren 8246 (HMAS 266579); Jiaohe, Qianjin forest farm, alt. 450 m, on rotten twigs, 23 July 2012, T. Bau, W.Y. Zhuang, Z.Q. Zeng, H.D. Zheng, Z.X. Zhu, F. Ren 8087b (HMAS 266578). Yunnan, Tengchong, on rotten twigs associated with other fungi, 16 September 2003, W.P. Wu W7095 (HMAS 183568).

Sequences. ITS (HM054151) and LSU (HM042437).

Habitat. On bark of deciduous trees, *Eucalyptus* sp., *Fagus* sp., *Gleditschia triacanthos*, *Salix* sp.

Distribution. Asia (China), Europe (France and Germany), Azores Islands.

Notes. The species was first placed in *Nectria*, then in *Neonectria* (Mantiri et al. 2001) and recently transferred to *Thelonectria* by Chaverri et al. (2011). It occurs on bark of recently killed trees, rarely on wood or leaves and is cosmopolitan in distribution (Brayford and Samuels 1993; Zhuang 2013).

Thelonectria yunnanica Z.Q. Zeng & W.Y. Zhuang, Phytotaxa 85(1): 19, 2013

Specimen examined. CHINA. Yunnan, Baoshan, on bark of an unidentified tree, 15 October 2003, W.P. Wu W7122 (HMAS 183564), ex-type culture: HMAS 188567.

Sequences. ACT (MF669049), ITS (FJ560438), LSU (MF669055) and RPB1 (MF669061).

Habitat. On bark.

Distribution. Asia (China).

Notes. *Thelonectria yunnanica* is only known from the type locality. It is phylogenetically related to *T. ostrina* (Figure 1). However, *T. ostrina* has a perithecial wall 25–40 µm while those of *T. yunnanica* are thicker 49–71 µm and have asci that are (56–)67–86(-98) × 7–12 µm while those of *T. yunnanica* are larger, 87–120 × 8.2–9.6 µm. Unlike *T. yunnanica*, *T. ostrina* does not forming microconidia in culture (Zeng and Zhuang 2013; Salgado-Salazar et al. 2015).

Excluded species

Thelonectria jungneri (Henn.) P. Chaverri & C. Salgado, in Chaverri, Salgado, Hirooka, Rossman & Samuels, Stud. Mycol. 68: 76, 2011

≡ *Nectria jungneri* Henn., Bot. Jb. 22: 75, 1895.
≡ *Neonectria jungneri* (Henn.) Samuels & Brayford, Mycologia 96(3): 580, 2004.

≡ *Macronectria jungneri* (Henn.) C. Salgado & P. Chaverri, in Salgado-Salazar, Rossman & Chaverri, Fungal Diversity 80: 448, 2016.

Specimen examined. CHINA. Guangdong, Dinghushan, on rotten twigs associated with other fungi, 9 October 1998, W.P. Wu W1871-2 (HMAS 183155).

Habitat. On various woody substrates, as well as other plant organic matter.

Distribution. Africa (Cameroon), Americas (Brazil, Costa Rica), Asia (China), possibly pantropical.

Notes. This fungus was originally described as *Nectria jungneri* and was transferred to *Neonectria* (Brayford et al. 2004) and *Thelonectria* (Chaverri et al. 2011). The recent work by Salgado-Salazar et al. (2016) indicated that it belongs to a separate genus *Macronectria* C. Salgado & P. Chaverri.

Discussion

The genus *Rugonectria* is characterised by the non-papillate, orange to red, conspicuously warted to rugose perithecial surface (Chaverri et al. 2011). The ascomatal anatomy, perithecial wall reactions to KOH and LA, features of asci and ascospores and asexual states indicate the placement of *R. microconidia* in this genus. The multi-locus sequence analyses confirm our morphological observations (Figure 1) and it is here described as a new species.

Historically, the nectriaceous fungi with cylindrocarpon-like asexual states were assigned to *Neonectria*. The accumulated morphological and phylogenetic data suggest that the genus was heterogeneous (Mantiri et al. 2001). Efforts were made towards establishment of a monophyletic *Neonectria* as well as its allies (Booth 1966, Rossman et al. 1999; Mantiri et al. 2001; Brayford et al. 2004). The previously recognised infrageneric groups within *Neonectria* are now recognised as separate genera, i.e. *Ilyonectria* for the *N. radicicola*-group, *Neonectria* sensu stricto for the *N. coccinea*-group, *Rugonectria* for the *N. rugulosa*-group and *Thelonectria* for the *N. mammoidea*/*N. veuillotiana*-groups (Chaverri et al. 2011). Since the establishment of *Thelonectria*, 45 species have been placed in the genus (www.indexfungorum.org). Salgado-Salazar et al. (2012, 2015) suggested that the criteria formerly used for generic differentiation were of insufficient sensitivity to accurately reflect the degree of species diversity within the group. Subsequently, Salgado-Salazar et al. (2016) emended the generic concept of *Thelonectria* by excluding *T. jungneri*, based on the molecular data and morphological characteristics.

The type species of *Thelonectria*, *T. discophora*, previously considered to be cosmopolitan, was first described based on material collected from Chile and was determined to be heterogeneous (Brayford et al. 2004). Salgado-Salazar et al. (2015) provided a revisionary treatment of the *T. discophora* species complex and recognised 16 cryptic species on the basis of the combined analyses of phylogeny and morphology. In this study, the new species *T. guangdongensis* is determined to be congeneric with *T. discophora*, while both the molecular data and morphological characteristics indicate that *T. guangdongenis*

is distinct from other species of *Thelonectria*. To date, 11 species of *Thelonectria* have been recorded from China (Teng 1936; Salgado-Salazar et al. 2012, 2015, 2016; Zeng and Zhuang 2012; Zhuang 2013). China is extremely diverse in its climate, vegetation, geographic structures and multiple niches. Our understanding of species diversity of the nectriaceous fungi will be significantly broadened in the near future.

Acknowledgements

The authors would like to thank Dr. A.Y. Rossman for her valuable comments and corrections and Drs. X.C. Wang, K. Chen and Y.B. Zhang for collecting specimens jointly for this study. This work was supported by the National Natural Science Foundation of China (nos. 31750001, 31570018, 31870012) and Frontier Key Program of Chinese Academy of Sciences (No. QYZDY-SSW-SMC029).

References

Booth C (1966) The genus *Cylindrocarpon*. Mycological Papers 104: 1–56.

Brayford D, Samuels GJ (1993) Some didymosporous species of *Nectria* with nonmicroconidial *Cylindrocarpon* anamorphs. Mycologia 85: 612–637. https://doi.org/10.2307/3760508

Brayford D, Honda BM, Mantiri FR, Samuels GJ (2004) *Neonectria* and *Cylindrocarpon*: the *Nectria mammoidea* group and species lacking microconidia. Mycologia 96: 572–597. https://doi.org/10.1080/15572536.2005.11832955

Castlebury LA, Rossman AY, Sung GH, Hyten AS, Spatafora JW (2004) Multigene phylogeny reveals new lineage for *Stachybotrys chartarum*, the indoor air fungus. Mycological Research 108: 864–872. https://doi.org/10.1017/S0953756204000607

Cedeño L, Carrero C, Quintero K, Pino H, Espinoza W (2004) *Cylindrocarpon destructans* var. *destructans* and *Neonectria discophora* var. *rubi* associated with black foot rot on blackberry (*Rubus glaucus* Benth.) in Merida, Venezuela. Interciencia 29: 455–460. https://doi.org/10.1038/sj.hdy.6800511

Chaverri P, Salgado C, Hirooka Y, Rossman AY, Samuels GJ (2011) Delimitation of *Neonectria* and *Cylindrocarpon* (Nectriaceae, Hypocreales, Ascomycota) and related genera with *Cylindrocarpon*-like anamorphs. Studies in Mycology 68: 57–68. https://doi.org/10.3114/sim.2011.68.03

Chernomor O, von Haeseler A, Minh BQ (2016) Terrace aware data structure for phylogenomic inference from supermatrices. Systematic Biology 65: 997–1008. https://doi.org/10.1093/sysbio/syw037

Crous PW, Luangsa-ard JJ, Wingfield MJ, Carnegie AJ, Hernández-Restrepo M, Lombard L, Roux J, Barreto RW, Baseia IG, Cano-Lira JF, Martín MP, Morozova OV, Stchigel AM, Summerell BA, Brandrud TE, Dima B, García D, Giraldo A, Guarro J, Gusmão LFP, Khamsuntorn P, Noordeloos ME, Nuankaew S, Pinruan U, Rodríguez-Andrade E, Souza-Motta CM, Thangavel R, van Iperen AL, Abreu VP, Accioly T, Alves JL, Andrade JP, Bah-

ram M, Baral H-O, Barbier E, Barnes CW, Bendiksen E, Bernard E, Bezerra JDP, Bezerra JL, Bizio E, Blair JE, Bulyonkova TM, Cabral TS, Caiafa MV, Cantillo T, Colmán AA, Conceição LB, Cruz S, Cunha AOB, Darveaux BA, da Silva AL, da Silva GA, da Silva GM, da Silva RMF, de Oliveira RJV, Oliveira RL, De Souza JT, Dueñas M, Evans HC, Epifani F, Felipe MTC, Fernández-López J, Ferreira BW, Figueiredo CN, Filippova NV, Flores JA, Gené J, Ghorbani G, Gibertoni TB, Glushakova AM, Healy R, Huhndorf SM, Iturrieta-González I, Javan-Nikkhah M, Juciano RF, Jurjević Ž, Kachalkin AV, Keochanpheng K, Krisai-Greilhuber I, Li YC, Lima AA, Machado AR, Madrid H, Magalhães OMC, Marbach PAS, Melanda GCS, Miller AN, Mongkolsamrit S, Nascimento RP, Oliveira TGL, Ordoñez ME, Orzes R, Palma MA, Pearce CJ, Pereira OL, Perrone G, Peterson SW, Pham THG, Piontelli E, Pordel A, Quijada L, Raja HA, Rosas de Paz E, Ryvarden L, Saitta A, Salcedo SS, Sandoval-Denis M, Santos Tab, Seifert KA, Silva BDB, Smith ME, Soares AM, Sommai S, Sousa JO, Suetrong S, Susca A, Tedersoo L, Telleria MT, Thanakitpipattana D, Valenzuela-Lopez N, Visagie CM, Zapata M, Groenewald JZ (2018) Fungal Planet description sheets: 785–867. Persoonia 41: 238–417. https://doi.org/10.3767/persoonia.2018.41.12

Cunningham CW (1997) Can three incongruence tests predict when data should be combined? Molecular Biology and Evolution 14: 733–740. https://doi.org/10.1093/oxfordjournals.molbev.a025813

Guu JR, Ju YM, Hsieh HJ (2007) Nectriaceous fungi collected from forests in Taiwan. Botanical Studies 48: 187–203.

Hall TA (1999) BioEdit: a user-friendly biological sequence alignment editor and analysis program for Windows 95/98/NT. Nucleic Acids Symposium Series 41: 95–98. https://doi.org/10.1021/bk-1999-0734.ch008

Hirooka Y, Rossman AY, Samuels GJ, Lechat C, Chaverri P (2012) A monograph of *Allantonectria*, *Nectria*, and *Pleonectria* (Nectriaceae, Hypocreales, Ascomycota) and their pycnidial, sporodochial, and synnematous anamorphs. Studies in Mycology 71: 1–210. https://doi.org/10.3114/sim0001

Kobayashi T, Hirooka Y, Natsuaki KT, Kawashima Y, Ushiyama K (2005) New canker diseases of *Abies veitchii* and *Acer crataegifolium* caused by *Neonectria castaneicola*. Journal of General Plant Pathology 71: 124–126. https://doi.org/10.1007/s10327-004-0172-1

Lombard L, van der Merwe NA, Groenewald JZ, Crous PW (2015) Generic concepts in Nectriaceae. Studies in Mycology 80: 189–245. https://doi.org/10.1016/j.simyco.2014.12.002

Lu BS, Hyde KD, Ho WH, Tsui KM, Taylor JE, Wong KM, Zhou Y, Zhou DQ (2000) Checklist of Hong Kong Fungi. Fungal Diversity Press, Hong Kong, 270 pp.

Luo J, Zhuang WY (2010) Three new species of *Neonectria* (Nectriaceae, Hypocreales) with notes on their phylogenetic positions. Mycologia 102: 142–152. https://doi.org/10.3852/08-224

Mantiri FR, Samuels GJ, Rahe JE, Honda BM (2001) Phylogenetic relationships in *Neonectria* species having *Cylindrocarpon* anamorphs inferred from mitochondrial ribosomal DNA sequences. Canadian Journal of Botany 79: 334–340. https://doi.org/10.1139/b01-002

Nirenberg HI (1976) Studies on the morphologic and biologic differentiation in *Fusarium* section *Liseola*. Mitteilungen aus der Biologischen Bundesanstalt für Land- und Forstwirtschaft 169: 1–117.

Nguyen LT, Schmidt HA, von Haeseler A, Minh BQ (2015) IQ-TREE: A fast and effective stochastic algorithm for estimating maximum likelihood phylogenies. Molecular Biology and Evolution 32: 268–274. https://doi.org/10.1093/molbev/msu300

Nylander JAA (2004) MrModeltest v2. Program distributed by the author. Evolutionary Biology Centre, Uppsala University.

Page RD (1996) TreeView: an application to display phylogenetic trees on personal computers. Computer Applications in the Biosciences 12: 357–358. https://doi.org/10.1093/bioinformatics/12.4.357

Rehner SA, Samuels GJ (1994) Taxonomy and phylogeny of *Gliocladium* analyzed from nuclear large subunit ribosomal DNA sequences. Mycological Research 98: 625–634. https://doi.org/10.1016/S0953-7562(09)80409-7

Ronquist F, Huelsenbeck JP (2003) MrBayes 3: Bayesian phylogenetic inference under mixed models. Bioinformatics 19: 1572–1574. https://doi.org/10.1093/bioinformatics/btg180

Rossman AY, Samuels GJ, Rogerson CT, Lowen R (1999) Genera of Bionectriaceae, Hypocreaceae and Nectriaceae (Hypocreales, Ascomycetes). Studies in Mycology 42: 1–248.

Salgado-Salazar C, Rossman AY, Samuels GJ, Capdet M, Chaverri P (2012) Multigene phylogenetic analyses of the *Thelonectria coronata* and *T. veuillotiana* species complexes. Mycologia 104: 1325–1350. https://doi.org/10.3852/12-055

Salgado-Salazar C, Rossman AY, Samuels GJ, Hirooka Y, Sanchez RM, Chaverri P (2015) Phylogeny and taxonomic revision of *Thelonectria discophora* (Ascomycota, Hypocreales, Nectriaceae) species complex. Fungal Diversity 70: 1–29. https://doi.org/10.1007/s13225-014-0280-y

Salgado-Salazar C, Rossman AY, Chaverri P (2016) The genus *Thelonectria* (Nectriaceae, Hypocreales, Ascomycota) and closely related species with cylindrocarpon-like asexual states. Fungal Diversity 80: 411–455. https://doi.org/10.1007/s13225-016-0365-x

Samuels GJ, Doi Y, Rogerson CT (1990) Hypocreales. Memoirs of the New York Botanical Garden 59: 6–108.

Samuels GJ, Brayford D (1994) Species of *Nectria* (*sensu lato*) with red perithecia and striate ascospores. Sydowia 46: 75–161.

Samuels GJ, Dodd S, Lu B-S, Petrini O, Schroers H-J, Druzhinina I-S (2006) The *Trichoderma koningii* aggregate species. Studies in Mycology 56: 67–133. https://doi.org/10.3114/sim.2006.56.03

Swofford DL (2002) PAUP*: phylogenetic analysis using parsimony (*and other methods). Version 4b10. Sinauer Associates, Sunderland.

Teng SC (1936) Additional fungi from China II. Sinensia. 7: 490–527.

Thompson JD, Gibson TJ, Plewniak F, Jeanmougin F, Higgin DG (1997) The ClustalX windows interface: flexible strategies for multiple sequences alignment aided by quality analysis tools. Nucleic Acids Research 25: 4876–4883. https://doi.org/10.1093/nar/25.24.4876

Vilgalys R, Hester M (1990) Rapid genetic identification and mapping enzymatically amplified ribosomal DNA from several *Cryptococcus* species. Journal of Bacteriology 172: 4238–4246. https://doi.org/10.1128/jb.172.8.4238-4246.1990

Wang L, Zhuang WY (2004) Designing primer sets for amplification of partial calmodulin genes from penicillia. Mycosystema 23: 466–473.

White TJ, Bruns T, Lee S, Taylor J (1990) Amplification and direct sequencing of fungal ribosomal RNA genes for phylogenetics. In: Innis MA, Gelfland DH, Sninsky JJ, White TJ (Eds) PCR protocols: a guide to methods and applications. Academic Press, San Diego, 315–322. https://doi.org/10.1016/B978-0-12-372180-8.50042-1

Zeng ZQ, Zhuang WY (2013) Four new taxa of *Ilyonectria* and *Thelonectria* (Nectriaceae) revealed by morphology and combined ITS and β-tubulin sequence data. Phytotaxa 85: 15–25. https://doi.org/10.11646/phytotaxa.85.1.3

Zeng ZQ, Zhuang WY, Ho WH (2012) A new species of *Rugonectria* (Nectriaceae) with four-spored asci. Mycosystema 31(4): 465–470.

Zhuang WY (2013) Flora fungorum sinicorum (Vol. 47). Nectriaceae et Bionectriaceae. Science Press, Beijing, 162 pp. [in Chinese]